



NTNU – Trondheim
Norwegian University of
Science and Technology

Wettability Variations within the North Sea Oil Field Frøy

Mathias Tangen

Earth Sciences and Petroleum Engineering

Submission date: June 2012

Supervisor: Jan-Åge Stensen, IPT

Norwegian University of Science and Technology

Department of Petroleum Engineering and Applied Geophysics

Acknowledgements

First of all, I would like to thank petroleum technology advisor Tormod Førland at Det norske oljeselskap for letting me write my master's thesis for Det norske and for giving me a practical and interesting subject to write about. Next, I would like to express my sincerest gratitude to reservoir engineers Erlend Øian and Geir Frode Kvilaas for a tremendous amount of help, for their infinite patience, for constructive discussions and feedback and in general for being so nice to me during my work on my thesis. You have been simply outstanding and I do not know how I could have written this thesis without your support, so again, thank you so much! Thank you to Det norske oljeselskap for supporting me financially by buying the book "Wettability" by Donaldson and Alam. Thank you also to Pål Skillingstad, Tor-Ole Jøssund and Grethe Schei at Det norske.

I would like to thank my NTNU supervisor, professor Jan Åge Stensen for feedback on my thesis. Thank you also to professor Ole Torsæter.

Abstract

Wettability is one of the most important parameters governing the rate of oil recovery from a porous medium. This thesis is a study of the wettability variations within the Frøy field in the North Sea, and its effect on the oil recovery. Several reports regarding the wettability and relative permeability of the Frøy field are available, and the conclusions from these reports are presented. The overall conclusion is that Frøy is on the oil-wet side of the wettability scale, with measured Amott-Harvey wettability indices ranging from -0.00189 to -0.73. An attempt was made to find wettability trends, relating the wettability index to variables such as distance above the water-oil contact, geological facies, permeability, the core's staining level and so on, based on the measured data. Unfortunately, no such trend was identified.

Only nine wettability measurements were available from the Frøy field while writing this thesis. This thesis concludes that in order to get a good statistical data set that can be used for establishing wettability trends, several wettability tests should be performed on cores sampled from a variety of distances above the water-oil contact, with different permeabilities and color staining levels, representing different rock types. And it is important to make sure that the cores have their original (native) wettability during the tests.

More than 50 simulation cases have been made and run during the work on this thesis, testing the effect of wettability variations on Frøy, using the Schlumberger reservoir simulation program Eclipse 100. Wettability variations are simulated by assigning different relative permeability curves to different saturation function regions in the reservoir. For this reason, five sets of relative permeability curves were made, that represents wettabilities ranging from slightly water-wet to oil-wet, and different combinations of these curves were used in the simulation cases. There are many uncertainties in the given data and there are different ways of initializing the simulation model which may affect the simulation results. These issues are discussed in a separate chapter of the thesis.

The simulation results showed that when the reservoir rock went from water-wet to oil-wet, the oil production went down, the water production went up, the water breakthrough occurred earlier and the oil recovery factor went down. The different producing wells were not equally affected by changes in the wettability.

Two important conclusions were drawn from the simulation results. Firstly, it is difficult to estimate the effect of wettability variations on the production profiles if not the aquifer support and the fault transmissibility factors are modeled correctly, since these parameters also affect the production. And secondly, it is the wettability of the bottom half of the 225 meter thick reservoir zone that affects the production profiles of the wells. The wettability of the top half of the reservoir zone hardly affects the production profiles at all.

Sammendrag

Nytt av året (2012) er at masteroppgavene ved NTNU skal ha et sammendrag både på norsk og engelsk. Dette er en norsk versjon av "Abstract" på den forrige siden.

Fukt (wettability) er en av de viktigste parametrene når det gjelder raten av oljeutvinningen fra et porøst medium. Denne oppgaven er en studie av fuktevariasjonene i Frøy-feltet i Nordsjøen, og hvordan disse påvirker oljeutvinningen. Flere rapporter som omhandler fukt og relativ permeabilitet på Frøy-feltet er tilgjengelig, og konklusjonene fra disse rapportene blir presentert. Den overordnede konklusjonen er at Frøy tilhører den oljefuktende siden av fukteskalaen, med målte Amott-Harvey-indeksler fra -0,00189 til -0,73. Et forsøk ble gjort på å finne fuktetrender ved å prøve å relatere fuktindeksen til variabler som avstand over vann-olje-kontakten, geologiske facies, permeabilitet, nivå av misfarging på kjerneprøvene og så videre, basert på de målte dataene. Dessverre ble ingen slike trender identifisert.

Bare ni fuktemålinger var tilgjengelig fra Frøy-feltet mens denne oppgaven ble skrevet. Oppgaven konkluderer med at for å få et godt statistisk datasett som kan brukes for å etablere fuktetrender, bør flere fuktetester utføres på kjerner som er tatt fra mange representative avstander over vann-olje-kontakten, med ulike permeabiliteter og nivåer av misfarging, og samtidig representere ulike bergarter. Det er viktig å sørge for at kjernene har sin opprinnelige fukting under testene.

Mer enn 50 simuleringer har blitt lagd og kjørt under arbeidet med denne masteroppgaven for å teste effekten av fuktevariasjoner på Frøy. Simuleringene er gjort med bruk av Schlumbergers reservoarsimuleringsprogram Eclipse 100. Fuktevariasjonene er simulert ved å tildele forskjellige relativ permeabilitetskurver til forskjellige metningsfunksjonsregioner i reservoaret. På grunn av dette ble det laget fem sett med relativ permeabilitetskurver, som representerer fuktekaraktistikker fra lett vannfuktende til oljefuktende, og ulike kombinasjoner av disse kurvene ble brukt i simuleringene. Det er mange usikkerheter i de gitte dataene og det finnes i tillegg forskjellige måter å initialisere simuleringsmodellen på som kan påvirke simuleringsresultatene. Disse problemstillingene er drøftet i et eget kapittel.

Simuleringsresultatene viste at når reservoaret gikk fra vannfuktende til oljefuktende gikk oljeproduksjonen ned, vannproduksjonen opp, vanngjennombruddet kom tidligere og utvinningsgraden gikk ned. De forskjellige produksjonsbrønnene ble i ulik grad påvirket av endringer i fukting.

To viktige konklusjoner ble trukket fra simuleringsresultatene. For det første er det vanskelig å anslå effekten av fuktevariasjoner på produksjonsprofilene uten at akviferstøtten og transmissibilitetsfaktorene gjennom forkastningene er modellert korrekt, ettersom disse parametrene også påvirker produksjonen. Og for det andre er det fuktekaraktistikken i den nedre halvdel av den 225 meter tykke reservoarsonen som påvirker produksjonsprofilene for brønnene. Fuktekaraktistikken i den øverste halvdel av reservoarsonen påvirker trolig ikke produksjonsprofilene i det hele tatt.

Table of contents

Acknowledgements.....	iii
Abstract.....	iv
Sammendrag.....	v
Table of figures	viii
List of tables	x
1 Introduction	1
2 Literature review.....	3
2.1 Reservoir parameters.....	3
2.1.1 Porosity	3
2.1.2 Permeability	3
2.1.3 Saturation.....	3
2.1.4 Surface and interfacial tension (IFT)	4
2.1.5 Contact angle and wettability	4
2.1.6 Capillary pressure.....	6
2.1.7 Relative permeability	8
2.2 Wettability in reservoir rocks.....	11
2.2.1 Measuring wettability	12
2.2.2 Restored state core versus native state core.....	14
2.2.3 The effect of wettability on oil recovery during waterflooding.....	15
2.2.4 Parameters affecting wettability	19
2.3 Summary of literature review	22
3 Review of Frøy studies related to relative permeability and wettability	23
3.1 Frøy introduction	23
3.2 Summary of previous studies related to SCAL analysis on Frøy	24
3.3 Wettability variations in the Frøy field	28
3.4 Summary on wettability trends	32
4 Reservoir simulation	35
4.1 Introduction	35
4.2 Description of the Frøy simulation model	36

4.3 New simulation cases for studying the effect of wettability on the Frøy reservoir performance ...	39
4.4 Introducing more SATNUMs for studying the effect of wettability variation on the reservoir performance	41
4.5 Simulation results	42
4.5.1 Results from simulation cases using only 1 SATNUM	42
4.5.2 Results from simulation cases using 4 and 6 SATNUMs	45
5 Discussion on the simulation results.....	49
5.1 Simulation cases using only 1 SATNUM	49
5.2 Simulation cases using 4 and 6 SATNUMs	50
5.3 Discussion on the validity of the presented data	52
6 Conclusions	57
7 Nomenclature	59
8 References	61
APPENDICES	67
A APPENDIX A – Key figures and tables regarding SCAL measurements on Frøy.....	69
B APPENDIX B – Data describing the PDO simulation model	75
C APPENDIX C – A modified copy of BO_8_001.DATA.....	77
D APPENDIX D – Simulation results	81

Table of figures

Figure 2.1 – Illustration of the nomenclature used for defining the contact angle (Torsæter and Abtahi 2003)	5
Figure 2.2 – Morrow’s relationship between receding and advancing contact angles as a function of intrinsic contact angle (Valvatne and Blunt 2004)	6
Figure 2.3 – Illustration of the capillary pressure as a function of water saturation (Torsæter and Abtahi 2003)	7
Figure 2.4 – The capillary pressure as a function of the water saturation profile (Holmes 2002)	7
Figure 2.5 – Typical relative permeability curves for a water-wet system	8
Figure 2.6 – The oil relative permeability generated from pore-network simulation is heavily affected by the rock wettability	10
Figure 2.7 – Illustration of the difference between a mixed-wet and fractionally wet system	11
Figure 2.8 – The relation between the Amott-Harvey index and the intrinsic contact angle (Spiteri et al. 2008)	12
Figure 2.9 – Relation between wettability relative permeability	14
Figure 2.10 – Comparison between native core, cleaned core and restored core relative permeabilities	15
Figure 2.11 – Oil recovery versus number of injected pore volumes of water	16
Figure 2.12 – Illustration of displacement processes on a macro scale	17
Figure 2.13 – Illustration of snap-off to the left and illustration of bypassing to the right	18
Figure 2.14 – Cumulative oil production versus number of injected pore volumes of water for different wetting characteristics	18
Figure 2.15 – Typical relationship between water saturation, distance above WOC and wettability	21
Figure 3.1 – Location of Frøy	23
Figure 3.2 – Location of the historical wells	26
Figure 3.3 – A vertical intersection in the E-W direction clearly shows that the 25/5-2 (A-2A) well is in the water zone	26
Figure 3.4 – Vertical E-W intersection through the Frøy field	29
Figure 3.5 – Measured wettability versus depth (TVD MSL)	31
Figure 3.6 – Measured wettability versus permeability (mD)	32
Figure 4.1 – Sequence stratigraphic model for the Sleipner and Hugin formations, showing the six reservoir units (PDO, Det norske 2008)	36
Figure 4.2 – Rs (purple) and saturation pressure (green) both show strong depth gradients (Frøy DG2 report, Det norske 2011)	37
Figure 4.3 – New calculated relative permeability curves	40
Figure 4.4 – Illustration of the division of the reservoir into 4 SATNUMs	42
Figure 4.5 – Illustration of the division of the reservoir into 6 SATNUMs	42
Figure 4.6 – Field performance as a function of wettability, 1 SATNUM region	43
Figure 4.7 – Comparison of simulation cases and historic performance, 1 SATNUM region SATNUM region	44
Figure 4.8 – Cumulative oil production as a function of wettability (figure split in two for readability) ...	45

Figure 4.9 – Field performance as a function of wettability variations using 4 and 6 SATNUMs compared to LC and SWW using 1 SATNUM.....	46
Figure 5.1 – The relation between the parameters alpha and beta and the intrinsic contact angle (Spiteri et al. 2008).....	54
Figure A.1 – Recommendations for Well 25/5-A1, Swi = 0.2 (ResLab Integration 2008).....	69
Figure A.2 – Recommendations for Well 25/5-A7, Swi = 0.2 (ResLab Integration 2008).....	70
Figure A.3 – Recommendations for Well 25/5-1, Swi = 0.2 (ResLab Integration 2008).....	71
Figure A.4 – Relative permeability curves generated by pore scale models (Numerical Rocks 2009).....	72
Figure A.5 – Relative permeability curves for wettability sensitivity study (Numerical Rocks 2009).....	73
Figure A.6 – Well correlations (Frøy PDO, Det norske) 2008).....	74
Figure B.1 – Relative permeability curves used by Det norske for the Frøy field.....	76
Figure B.2 – Capillary pressure curve used by Det norske for the Frøy field.....	76
Figure D.1 – Performance of A1 as a function of wettability, 1 SATNUM region.....	81
Figure D.2 – Comparison of simulation cases and historic performance of A1, 1 SATNUM region SATNUM region.....	82
Figure D.3 – Performance of A4 as a function of wettability, 1 SATNUM region.....	83
Figure D.4– Comparison of simulation cases and historic performance of A4, 1 SATNUM region SATNUM region.....	84
Figure D.5 – Performance of A5 as a function of wettability, 1 SATNUM region.....	85
Figure D.6 – Comparison of simulation cases and historic performance of A5, 1 SATNUM region SATNUM region.....	86
Figure D.7 – Performance of A6 as a function of wettability, 1 SATNUM region.....	87
Figure D.8 – Comparison of simulation cases and historic performance A6, 1 SATNUM region SATNUM region.....	88
Figure D.9 – Performance of A7 as a function of wettability, 1 SATNUM region.....	89
Figure D.10 – Comparison of simulation cases and historic performance of A7, 1 SATNUM region SATNUM region.....	90
Figure D.11 – Performance of A8 as a function of wettability, 1 SATNUM region.....	91
Figure D.12 – Comparison of simulation cases and historic performance of A8, 1 SATNUM region SATNUM region.....	92
Figure D.13 – Performance of A1 as a function of wettability variations, 4 SATNUMs regions.....	93
Figure D.14 – Performance of A1 as a function of wettability variations, 6 SATNUMs regions.....	94
Figure D.15 – Performance of A7 as a function of wettability variations, 6 SATNUMs regions.....	95
Figure D.16 – Field performance, comparing the SWW and LC cases with simulation cases including aquifer and fault transmissibility factors.....	96
Figure D.17 – Field performance, comparing the SWW and LC cases with simulation cases using the SWL initialization method (PC = 0).....	97
Figure D.18 – Field performance, comparing the SWW and LC cases with simulation cases including Spiteri et al.'s trapping model.....	98
Figure D.19 – The reservoir pressure has dropped below the bubble point pressure at the top of the horst structure at the end of the simulation period.....	99

List of tables

Table 2.1 – Relation between the wetting index, contact angle and wetting condition.....	5
Table 2.2 – Recommended values of Corey parameters for different wetting characteristics.....	9
Table 3.1 – Wettability measurements performed by Geco Petroleum Laboratory (1988)	24
Table 3.2 – Recommended Corey parameters and saturation end points (ResLab 2007)	25
Table 3.3 – Wettability measurements performed by Weatherford Laboratories (August 2009).....	28
Table 3.4 – Core properties, Geco (1988)	29
Table 3.5 – Core properties, Weatherford (2009)	30
Table 3.6 – Core properties, Selboe (2010)	30
Table 3.7 – Properties of the cores.....	31
Table 4.1 – Relationship between geological formation, reservoir unit and simulation layer gradients (Frøy DG2 report, Det norske 2011)	37
Table 4.2 – Grid properties in the simulation model.....	37
Table 4.3 – End points and Corey parameters for calculation of new relative permeability curves.....	40
Table 4.4 – Saturation end points used in the new simulation cases.....	41
Table 5.1 – Thickness of SATNUM 2, LC.....	50
Table 5.2 – Thickness of SATNUM 2, SWW.....	51
Table 5.3 – Thickness of the reservoir zone above SATNUM 2, LC.....	51
Table 5.4 – Thickness of the reservoir zone above SATNUM 2, SWW.....	51
Table 5.5 – Values of alpha and beta for the different sets of relative permeability curves	55
Table A.1 – Recommendations for Well 25/5-A1, $S_{wi} = 0.2$ (ResLab Integration 2008)	69
Table A.2 – Recommendations for Well 25/5-A7, $S_{wi} = 0.2$ (ResLab Integration 2008)	70
Table A.3 – Recommendations for Well 25/5-1, $S_{wi} = 0.2$ (ResLab Integration 2008).....	71
Table A.4 – Simulated drainage data (Numerical Rocks 2009)	72
Table A.5 – Simulated waterflood data (Numerical Rocks 2009)	72
Table A.6 – Input data for wettability sensitivity study (Numerical Rocks 2009).....	73
Table A.7 – Endpoints and optimized LET-parameters for simulated relative permeability curves (Numerical Rocks 2009)	73
Table B.1 – Oil-water saturation function table used by Det norske (table split in two)	75

1 Introduction

Det norske oljeselskap ASA has a 50 % ownership and is the current operator on the North Sea oil field Frøy. A plan for development and operation (PDO) was delivered in 2008. Questions regarding how the geochemistry will affect the productivity of the reservoir were raised by the Norwegian Petroleum Directorate (NPD), and based on this Det norske initiated several studies. One of the topics in these studies is the wettability. Det norske gave the author of this thesis the following objectives:

The main objective is to find out if the relative permeability curves that are currently used in the simulation model are adequate to model the Frøy wettability.

1. Systematize the currently available SCAL data on Frøy which are related to relative permeability and wettability.
2. Based on objective 1, investigate if it is possible to establish wettability trends which can relate the Frøy wettability to e.g. distance above the water-oil contact, geological facies (mineralogy) or other reservoir parameters.
3. If trends can be established:
 - a. Implement the trends into the reservoir simulation model.
 - b. Compare the results from the new simulation model with historical production data.
4. If trends cannot be established because of lack of data, give recommendations for further work on this topic.

In this master's thesis the Frøy wettability and its effect on the productivity will be investigated by reviewing the available reports on wettability and by running reservoir simulations using the Schlumberger programs Eclipse and Petrel. The thesis is divided into six chapters and the outline is as follows:

- Chapter 1 is the introduction. This chapter defines the main objectives of the thesis.
- Chapter 2 is a general literature review on reservoir parameters with a special focus on wettability in reservoir rocks.
- Chapter 3 reviews the SCAL reports currently available on Frøy, fulfilling objective 1 and 2.
- Chapter 4 is the reservoir simulation part. Simulation cases are defined and run. The key results are presented.
- Chapter 5 is a discussion of the results presented in Chapter 4.
- The conclusions of this master's thesis are given in Chapter 6.

2 Literature review

2.1 Reservoir parameters

The text presented in this subchapter is a modified copy of a subchapter in the Specialization Project (Tangen, 2011), written by the same author as for this master's thesis.

2.1.1 Porosity

Porosity is a measure of the storage capacity of a reservoir and is defined as the ratio of the pore volume to bulk volume (Torsæter and Abtahi 2003).

$$\phi = \frac{\text{pore volume}}{\text{bulk volume}} = \frac{\text{bulk volume} - \text{grain volume}}{\text{bulk volume}} \quad (2.1)$$

We distinguish between total (absolute) porosity and the effective porosity. The total porosity is the ratio of all the pore spaces in the rock to the bulk volume of the rock, while the effective porosity ϕ_e is the ratio of the interconnected pore space to the bulk volume of the rock. The porosity is given as a fraction or as a percent.

2.1.2 Permeability

Permeability is a measure of a porous media's ability to transmit fluids (Torsæter and Abtahi 2003). Together with porosity, permeability is one of the most important rock properties, and it depends among other things on the porosity and the grain size distribution. When more than one fluid is present in a porous medium, the permeability of a given fluid is called the effective permeability of that fluid. Permeability is usually given in millidarcies.

2.1.3 Saturation

For a given porous rock, fluid saturation is defined as the ratio of the volume of the fluid to the pore volume of the rock (Torsæter and Abtahi 2003). In a water, oil and gas system, the respective saturations are defined as

$$S_w = \frac{V_w}{V_p}, \quad S_o = \frac{V_o}{V_p}, \quad S_g = \frac{V_g}{V_p} \quad (2.2)$$

Where V_w , V_o , V_g and V_p are water, oil, gas and pore volumes respectively.

$$S_w + S_o + S_g = 1 \quad (2.3)$$

If the pore volume is referred to as the interconnected pore volume only, we refer to the saturation as the effective saturation. We can also use a normalized value of the saturation where the irreducible saturations are subtracted from the bulk saturations. Saturation is given as a fraction or as a percent.

Connate water saturation is the in situ water which has been present in the sediment since the burial and diagenesis of the rock. The irreducible water saturation S_{wirr} is the lowest water saturation obtainable when a water displacement process is occurring. Increasing the capillary pressure will not reduce the water saturation below S_{wirr} . The residual oil or gas saturation S_{or} or S_{gr} is the ultimate trapped value of oil or gas after the capillary pressure is decreased from a high positive value to a high negative value, and finally, the critical water saturation is defined as the highest water saturation for which the water is immobile.

2.1.4 Surface and interfacial tension (IFT)

Surface tension is the tendency of a liquid to expose a minimum free surface, and it may be defined as the contractile tendency of a liquid surface exposed to gases. The interfacial tension (IFT) is a similar tendency which exists when two immiscible liquids are in contact. Surface and interfacial tension of fluids result from molecular properties occurring at the surface or interface (Torsæter and Abtahi 2003).

Molecules in a given fluid are attracted to each other by an electrostatic force called cohesion. If several fluids are present in a system, cohesive forces also exist between the different fluids. In a water/oil/gas system, the intramolecular forces (within a fluid) are often greater than the intermolecular forces (between two or more fluids), causing the different fluids to be immiscible. In such systems, the area of the contact surfaces is minimized. If a solid is introduced to the system, the molecules are attracted to the solid by an electrostatic force called adhesion (Zolotukhin and Ursin 2000).

2.1.5 Contact angle and wettability

When a liquid comes in contact with a solid surface, the liquid either spreads out on the surface or forms drops on the surface (Torsæter and Abtahi 2003). If the liquid spreads out, we say that the liquid is wetting the surface, while in the other case a contact angle $\theta > 0$ will develop between the surface and the drop. If we have more than one fluid present in the system, one of the fluids (the most adhesive one) has a higher tendency of wetting the surface than the other fluids. We call this fluid the wetting phase and a measure of how much the fluid is wetting can be determined by the contact angle. This angle reflects the equilibrium between the fluids' interfacial tension and the fluids' individual adhesive attraction to the solid (Zolotukhin and Ursin 2000). In some cases the different fluids can have equal affinity to the solid surface. We call this a neutral system. The process of decreasing the wetting phase saturation is defined as drainage. The opposite, increasing the wetting phase saturation is defined as imbibition.

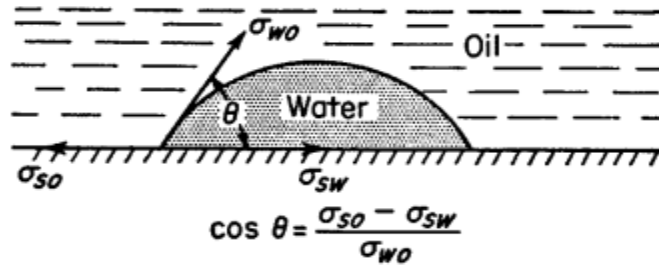


Figure 2.1 – Illustration of the nomenclature used for defining the contact angle (Torsæter and Abtahi 2003)

In figure 2.1, σ_{so} , σ_{sw} and σ_{wo} are the interfacial tensions between the solid and oil, solid and water and water and oil, respectively. Torsæter and Abtahi (2003) give the following table that relates the contact angle to the wettability.

Wetting Index $\cos\theta$	Contact angle θ	Wetting condition
1.0	0°	completely water wetted
0	90°	neutral system
-1.0	180°	completely oil wetted

Table 2.1 – Relation between the wetting index, contact angle and wetting condition

When more than 50 % of the rock surface is wet by water in a water/oil/rock system, the rock is considered water-wet (Donaldson and Alam 2008). The smallest pores and crevices are fully saturated with water, and the water also coats the grains in bigger pores as surface films, surrounding the oil that exists as droplets in the center of the pore bodies. The oil can exist as globules, which means that oil can be connected between two or more pores, but the oil is not a continuous phase unless the water saturation is very low. In a water-wet system the water will exist as a continuous phase and wets the surfaces even if we reduce the saturation to the irreducible water saturation. Another core of the same reservoir rock that is 100 % water-filled will not spontaneously imbibe oil (Donaldson and Alam 2008). For an oil-wet rock the roles of water and oil is the opposite compared to the water-wet case. Oil fills the smallest pores and crevices and coats the surfaces of the grains, while the water exists in the center of the pore bodies. The behavior of oil for an oil-wet core is the same as for water in a water-wet core described above.

We can divide the contact angle into an advancing contact angle θ_A and a receding contact angle θ_R . Because of surface roughness, the advancing contact angle (which is measured during increase in wetting phase saturation) is typically found to be significantly larger than the receding contact angle

(reduction in wetting phase saturation) (Valvatne and Blunt 2004). The phenomenon that the contact angle during drainage is different than the contact angle during imbibition is called contact angle hysteresis. In 1975, Morrow introduced the intrinsic contact angle which gives the relationship between the advancing and receding contact angles.

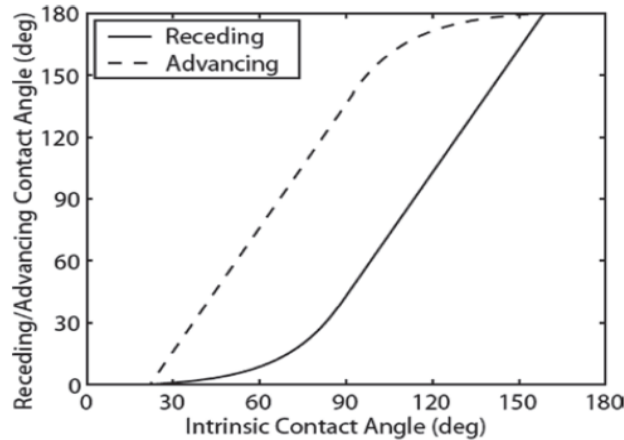


Figure 2.2 – Morrow’s relationship between receding and advancing contact angles as a function of intrinsic contact angle (Valvatne and Blunt 2004)

2.1.6 Capillary pressure

The pressure difference across the interface of two immiscible fluids in a porous medium is called the capillary pressure (Torsæter and Abtahi 2003), and is defined as the following:

$$P_c = P_{\text{non-wetting}} - P_{\text{wetting}} \quad (2.4)$$

The pressure difference comes from the difference in the cohesive and adhesive forces acting on the fluids (Zolotukhin and Ursin 2000). During a drainage process, the capillary pressure will increase, while during an imbibition process the capillary pressure will decrease. We often give the capillary pressure as a function of water saturation, but it is also dependent of the interfacial tensions, the contact angle, porosity and permeability.

In figure 2.3 we see that the capillary pressure curve also is dependent on the saturation direction (imbibition or drainage). If we have a flow reversal, the capillary pressure curve will not retrace its own path. This phenomenon is called capillary pressure hysteresis and is among other things caused by hysteresis in the contact angle. Figure 2.4 shows the capillary pressure as a function of the saturation profile of the reservoir. The free water level (FWL) is where the capillary pressure of water and oil equals zero. The water-oil contact (WOC) occurs where the capillary pressure equals the pore entry (threshold) pressure. During primary oil migration into the reservoir, the capillary pressure must be equal to or higher than the threshold pressure for oil to be able to enter the pore and displace the water

(Donaldson and Alam 2008). In the vertical saturation profile, the water saturation will be highest close to the WOC and it will decrease with increasing distance above the WOC until it at some elevation level reaches the irreducible water saturation. At this level, the capillary pressure is at its highest. The depth interval from the FWL to the zone where $S_w = S_{wi}$ is known as the transition zone. Usually both the oil and water is mobile in this zone and it can vary between a few meter in thickness up to several hundred meters (Jackson et al. 2005).

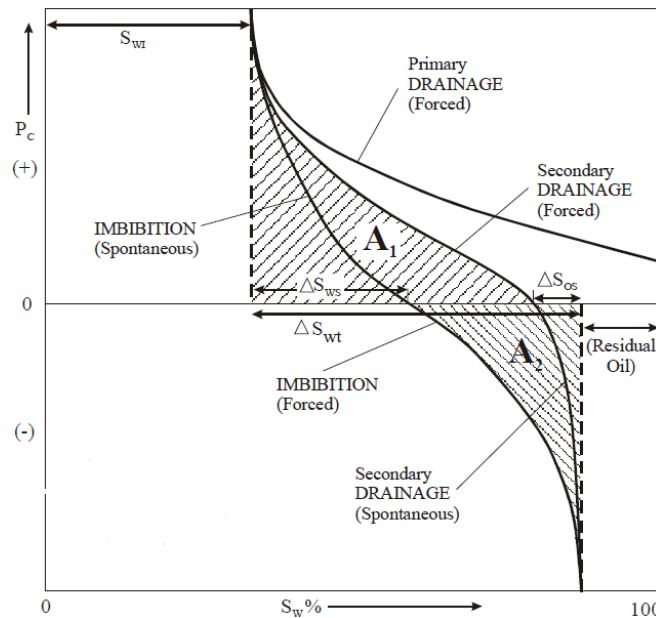


Figure 2.3 – Illustration of the capillary pressure as a function of water saturation (Torsæter and Abtahi 2003)

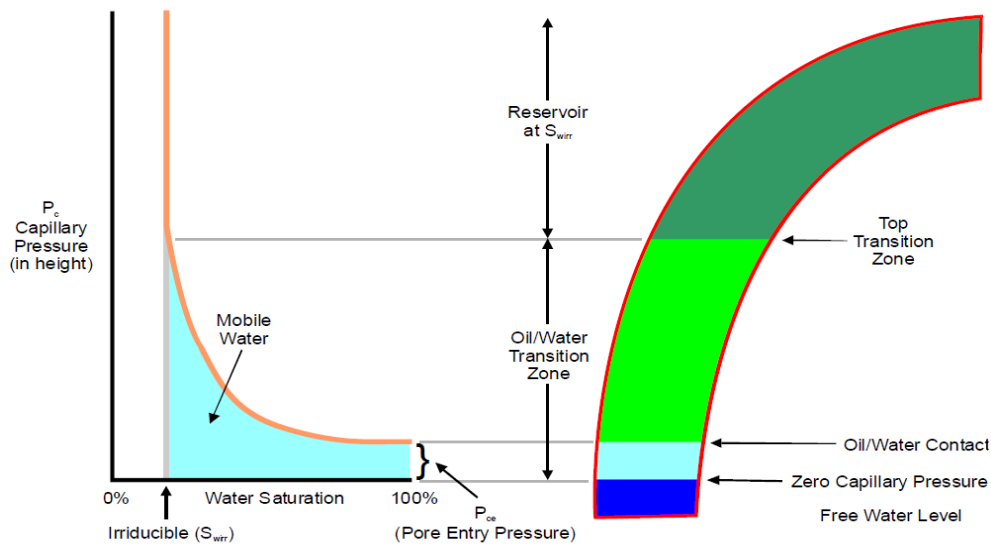


Figure 2.4 – The capillary pressure as a function of the water saturation profile (Holmes 2002)

2.1.7 Relative permeability

The relative permeability of a phase is defined as the ratio of the effective permeability of the phase in interest, to the absolute or total permeability (Torsæter and Abtahi 2003). For example, the relative permeability to oil is defined as

$$k_{ro} = \frac{k_o}{k} \quad (2.5)$$

Relative permeability is often plotted as a function of saturation, but it is also strongly dependent on the saturation history, wettability and pore geometry.

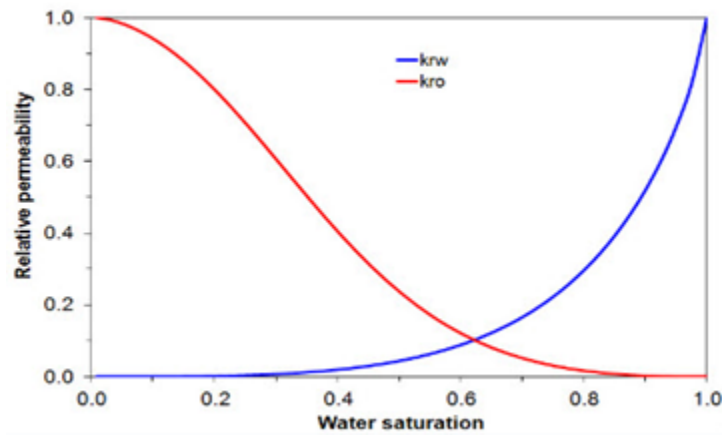


Figure 2.5 – Typical relative permeability curves for a water-wet system

If relative permeability is measured in the lab, one will obtain the endpoints of the relative permeability curves and some data points in between. Perhaps the most standard procedure in the industry is to interpolate between the data points to obtain the complete curves by using the modified Brooks and Corey model (Goda and Behrenbruch 2004)

$$k_{ro} = k_{ro}(\text{at endpoint}) \cdot \left(\frac{1 - S_w - S_{or}}{1 - S_{wirr} - S_{or}} \right)^{n_o} \quad (2.6)$$

$$k_{rw} = k_{rw}(\text{at endpoint}) \cdot \left(\frac{S_w - S_{wirr}}{1 - S_{wirr} - S_{or}} \right)^{n_w} \quad (2.7)$$

where n_o is called the Corey exponent for oil and n_w is the Corey exponent for water. The Corey exponents are changed until we get a good match with the experimental data. Goda and Behrenbruch (2004) suggest the following Corey parameters for different wetting characteristics:

Wetting Conditions	n_o	n_w
Oil Wet (OW)	6 - 8	2 - 3
Slightly Oil Wet (SOW)	2 - 6	2 - 4
Slightly Water Wet (SWW)	2 - 6	4 - 6
Water Wet (WW)	2 - 4	6 - 8

Table 2.2 – Recommended values of Corey parameters for different wetting characteristics

Another model that is increasing in popularity is the LET model (Lomeland, Ebeltoft and Thomas 2005) which is an improvement of the modified Brooks and Corey model. The LET model is proved to give better fits with SCAL-data because the model uses three shape factors instead of one.

$$k_{ro} = \frac{(1-S_w)^{L_o}}{(1-S_w)^{L_o} + E_o S_w^{T_o}} \quad (2.8)$$

$$k_{rw} = \frac{k_{rw}(\text{at endpoint}) S_w^{L_w}}{S_w^{L_w} + E_w (1-S_w)^{T_w}} \quad (2.9)$$

where L_o , E_o , T_o and L_w , E_w , T_w are the shape factors for the oil and water relative permeability curves respectively, and S_w is a normalized value of water saturation.

Geffen et al. (1951) were the first ones to report that there can be a big difference between the observed (measured) drainage and imbibition relative permeability (relative permeability hysteresis). When water is the wetting phase and no gas is present, we observe the biggest difference in the oil phase (Land 1968; Killough 1976; Carlson 1981), but also the water phase display hysteresis. The water phase hysteresis is so small that the assumption of a reversible water phase relative permeability is not too restrictive (Killough 1976).

It is important to include hysteresis in the saturation functions in simulation models. Killough reports that the simulation results obtained when including hysteresis are significantly different from results of “conventional” simulations. He specifically mentions that hysteresis should be included in water-coning simulations, gas cap shrinkage simulations and simulations of waterflooding in the presence of free gas saturation. Today, water alternating gas (WAG) injection is frequently used for improving oil recovery. During WAG injection, we will alternate between drainage and imbibition. When simulating a reservoir where WAG injection is used, it is crucial that hysteresis is included to predict recoveries accurately. Carlson (1981) reports that when using drainage data instead of imbibition data in a gas reservoir with a strong water drive, the predicted recoveries can be twice the amount actually observed.

Data provided by Numerical Rocks, generated by pore-scale simulation models, show that the relative permeability is heavily affected by the wettability of the rock. The main reason why we have hysteresis

in the relative permeability for the nonwetting phase is that during imbibition, some of the nonwetting phase gets trapped (Geffen et al. 1951). This also affects the capillary pressure (Land 1968). Hence, in order to understand relative permeability hysteresis it is important to investigate the governing trapping mechanisms during fluid displacement.

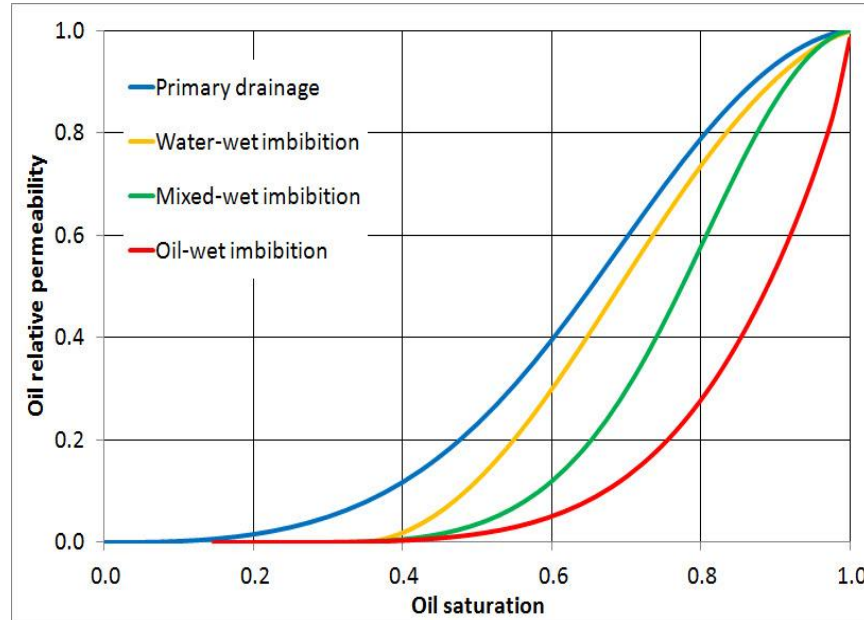


Figure 2.6 – The oil relative permeability generated from pore-network simulation is heavily affected by the rock wettability

In figure 2.6, one should notice that the curvature of the imbibition (waterflood) curve increases when the wettability goes toward more oil-wet. When reproducing these curves numerically with the Corey model, the high curvature is accounted for by using a high value of the Corey exponent for oil. We can also see that for an oil-wetted system, the oil relative permeability is extremely low for high water saturations and that the theoretical residual oil saturation is very low. The industry often refers to oil-wet relative permeability curves as “creeping” curves because of their shapes. It is important to emphasize that the curves in figure 2.6 are synthetic curves and may be slightly misleading. In practice the residual oil for oil-wet rocks will be higher and strongly dependent on number of injected pore volumes of water. The relationship between relative permeability and wettability will be discussed in more detail in a later section.

2.2 Wettability in reservoir rocks

Wettability is the parameter that will be focused on the most in this paper. It is the most important parameter regarding the rate of oil recovery from a porous media (Donaldson and Alam 2008). The wettability controls the displacement and trapping mechanisms in the reservoir. This will affect the endpoints and shapes of the relative permeability and capillary pressure curves and the saturation distribution of the different fluids after waterflooding. In other words, wettability directly affects how much oil we can recover from the reservoir with waterflooding and how the remaining oil will be distributed throughout the reservoir.

Many papers have been published over the last sixty years, describing the wettability characteristics in reservoir rocks. In the earliest papers, even though some authors argued that heterogeneous wettability was normal, the standard was to assume that the wetting characteristic was uniform throughout the reservoir (Agbalaka et al. 2008). It was also common practice to assume that the rock was very strongly water-wet (Morrow 1990). The reservoir rock is initially completely water-filled. When oil starts migrating into the reservoir, the early authors assumed that the oil would fill the center of the greatest pores, but a thick water film would separate the oil from the grain surfaces. The fact that core experiments showed that other wettability states than strongly water-wet can occur was often explained by damage of the core during core recovery (Morrow 1990). But further investigations led to the current understanding, that most reservoir rocks are not strongly water-wet and that heterogeneous wettability is the normal condition in oil reservoirs (Agbalaka et al. 2008).

For uniformly-wet media, the rock can be water-wet, intermediate-wet or oil-wet, depending on the contact angle. Terms like strongly- or very strongly water-wet and weakly-oil-wet and so on has also been used loosely in the literature, but these terms do not have a clear definition and is quite subjective from author to author. In the case of non-uniformly wetted reservoirs, there are two systems that are of interest. Brown and Fatt (1956) introduced the term fractionally-wet, while Salathiel (1973) introduced the term mixed-wet. Dixit (1999) has the following definitions of fractionally-wet and mixed-wet: In a mixed-wet system the *largest* pores containing oil after primary drainage becomes oil-wet and the smaller pores and crevices remain water-wet while for a fractionally wet system, a certain fraction of the pores containing oil *randomly* becomes oil-wet. The main difference is that the oil is a continuous phase in a mixed-wet system. This is not the case for a fractionally-wet system where the oil-wet pores are scattered (Donaldson and Alam 2008).

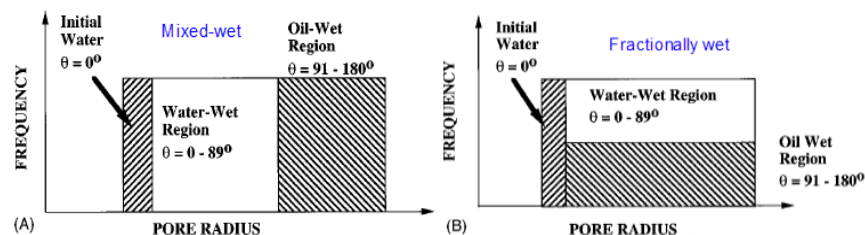


Figure 2.7 – Illustration of the difference between a mixed-wet and fractionally wet system

2.2.1 Measuring wettability

The contact angle is as mentioned a direct measurement of wettability. Popular methods are the Sessile Drop method and the Modified Sessile Drop method (Ghedan et al. 2010). In these methods, a drop of oil is placed on top of a flat, polished mineral crystal plate (Sessile Drop) or between two moveable, flat, polished crystal plates (Modified Sessile Drop). The plates are aged with formation brine to reproduce the reservoir wettability. There is a big difference between a heterogeneous reservoir rock and a flat, polished surface, which means that the validity of these methods is questionable.

Amott (1959) suggested a method of relating the wettability to the displaced volumes during a centrifuge test which is widely used in the industry. First, water is displaced by oil in a centrifuge or by the use of a high flowing pressure gradient until we reach the irreducible water saturation of the core. Then the core is immersed in water such that water will be imbibed spontaneously. The volume of spontaneously imbibed water $S_{w,sp}$ will be measured. The water saturation is further increased by forced displacement of oil by water. The wettability index to water is given as the ratio of the volume of the spontaneously imbibed water, to the total increase in water saturation after spontaneous and forced imbibition.

$$WI_{w,Amott} = I_w = \frac{S_{w,sp}}{\Delta S_w} = \frac{S_{w,sp}}{S_{w,sp} + S_{w,f}} \quad (2.10)$$

Then the core can be immersed in oil such that a similar experiment can be done to obtain the wettability index to oil. The values of the indices range between zero and unity. The closer I_w is to 1, the more water-wet the core is. Similarly, the closer I_o is to 1, the more oil-wet the core is. Often the wettability is given by the Amott-Harvey index, I_{wo} which is the difference between the wettability index to water and the wettability index to oil. The Amott-Harvey index ranges between -1 (strongly oil-wet) and 1 (strongly water-wet). Spiteri et al. (2008) provides a correlation between the intrinsic contact angle (introduced by Morrow) and the Amott-Harvey index.

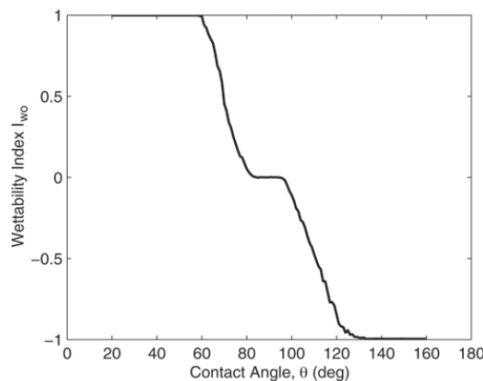


Figure 2.8 – The relation between the Amott-Harvey index and the intrinsic contact angle (Spiteri et al. 2008)

Donaldson et al. (1969) presented the USBM method which also is a popular method in the industry as a measure of wettability. Drainage and imbibition capillary pressure is measured during displacement processes similar to the ones in the Amott method. The USBM wettability index is defined by the following equation

$$WI_{\text{USBM}} = \log\left(\frac{A_1}{A_2}\right) \quad (2.11)$$

Where A_1 is the area under the secondary drainage curve (drainage from residual oil) and A_2 is the area under the negative imbibition curve (figure 2.3). The USBM index ranges between -1 (strongly oil-wet) and 1 (strongly water-wet), which is the same scale as for the Amott-Harvey index. Weaknesses of the Amott and USBM methods are that the Amott test is unable to distinguish important degrees of water-wetness and the USBM test is unable to recognize strongly oil-wet and strongly water-wet systems (Yildiz 2010). The Amott test is insensitive near neutral wettability and the USBM method cannot see the difference between mixed-wet and fractionally wet reservoirs (Ghedan 2011). The Amott test, USBM test and measurements of the contact angle are quantitative methods of measuring wettability. Another quantitative method is Thin Layer Wicking (Yildiz 2010). More qualitative methods of measuring wettability includes imbibition rate tests, nuclear magnetic resonance (NMR) tests, reservoir logs and microscopic examination (Yildiz 2010), but will not be discussed here.

Owens and Archer (1971) showed how the wetting state affects the relative permeability curves for Berea and Torpedo sandstones. The shape and endpoints of the relative permeability curves can also be used as a qualitative measurement of the wettability. They conclude that oil relative permeability decreases and water relative permeability increases when the wettability goes from water-wet to oil-wet. This is in agreement with the data given by Numerical Rocks in figure 2.6. Craig (1971) give the following rule of thumb, known as Craig's rule: For water-wet systems the connate water saturation is usually greater than 20-25 % of the pore volume. The saturation at which the oil and water relative permeabilities are equal is usually greater than 50 % water saturation, and the relative permeability to water at maximum water saturation is generally less than 30 %. For oil-wet systems the connate water saturation is generally less than 15 % of the pore volume and frequently less than 10 %. The saturation at which the relative permeabilities are equal is usually less than 50 % water saturation, and the relative permeability to water at maximum water saturation is greater than 50 % and approaching 100 %. Figure 2.9, taken from Donaldson and Alam (2008) shows the water and oil relative permeability for sandstones with different wettabilities. We can see that with increasing oil-wetness, the water relative permeability for maximum water saturation increases, and the curvature (Corey parameter) for oil relative permeability increases.

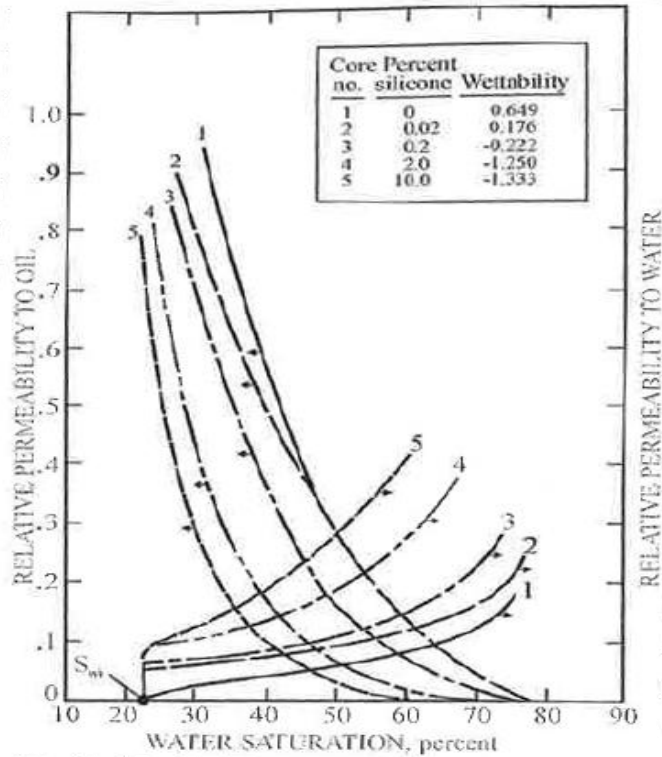


Figure 2.9 – Relation between wettability relative permeability

2.2.2 Restored state core versus native state core

When taking core samples from the reservoir, the core wettability will be more or less altered. Both the drilling mud, which contaminates the core, and the changes in temperature and pressure when the core is brought to the surface will induce wettability changes in the core. If one suspects that the wettability has been altered, the wettability must be restored in order to get reliable results during flow experiments. First, the core plug must be cleaned in order to remove the wettability-altering components. Polar compounds and precipitated asphaltenes are removed since there is no way of knowing if these components are native to the core, or if they occurred after exposure of ambient pressure and temperature (Wendel et al. 1987). Cleaning procedures, using the solvent toluene and the Soxhlet or Dean-Stark apparatus are described in Torsæter and Abtahi (2003) and will not be discussed here. After cleaning, the cores will be dried in an oven. When the core is dry, water (often synthetic laboratory water) is introduced to the core. Then, some of the water is displaced by oil (crude oil from the field or synthetic laboratory oil) to establish the correct initial water saturation. The use of mineral (laboratory) oil is common because crude oil often precipitate polar compounds at ambient temperature, hence, the experiments must be performed at elevated temperatures when using crude oil. In other cases crude oil is simply not available and mineral oil must be used instead. Sometimes mineral oil is used for establishing initial water saturation because it has a more favorable viscosity than crude oil which makes it easier to displace the water. When the correct initial water saturation is obtained, the mineral oil is displaced with crude oil at elevated temperature (Selboe 2010). The core is

then aged for several days in a heating cabinet to re-establish the in-situ wettability. After this procedure, the core is a so called restored state core.

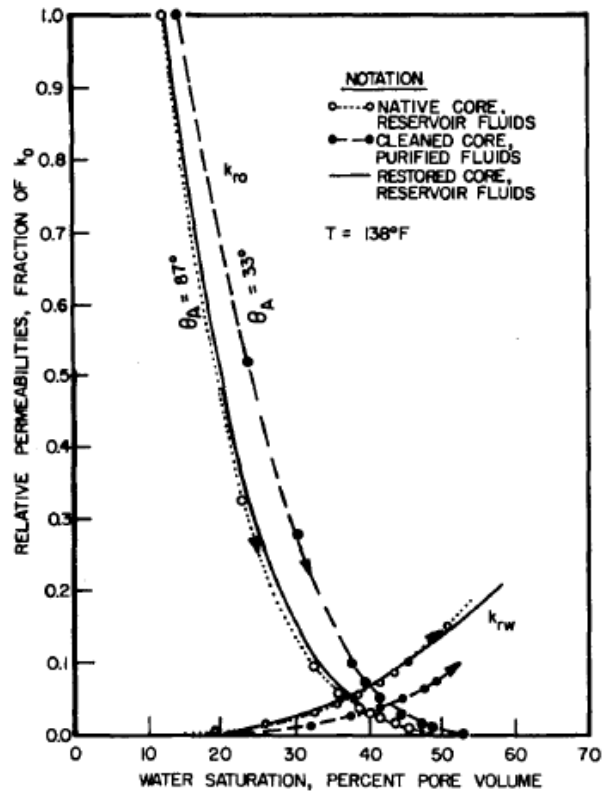


Figure 2.10 – Comparison between native core, cleaned core and restored core relative permeabilities

On the other hand, a native state core is a core where the wettability alterations are minimized. This is obtained by coring with a mud that does not contain surfactants or other chemicals that can alter the wettability and by packaging and storing the cores in a way that preserve the cores (Wendel et al. 1987). Some authors distinguish between cores taken with oil-based mud (“native state cores”) and water-based mud (“fresh state cores”). In this text, cores with unaltered wettability will be referred to as native state cores, regardless of drilling fluid used. Plugs taken from native state well preserved cores, so called seal peels, are in the industry considered to give the most valid results in core flooding experiments. If the drilling mud has not considerably affected the core and the other conditions (pressure and temperature) have been preserved, there is no need to clean the core before performing relative permeability and wettability measurements.

2.2.3 The effect of wettability on oil recovery during waterflooding

Injection of water is the most widely applied secondary recovery process in the world. By injecting water, the oil can be produced without having problems with pressure loss in the reservoir, and the injected water can displace the oil towards the producing wells. However, the oil recovery is affected by

the wettability of the rock. Numerous experiments have been performed in the laboratories and many articles have been published in order to try to understand how wettability affects the oil recovery during waterflooding. A review of some of the literature shows that there has been some disagreement about what the ideal wettability is, but most authors agree that the lowest residual oil is obtained somewhere close to neutral wettability.

Amott (1959) reports that several authors in the 1950's have found that preferentially water-wet systems result in higher waterflood oil recovery than preferentially oil-wet systems and that other authors have found that wettabilities close to neutral give higher recovery than strongly water-wet or strongly oil-wet systems. Amott also found that wettabilities close to neutral give lower residual oil for Ohio sandstones than either extreme on the wettability scale will give. But he emphasizes the fact that since there has not been a generally accepted standard on how to define the wettability scale from strongly water-wet to strongly oil-wet, his results are not necessarily in disagreement with the other authors that found the highest recovery for water-wet cores.

Donaldson et al. (1969) performed waterflood tests on torpedo sandstones. They plotted oil recovery versus number of injected pore volumes of water for different wetting characteristics.

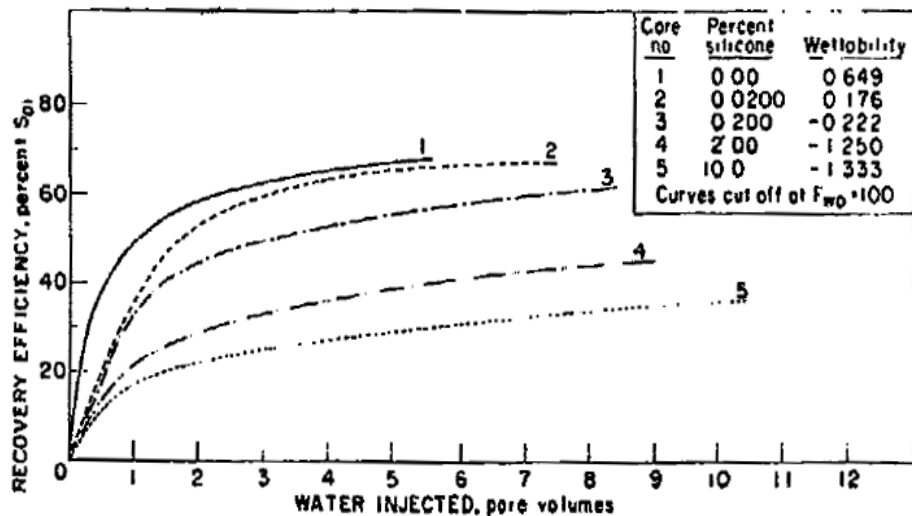


Figure 2.11 – Oil recovery versus number of injected pore volumes of water

As can be seen in the figure, the most efficient recovery is obtained for water-wet rocks (curve 1), while curve 2 shows that with continued waterflooding, the recovery for close to neutral systems (weakly water-wet) can be higher than for water-wet systems. Curve 4 and 5 show that the recovery is low and highly dependent on number of pore volumes injected for oil-wet systems. These findings are in agreement with several other published articles (Owens and Archer 1971; Salathiel 1973; Morrow 1990; Morrow et al. 1994; Jadhunandan and Morrow 1995; Hamon 2000; Donaldson et al. 2008).

To understand why wettability has such a big effect on residual oil saturation, we must take a deeper look at the governing displacement processes for different values of wettability. In every reservoir rock, water is initially filling the pore space and the reservoir is assumed to be completely water wet. As the sediments get buried deeper and deeper, oil starts migrating from the source rock. If we have a cap rock that can act as a seal, oil can start accumulating and an oil field will form. Oil will displace some of the water when it migrates in to the reservoir. This is a drainage process because we are decreasing the wetting phase saturation. Oil will enter the biggest pores first with a piston-like displacement, pushing the water into the crevices and pore throats and the capillary pressure will increase (Spiteri et al. 2008). In some throats and pores the oil will come in contact with the surface of the rock and alter the wettability of the rock.

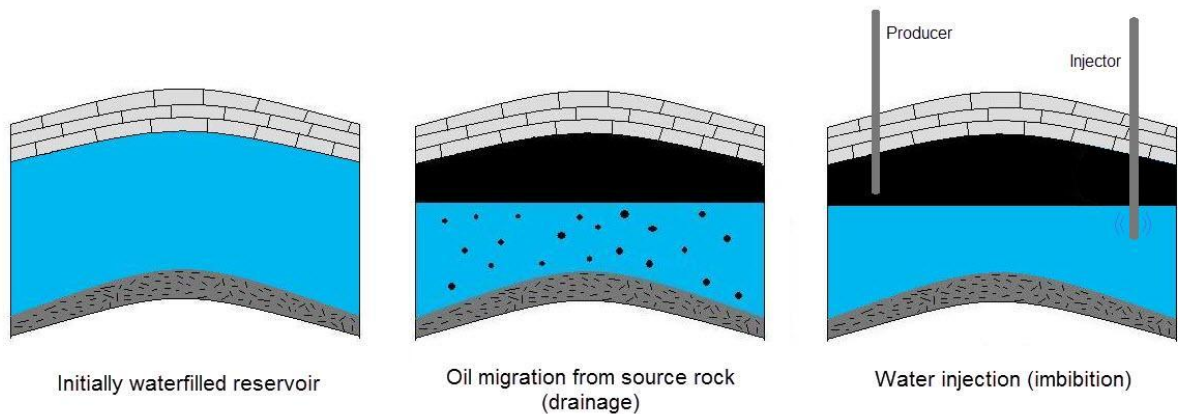


Figure 2.12 – Illustration of displacement processes on a macro scale

During imbibition we can have several oil displacement and trapping mechanisms. Which process that will dominate depends on the wettability characteristic of the rock (Spiteri et al. 2008). In the literature (Lenormand et al. 1983; Valvatne and Blunt 2004) we can read about snap-off, cooperative pore-body filling and bypassing. If the water saturation increases after primary drainage of a water-wet reservoir rock, the water will start filling the smallest pores and pore throats, pushing the oil into the largest pores. Some of the pores that are filled with oil will be snapped off from the other oil-filled pores, leaving the oil in the snapped off pores in a discontinuous immobile state (figure 2.13). The mobile oil is pushed in front of the displacing water towards the producing well and the oil relative permeability is high. Waterflood experiments (Donaldson and Alam 2008) show that water breakthrough occurs at approximately one pore volume of injected water and that almost no oil is produced after breakthrough.

For mixed-wet rocks the smallest pores and crevices will be water-wet, while the bigger pores will be oil-wet. Some oil may become trapped during imbibition because of bypassing. Water creates its own path around big globules of oil, leaving the globules of oil unable to move. Fingers of water move through the water-wet pores reaches the producing well before the oil front, causing the breakthrough to occur earlier than for water-wet rocks. But more oil is produced after breakthrough because of surface film drainage from the continuous oil-wet pores, causing the ultimate recovery to be higher than for water-wet cases (Donaldson and Alam 2008). In some cases gravity segregation can occur in mixed-wet

reservoirs, causing the oil to drain upwards along films of oil in oil-wet pores, resulting in unusually low residual oil saturations (Salathiel 1973).

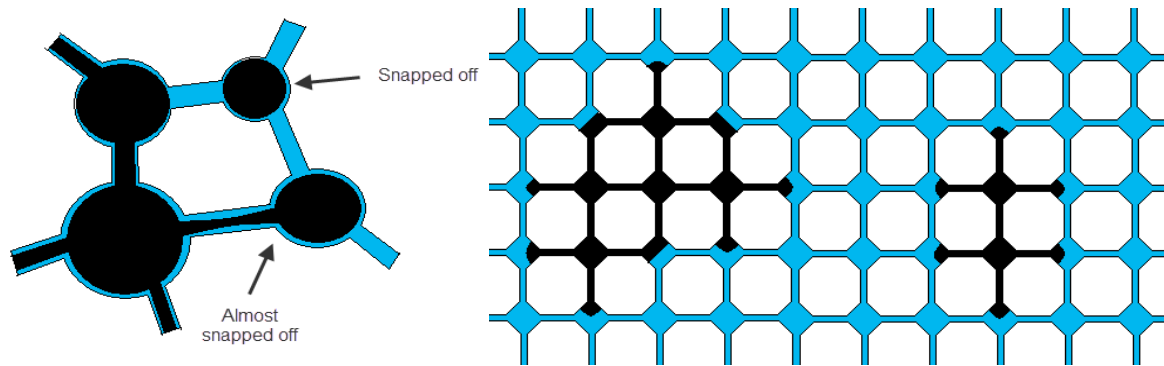


Figure 2.13 – Illustration of snap-off to the left and illustration of bypassing to the right

During imbibition of oil-wet rocks, the oil will fill the corners and crevices of the rock and the water will move through the center of the pore bodies and throats with a piston-like movement. Continuous fingers of water will rapidly reach the producing well and most of the oil will be produced post breakthrough. The relative permeability to oil is low, and the recovery which is strongly dependent on volume of injected water will also be lower than for other wetting states (Donaldson and Alam 2008).

The following simplified figure (taken from Donaldson and Alam 2008) summarizes the current understanding on how wettability affects oil recovery. The least recovery is obtained from oil-wet reservoirs and the highest oil recovery is accomplished when the wettability is close to neutral. Very low residual oil saturations may be reached when surface film drainage proposed by Salathiel (1973) occurs in mixed-wet reservoirs.

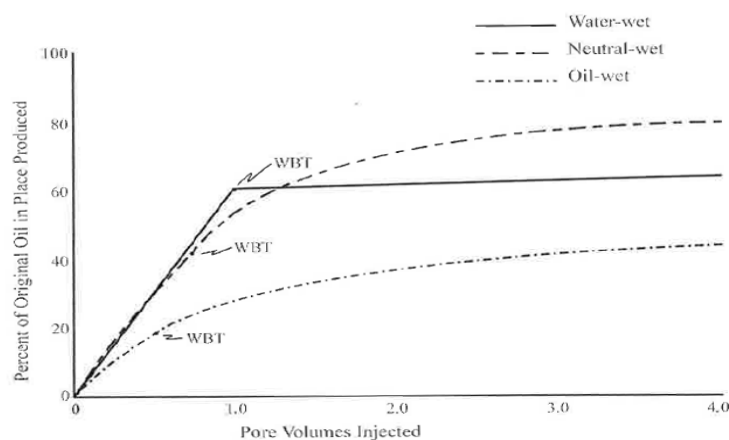


Figure 2.14 – Cumulative oil production versus number of injected pore volumes of water for different wetting characteristics

2.2.4 Parameters affecting wettability

The focus up to this point has been the general definition of wettability, how we can measure wettability, and how wettability affects production and residual oil saturation. Another important aspect is the parameters affecting wettability and the explanation of why some reservoir rocks goes from water-wet to mixed-wet or oil-wet when oil migrates into the reservoir. Wettability is generally considered as a rock property, but there are several parameters affecting the wettability in oil reservoirs. A review of the literature shows that the wettability in reservoir rocks depends on

- Rock mineralogy
- Rock quality (permeability)
- Properties and composition of the oil, including the asphaltene content
- Properties and composition of the formation water, including pH and salinity
- Reservoir conditions (temperature and pressure)
- Saturation and saturation history

In the following, conclusions from several articles that investigate the relation between wettability and other parameters or variables will be presented. It is important to emphasize that wettability is a very complex variable that is still not fully understood. There is still a lot of research going on trying to understand how the wettability affects the productivity of a reservoir, and how wettability itself is affected by other parameters or variables. The presentation of the articles below may give an indication on how wettability depends on other parameters, but one should be aware that the articles do not give definite answers and that the wettability can behave differently under other settings or conditions. Caution should be made when predicting wettability based on other parameters.

Morrow (1990) emphasizes that the wettability depends on the stability of the water film between the oil and the rock. This film is generally much less than 100 nm thick. If the water film becomes unstable, polar compounds from crude oil can adsorb onto the rock and alter the wettability permanently (from water-wet to oil-wet). This suggests that the thickness of the water film is important. One group of polar components in the crude oil that has been studied is the asphaltenes, which are high-molecular-weight colloidal particles suspended in the crude oil (Morrow 1990). By removing the asphaltenes from the crude oil, Morrow observed that the oil did not adsorb onto the rock surface for low values of pH. But the presence of asphaltenes is not a guarantee for wettability alteration, and an increasing content of asphaltenes does not necessarily mean that the rock becomes oil-wet more easily. Buckley et al. (1998) describe the interactions between the crude oil, brine and solid. They emphasize that the extent of asphaltene precipitation depends on the crude oil's ability to act as solvent for its asphaltenes. Poor solvents precipitate more asphaltenes, enhancing the wettability alteration while good solvents can keep the asphaltenes in the oil phase. Some oils that are good solvents at reservoir conditions may experience asphaltenes destabilization during production because of depressurization (Al-Maarmari and Buckley 2003), indicating that the wettability is also dependent on the pressure. In Prudhoe Bay, the asphaltene content increases with depth (Jerauld and Rathmell 1997), but the reservoir rock is also

more water-wet with increasing depth, indicating that the wettability is more dependent on initial water saturation than the asphaltene content.

The properties of the formation water affect wettability in several ways (Buckley et al. 1998). Both the oil and the solid become electrically charged in the presence of water. The polar groups at the surface of the solid or in the oil at the oil-water interface can gain a proton from the brine and become positively charged or give away a proton to the brine and become negatively charged. From basic chemistry we know that the proton concentration (or in other words the H^+ , or more precisely the H_3O^+ concentration) of a fluid is the definition of pH, which means that these interactions affect the pH of the system. When the oil and the solid have the same sign of the electrical charge (both positive or both negative), they repel each other and a stable water film can exist in between, maintaining a water-wet system. If one is positive and the other is negative, attractive electrical forces between the crude oil and solid can destabilize the water film, and asphaltenes can precipitate on the rock, thus altering the wettability. The importance of the pH is given by Morrow (1990) who found that for a given oil, only slight changes in pH at close to neutral conditions can cause a drastic change in adhesion behavior of the oil. Jerauld and Rathmell (1997) found that for reservoir rocks from Prudhoe Bay, low pH resulted in more oil-wet contact angles while pH above 7 gave water-wet tendencies. With all this in mind, it is important to be aware that calcite has a more positive surface charge than quartz and clay minerals have a negative surface. This indicates that the rock mineralogy and the distribution of rock minerals in the reservoir affect the wettability. Jerauld and Rathmell (1997) report that kaolinite clays are often oil-wet in Prudhoe Bay rocks. Ghedan (2010) writes that quartz is extremely water-wet and that sandstones are moderately water-wet, while carbonates tend to be oil-wet.

Jadhunandan and Morrow (1995) performed more than 50 slow-rate waterflood experiments on Berea sandstones and measured wettability. They wanted to identify the dominant variables controlling the wettability in crude oil/brine/rock (COBR) systems. Their study shows that the wettability depends on the aging temperature, initial water saturation and the composition of both the brine and the crude oil. They found that by increasing the initial water saturation, the Amott-Harvey index increases (more water-wet), but by increasing the aging temperature, the wettability index decreased (more oil-wet). For all comparable conditions, aging a core with Moutray oil resulted in a lower wettability index than by aging a core with ST-86 oil, indicating that oil composition affects wettability. The Amott-Harvey index for the core aged with Moutray oil was more sensitive to the calcium ion content of the brine than the Amott-Harvey index for the core aged with ST-86 oil. For Moutray oil, the wettability decreased with increasing calcium ion content. Jadhunandan and Morrow (1995) does not explain why the calcium ion content in the brine affected the wettability, but a possible explanation is that the calcium ions lowered the pH because calcium reacted with the hydroxide ions and formed salts of $Ca(OH)_2$ and therefore reducing the basic component (OH^-) of the brine, resulting in altered wettability. Another possibility is that the positively charged calcium ions can bring a negatively charged oil phase closer to a negatively charged solid, causing the water film to be destabilized.

Hamon (2000) studied experimental results from reservoir cores under reservoir conditions. The core samples covered a large permeability range and were sampled from different heights above the WOC.

The goal of his study was to find trends in the wettability variations throughout the reservoir, focusing on the effect of permeability and structural position of the core. He found that the wettability index to water decreased with increasing height above the WOC. This is in agreement with other authors (Jerauld and Rathmell 1997; Jackson et al. 2005; Donaldson and Alam 2008). There was some scatter in the wettability index for a given height, but it can be explained with difference in rock quality. Hamon found that the higher the permeability, the less water-wet the sample. Jackson et al. (2005) discuss the effect of initial water saturation on wettability, which perhaps is the most important parameter affecting wettability. Several oil fields have a significant transition zone where the lowest oil saturation is found at the base or bottom and the highest oil saturation is found at the top of the transition zone. Because of the high water saturation close to the water water-oil contact, this part of the reservoir usually is water-wet. The water saturation decreases with increasing distance from the WOC, causing the coating water film to be thin and unstable, and polar compounds from the oil can deposit on the rock and alter the wettability. Donaldson and Alam (2008) present the following figure which can summarize the typical relationship between the water saturation, height above the water-oil contact and wettability.

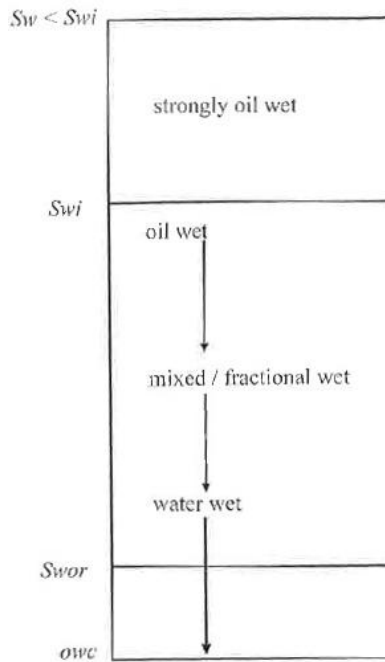


Figure 2.15 – Typical relationship between water saturation, distance above WOC and wettability

The last subject that will be mentioned in this chapter is the altering of wettability during production for enhanced oil recovery (EOR). When we know how the wettability is affected by different parameters, we can use this knowledge to our advantage and alter the wettability to maximize the recovery. One way of altering wettability is by using surfactants. A surfactant is a chemical compound that lowers the interfacial tension between two fluids. Seethepalli et al. (2004) found that anionic (negative ion) surfactants changes oil-wet carbonates to intermediate/water-wet for a West Texas crude oil and also lowers the interfacial tension between the oil and water phases, but field-scale evaluations were not

made. They also report that other authors have found that cationic (positive ion) surfactants can change the wettability towards more water-wet, but these surfactants are expensive. Yu et al. (2008) suggest that injecting seawater gives a higher recovery than injecting formation water in oil-wet carbonates because the sulphate ions in the seawater alter the wettability towards increased water-wetness. They do not mention the possible scaling problems that can occur when seawater and formation water are mixed. An increasingly popular EOR method is the injection of low salinity water which can lead to low residual oil saturations in cases where the reservoir rock is oil-wet because of a high content of clay minerals (Vledder et al. 2010). Bivalent cations like Ca^{2+} and Mg^{2+} can act as a bridge between the negatively charged oil and the negatively charged clay minerals. By injecting low salinity water, the concentration of the cations decreases, and the negatively charged oil and clays will repel each other and the clays will no longer be oil-wet. Vledder et al. (2010) presents the successful wettability alteration by injection of low salinity water in the Omar field in Syria. Roosta et al. (2009) found that when calcite, glass and quartz had undergone wettability alteration by precipitation of asphaltenes, hot steam could reverse the alteration path toward water-wetness by washing out the precipitated asphaltenes from the surfaces. But they also found that mica (clay) changed towards more oil-wet after steam treatment if the mica originally turned oil-wet by the mechanism of polar interactions. This means that in clay rich reservoirs, steam injection can cause the opposite effect than the one intended.

2.3 Summary of literature review

A review of the literature shows that the wettability is a very complex parameter which is dependent on many variables in the reservoir. These include properties of the rock and properties of the oil and brine and the reservoir conditions, suggesting that the wettability is a result of the equilibrium between the forces acting on the solid and the fluids present in the system. Wettability affects the endpoints and shapes of the relative permeability curves and capillary pressure curves, and also the fluid saturation distribution in the reservoir. Several methods, including both quantitative and qualitative methods of measuring wettability have been presented, with a special focus on the Amott and USBM methods. Different wettability characteristics of a reservoir rock leads to different oil displacement mechanisms on a pore-scale level. The wettability also affects the residual oil saturations. The current view is that wettabilities close to neutral gives the lowest residual oil and therefore the highest recovery. Hence, the knowledge of the wettability state of a given reservoir and how it can be altered to lower the residual oil is crucial in enhanced oil recovery projects. Because of its complexity, the wettability is still a variable that is not fully understood, and research is continuously ongoing.

3 Review of Frøy studies related to relative permeability and wettability

3.1 Frøy introduction

The information in this introduction is taken from the Frøy PDO and Frøy PDO Subsurface Support Document (Det norske 2008). The Frøy field is an oil field that was discovered in 1987 by Elf Petroleum Norge AS (now Total) in the North Sea. Frøy is located about 32 km south-east of the Frigg field and 25 km north-east of the Heimdal field in Blocks 25/5 and 25/2. Frøy is now covered by the Production License 364 partnership, where Det norske oljeselskap (operator) and Premier Oil own 50 % each.

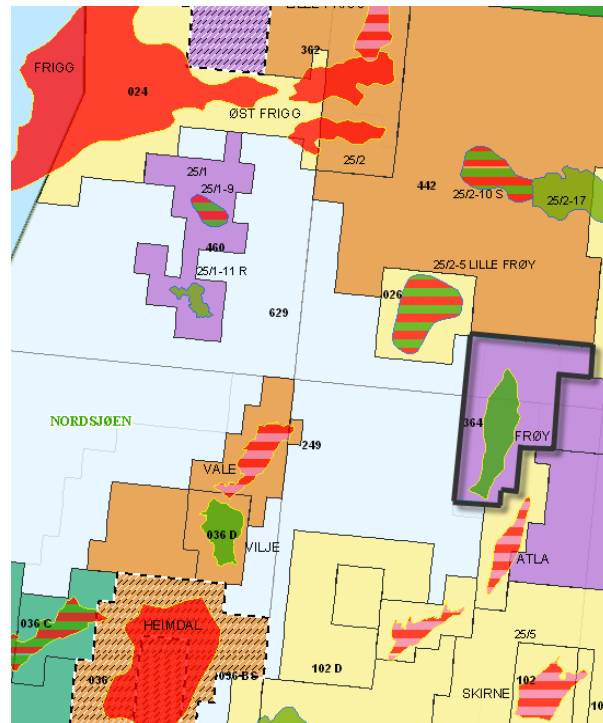


Figure 3.1 – Location of Frøy

Elf developed the field with six production wells and four seawater injection wells. Production started in 1995 and lasted six years. Elf was able to produce 5.9 MSm³ of oil and 1.7 GSm³ of gas before the field was shut down due to technical problems (scaling) and also low oil prices. The entire infrastructure except pipelines and cables was removed before the area was relinquished.

Det norske together with Premier Oil plan to redevelop the field with several producers and injection wells. Water alternating gas (WAG) and simultaneous injection of gas and water (SWAG) are under consideration for enhanced oil recovery. A plan for development and operation (PDO) was submitted to the Ministry of Petroleum and Energy in 2008. In the PDO, the estimated economic recovery was around 7.5 MSm³ of oil. The Frøy redevelopment is currently on hold.

3.2 Summary of previous studies related to SCAL analysis on Frøy

The first measurements of relative permeability and capillary pressure on Frøy were conducted by Elf during the late 80's and early 90's. The reports from Elf are confidential and were not available when writing this thesis. Geco Petroleum Laboratory (1988) performed an experimental program on five core samples from 25/5-1. Both oil-water relative permeability and oil-gas relative permeability were measured with unsteady state experiments. They measured spontaneous and forced imbibition (and drainage) and calculated the displacements ratios. From these ratios it is easy to calculate the Amott-Harvey index. They found the following:

Depth [MD]	I_w	I_o	I_{wo}
2993.12	0.00	0.200	-0.200
2998.18	0.00	0.430	-0.430
3013.15	0.00	0.114	-0.114
3022.1	0.02	0.113	-0.111
3040.33	0.00	0.369	-0.369

Table 3.1 – Wettability measurements performed by Geco Petroleum Laboratory (1988)

The data show that the wettability of the core samples seems to be slightly oil-wet. However, the data are questionable because of the sample preparations before performing the flow experiments. The cores were cleaned with toluene, but there was no attempt of restoring the original wettability by aging the cores with crude oil (cf. figure 2.10). Instead, mineral oil and synthetic brine were introduced to the core immediately after cleaning, and the flow experiments were performed at ambient conditions.

NTNU evaluated the data from Geco in 2006 and ResLab Integration (now Weatherford Petroleum Consultants) further evaluated the data in 2007 to find which experiments that could be used for validation with the numerical simulator Sendra. Sendra is a two-phase core flow simulator specially designed to simulate and verify SCAL experiments. Sendra requires production and differential pressure or injection rates as input and calculates relative permeability curves through an automated history matching approach. The required data were not available for the water-oil experiments in the report from Geco, hence ResLab had to create synthetic data based on the reported relative permeabilities and the assumption of negligible capillary pressure in order to be able to use the Sendra simulator. ResLab's conclusion based on the Sendra simulations was that none of the oil-gas relative permeability experiments could be recommended for further use. They also questioned the water-oil relative permeability data because of the questionable core preparations mentioned above.

However, ResLab presented the results from the water-oil Sendra simulations and gave recommendations for the relative permeability endpoints and Corey parameters. These recommendations are also the values that Det norske chose to use in the PDO (August 2008):

Case	N_o	N_w	S_{or}	$k_{rw}(S_{or})$
High	5.0	1.8	0.05	0.6
Base	5.5	1.3	0.08	0.8
Low	6.0	1.0	0.12	1.0

Table 3.2 – Recommended Corey parameters and saturation end points (ResLab 2007)

The recommended values clearly indicate an oil-wetting system. The Corey parameter is high, the residual oil is very low and the relative permeability of water at maximum water saturation is high (cf. figure 2.9 and Craig's rule)

ResLab Reservoir Laboratories (April 2008) (now Weatherford Laboratories) was engaged by Det norske to provide recommendations for analyses based upon field requirements for submission of PDO. Because of the presence of heavy oil components in the Frøy oil, Reslab came to the conclusion that several experiments, both using native state cores and restored state cores, should be initiated to reduce the uncertainty related to which properties are native to the core, and which properties are observed because of wettability alteration during coring.

Sintef (July 2008) investigated the heavy polar compounds of the Frøy field, but was unable to find out how the compounds influence the wettability on Frøy. They observed polar-rich compounds in the rock extracts from coarse-grained, highly porous and intensely brown stained sandstones. This may relate the asphaltene content, hence wettability, to the staining level of the rock. Sintef recommended that the staining level and its effect on the productivity of the reservoir should be studied further.

The Norwegian Petroleum Directorate (NPD) received the PDO in 2008, but raised questions related to how the geochemistry on Frøy will affect the productivity of the reservoir. Because of these questions, Det norske initiated several studies in 2008 and 2009, involving ResLab Integration, Fugro Geolab Nor, Numerical Rocks and Weatherford Laboratories to increase the understanding of the geochemistry. Stensen and Fjørland (2009) summarized the conclusions from these studies in a report. All these studies deals with wettability and relative permeability issues and are of interest for this thesis and will be presented in the following in chronological order.

To reduce the uncertainty in the water-oil relative permeabilities, Det norske sent eight Elf Aquitaine Production flow experiment reports that cover 25/5-1, 25/5-A1, 25/5-2, 25/5-A4 and 25/5-A7 to ResLab Integration for validation in August 2008. Their work led to the following conclusions:

- 25/5-A1 and 25/5-A7 contained enough data to be verified by the numerical simulator Sendra and was recommended for further use.
- Even though the data from 25/5-1 were not sufficient to be verified by Sendra, it coincided with data from 25/5-A1 and 25/5-A7 and was for this reason recommended for further use.

- The data from 25/5-A4 were too limited and were non-conclusive and were therefore not recommended for further use.
- Data from 25/5-2 showed very water-wet behavior and were therefore not recommended for further use.

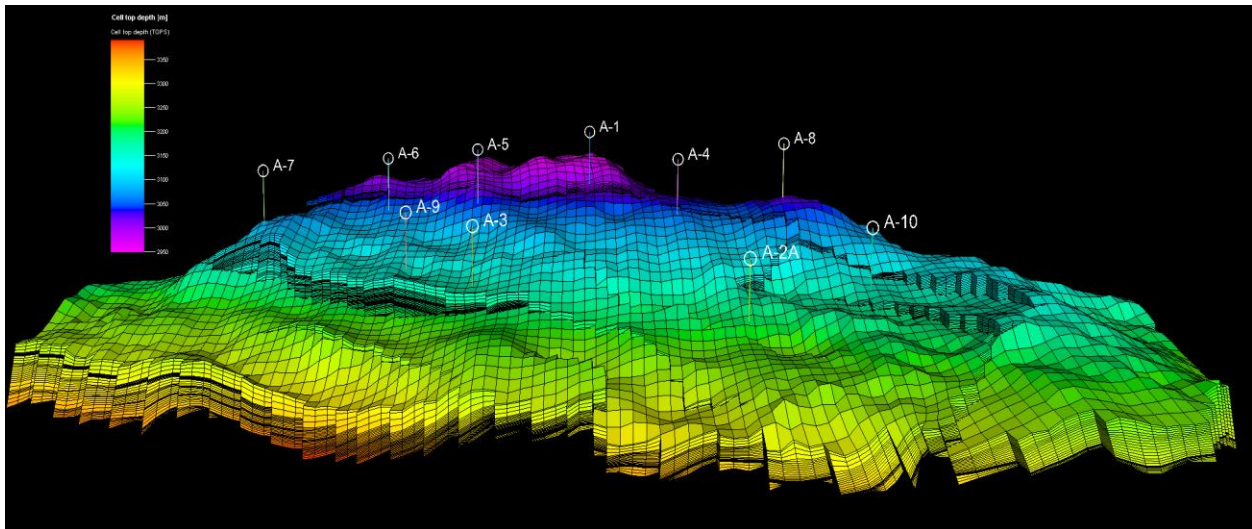


Figure 3.2 – Location of the historical wells

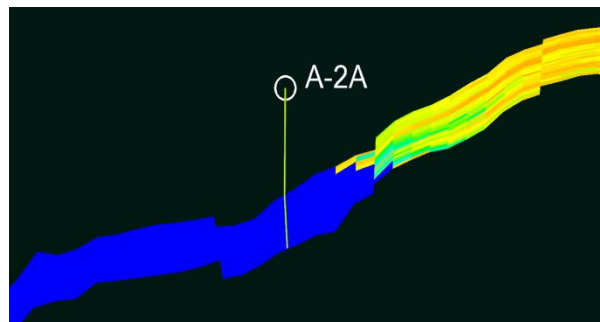


Figure 3.3 – A vertical intersection in the E-W direction clearly shows that the 25/5-2 (A-2A) well is in the water zone

The core preparations made before measuring the relative permeability in these experiments can be summarized with the following, which is a typical restored state procedure:

- Cleaning of the core with miscible solvents like toluene and isopropanol
- Drying in oven at 80 °C
- Saturating the cores with synthetic brine
- The initial water saturation is established by introducing laboratory oil
- Laboratory oil is replaced by crude oil and the cores are aged for 10 days under reservoir pressure and temperature to obtain reservoir wettability

- The crude oil is displaced with laboratory oil before performing relative permeability measurements at ambient conditions

One of the reasons why the crude oil is displaced with laboratory oil is that the crude oil can precipitate asphaltenes when the pressure and temperature is lowered to ambient conditions. ResLab Integration concludes that the aging procedure probably is adequate to mimic the reservoir wettability, but recommends that experiments with original fluids under full reservoir conditions also should be performed, in order to find the “true” wettability of the reservoir, which can be compared to these experiments. Based on their work, ResLab recommended that Sendra verifications should be performed on the relative permeability data from the wells 25/5-1, 25/5-A1 and 25/5-A7. Det norske accepted the recommendations from ResLab.

ResLab Integration (September 2008) ran Sendra simulations for verification of the relative permeability data from the wells 25/5-1, 25/5-A1 and 25/5-A7. Based on the simulations they gave recommendations for the relative permeability endpoints and Corey parameters for each of the wells. These recommendations (which can be seen in Appendix A) are in good agreement with the ones presented in table 3.2.

Fugro Geolab Nor (March 2009) investigated how the heavy hydrocarbons, the polar content and tar mats affect the productivity of the Frøy field, following up the study performed by Sintef in 2008. The heaviest staining was observed in samples from the oil zones where the permeability and initial oil saturation was high. This may indicate that the cores with heavy staining tend to be oil-wet because these are the cores with the lowest water saturation.

Numerical Rocks (April 2009) reconstructed four pore scale models based on thin section images from core plugs from Well 25/5-1 and 25/5-A1 using the relatively new eCore technology. Numerical flow simulations were then performed on the pore scale models to obtain capillary pressure and relative permeability data. The data show neutral-wet to slightly oil-wet behavior (WI_{Amott} from 0 to -0.25). Numerical rocks also performed a sensitivity study of the effect on the relative permeability by changing the wettability index from -0.4 to 0.4. The resulting residual oil saturations were 0.03 and 0.19, respectively. The other results can be seen in Appendix A.

The latest study initiated by Det norske on the geochemistry on Frøy is a wettability study performed by Weatherford Laboratories (August 2009). 55 wax preserved 4 inch whole core samples (seal peels) from 25/5-1, 25/5-A1 and 25/5-A7 were available for testing. Based on CT scanning, Weatherford graded the cores with respect to homogeneity on a scale from 1 to 3, where 3 was acceptable, 2 questionable and 1 unsuitable. They also wanted to select cores that covered a range of permeabilities and a range of staining levels. Based on these criteria, they chose three cores from 25/5-A1 and performed wettability tests. The composition of the formation water on Frøy is unknown, but it is assumed that the known composition of the formation water at the Volve field can be used as an analogue. Synthetic brine with the Volve composition was therefore used in the experiments. No crude oil was available for testing the native state core. A non-polar laboratory oil (Isopar L) was used instead. The experiments were

performed under ambient conditions. However, Weatherford considers the native wettability to be retained. The results from their experiments can be summarized with the following table:

Core depth [m]:	3186.62	3228.62	3232.76
USBM	-0.12	-0.91	-0.78
Amott-Harvey	-0.01	-0.73	-0.39

Table 3.3 – Wettability measurements performed by Weatherford Laboratories (August 2009)

As described earlier, the Amott method and USBM method is based on measuring the volumes from spontaneously and forced imbibition and drainage. However, in these experiments it was decided to cut the spontaneous cycles owing to time constraints and expected possible long spontaneous production times. Instead of measuring true spontaneously imbibed or drained volumes, Weatherford used the lowest speed on the centrifuge (lowest displacement pressure) and referred to the produced volumes as “pseudo-spontaneous” produced volumes. The pseudo-spontaneous produced volumes were then used in the calculation of the wettability indices. Since pressure is applied, the pseudo-spontaneous volumes will be higher than the real spontaneous volumes. This leads to uncertainty in the calculated wettability indices. Both water and oil imbibed pseudo-spontaneously into all three cores. The shallowest core shows close to neutral wettability, while the two deeper cores show oil-wet to strongly oil-wet behavior. These findings are in good agreement with the earlier wettability evaluations (based on relative permeability) by Elf.

Based on the results from the geochemistry reports initiated by Det norske in 2008 and 2009, Stensen and Førlund (2009) concluded that these studies supported the estimated parameters in the PDO, and that there is no reason to believe that the geochemistry will have an important additional effect on the Frøy productivity compared to the effect already reported in the PDO.

The currently last study related to SCAL on Frøy can be found in a NTNU master’s thesis (Selboe 2010). The purpose of the thesis was to look at the wettability effects on low salinity waterflooding. A core plug from 25/5-A1 (sent to NTNU from Weatherford during Weatherford’s studies in 2009) was saturated and aged with Frøy crude oil to restore original wettability. An imbibition cell and a centrifuge was used to measure spontaneous and forced production of water and oil, and the Amott-Harvey index was calculated. Selboe found the wettability to be mixed-wet (spontaneous imbibition of both oil and water). The wettability index was -0.00189.

3.3 Wettability variations in the Frøy field

A goal with this master’s thesis is to try to find wettability trends in the Frøy reservoir. From the literature we know that a typical reservoir is water-wet close to the WOC and the wettability changes towards mixed-wet and oil-wet upwards in the oil zone. We also know that the water-wetness decreases with increased permeability (Hamon 2000) and that the wettability is rock type dependent.

For these reasons it is important to find out where the core samples are taken from in the reservoir. According to the 2008 PDO, the WOC is located at 3175 MSL TVD and is at the same depth throughout the reservoir. The reservoir thickness is at its maximum close to 70 m, but because Frøy is a tilted reservoir, the distance between the WOC and top reservoir can be up to approximately 225 m. The depths of the core samples are given in measured depth from the rotary kelly bushing (MD RKB). These depths must be converted to TVD MSL in order to be comparable with the WOC.

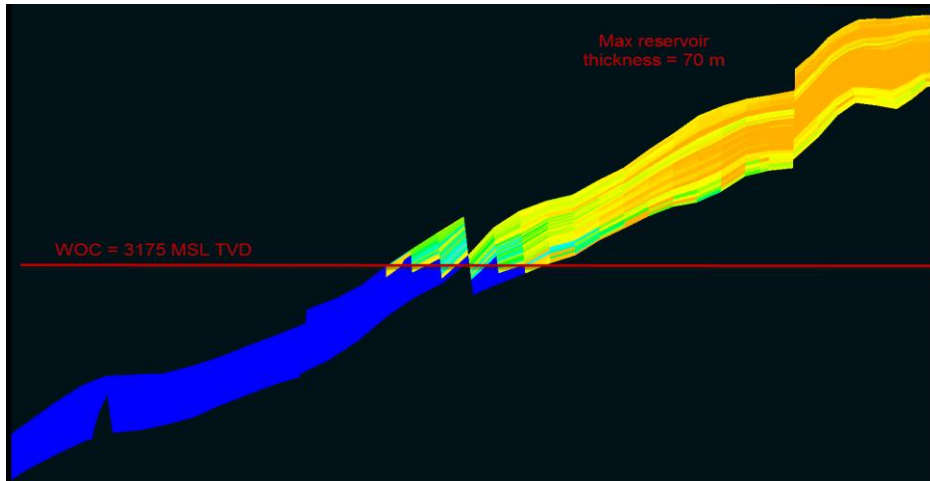


Figure 3.4 – Vertical E-W intersection through the Frøy field

The first wettability measurements were as mentioned performed on cores from 25/5-1 by Geco Petroleum in 1988. In the report a mineralogy description of the cores and the permeabilities are given. No deviation data is available for this well, but according to a petro physicist from Det norske, one can assume that the well is perfectly vertical and that the distance between RKB and MSL is 25 m. The TVDs can then be calculated.

Depth [MSL TVD]	I_{wo}	Permeability [mD]	Mineralogy
2968.12	-0.200	297	Grey sandstone with pyrite and mica
2973.18	-0.430	258	Redish-brown sandstone with siderite, mica and coal
2988.15	-0.114	18	Light-grey sandstone with siderite, mica and some pyrite
2997.1	-0.111	533	Light-grey sandstone with mica and pyrite
3015.33	-0.369	274	Light-grey sandstone with mica and coal

Table 3.4 – Core properties, Geco (1988)

According to the well correlation (PDO, Det norske 2008), which can be seen in Appendix A, the reservoir zone lays in the depth interval 2958 - 3034 MSL TVD for Well 25/5-1, which means that the core samples are taken from practically the whole reservoir zone. We can see that there is not much variation in the wettability. These results show that the whole reservoir zone in the 25/5-1 area is slightly oil-wet. But as mentioned, it is difficult to know exactly how representative these measured

values are because of the questionable sample preparations. The original wettability was not restored after the cleaning process, which may lead to erroneous results.

The wettability measurements by Weatherford (2009) were performed on cores from Well 25/5-A1. An “End of Well” drilling report is available for this well (Elf Petroleum 1993) which can be used for finding the relationship between the measured and true vertical depths. The following information can then be drawn from the report from Weatherford:

Depth [MSL TVD]	Permeability [mD]	Staining level	USBM	I_{wo}
3011	50	low	-0.12	-0.01
3049	400	med	-0.91	-0.73
3053	750	heavy	-0.78	-0.39

Table 3.5 – Core properties, Weatherford (2009)

According to the well correlation (PDO, Det norske 2008), the reservoir zone is located in the depth interval 3000 - 3073 MSL TVD for Well 25/5-A1, which means that the samples are taken from representative locations of the reservoir zone. We can see that the wettability varies between neutral or mixed-wet to strongly oil-wet. The core preparations were good, and the original wettabilities are considered retained. However, a problem with these measurements is as mentioned that no true spontaneous imbibitions were measured, instead the lowest speed on the centrifuge was used, and “pseudo-spontaneous” imbibitions were measured instead and used in the wettability calculations. For this reason, the absolute values of the wettability indices are probably lower (less oil-wet). Hence, the results from Weatherford are in good agreement with the results from Geco.

The wettability test by Selboe (2010) was performed on a core from Well 25/5-A7. An “End of Well” drilling report is available (Elf Petroleum 1995) which can be used for calculating the core sample’s TVD. From the well correlation (PDO, Det norske 2008) we can see that the reservoir zone is located between 3085 and 3161 MSL TVD. The core was taken from 3121 MSL TVD.

Depth [MSL TVD]	Permeability [mD]	Staining level	I_{wo}
3121	≈2300	heavy	-0.00189

Table 3.6 – Core properties, Selboe (2010)

The Frøy field is a heterogeneous field and several rock types are defined based on depositional environment. The well correlation in the PDO can be used for classifying the cores into different rock types. The table below summarizes the information about the 9 cores studied in this chapter.

Depth [MSL TVD]	Rock type	Permeability [mD]	Wettability [I_{wo}]
2968	Shoreface sand	297	-0.2
2973	Intertidal sand	258	-0.43
2988	Channel sand	18	-0.114
2997	Subtidal sand	533	-0.111
3011	Shoreface sand/Coal	50	-0.01
3015	Channel sand	274	-0.369
3049	Channel sand	400	-0.73
3053	Channel sand	750	-0.39
3121	Channel sand	2300	-0.00189

Table 3.7 – Properties of the cores

We can see that channel sands is the only rock type that is represented with more than one core. Since we need at least two data points to be able to establish a trend, it is impossible to find wettability trends for rock types other than channel sands. In the figures below, the wettability is plotted versus depth and permeability, respectively. The data points that are considered unreliable (data from Geco, 1988), because the original wettability was not restored, are marked with a red color and the cores from channel sands have triangle marks instead of squares.

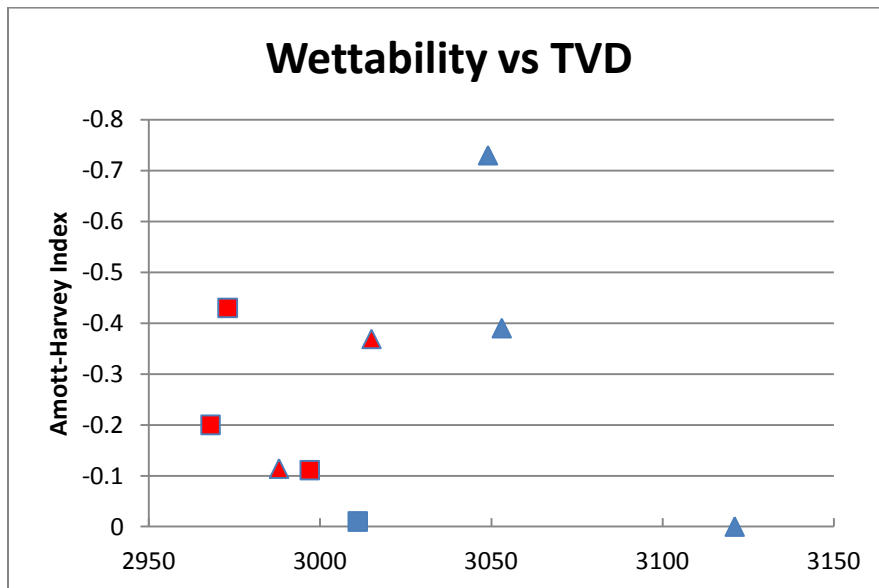


Figure 3.5 – Measured wettability versus depth (TVD MSL)

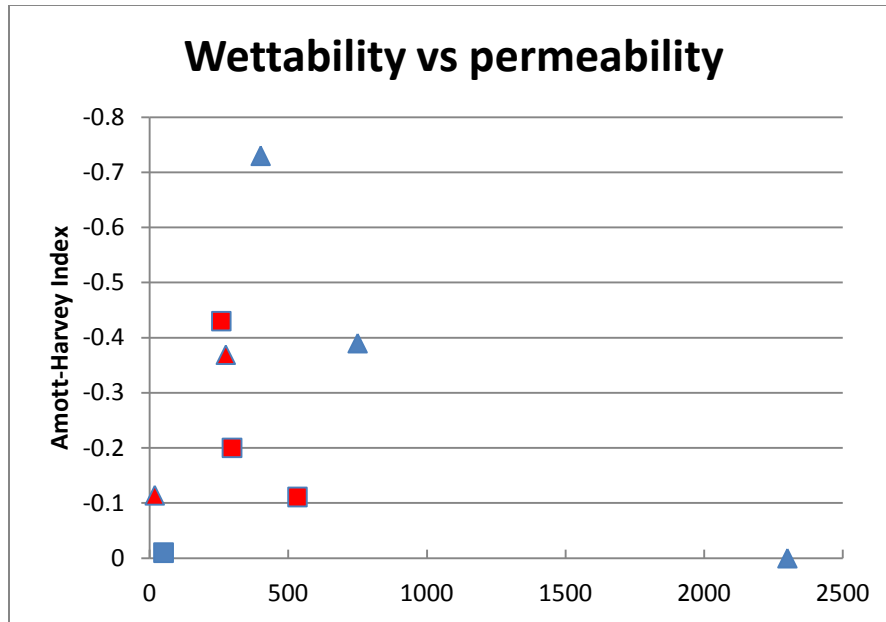


Figure 3.6 – Measured wettability versus permeability (mD)

If we look at the total picture, including the whole data set, we observe that the data are very scattered and that it is hard to see any clear wettability trends with respect to depth or permeability. If we exclude the most unreliable data (marked in red), we still can't see any clear trends. According to the data considered most reliable, the oil-wet rocks are found in the middle of the reservoir (depth wise), at around 3050 MSL TVD, while the wettability is close to neutral at the depths 3011 and 3121 meters. The close to zero wettability value of the core at 3011 meters may be explained with its low permeability. According to Hamon (2000), the oil-wetness decreases with decreasing permeability. The deepest core has the highest permeability, but has close to neutral wettability. This may be explained with the fact that it is a lot closer to the WOC than the other cores, but still we should be aware that it is more than 50 meters above the WOC. The blue triangles in the wettability versus permeability plot, which represents the "reliable" measurements of the channel sands, can actually be approximated with a straight line and is the subset of these data that resembles a trend the most. But we really should have more than three data points to be confident that this actually is a trend and not three points that accidentally falls on the same line. In addition, these three points tells us that the wettability goes towards more water-wet when the permeability increases, which is the opposite conclusion compared to what is written in the literature.

3.4 Summary on wettability trends

The wettability measurements currently available on Frøy are presented. They all suggest that Frøy is on the oil-wetting side of the wettability scale. Qualitatively we can see that the relative permeability curves presented by ResLab Integration (2008) for 25/5-1, 25/5-A1 and 25/5-A7 also indicates wettabilities on the oil-wetting side. But the measurements also show high scatter with Amott-Harvey

indices ranging from zero to -0.73. The conclusion of this study must be that there are not enough reliable wettability measurements available to be able to establish wettability trends in the Frøy field. The wettabilities observed cannot be related specifically to permeability, staining level, rock type or distance above the WOC, simply because the data points are too few and some of them too unreliable. Except from the core used in Selboe's master's thesis, the cores are taken from the top of the structure, more than 100 meters above the WOC. Perhaps the rock tends to be more water-wet closer to the WOC. Several wettability tests using the same procedure as Weatherford (2009) but by measuring true spontaneous imbibition instead of "pseudo-spontaneous" imbibition should be done in order to provide a good statistical dataset that can be used for establishing wettability trends. The samples should represent different permeabilities, staining levels, distances from the WOC, rock types and parts of the reservoir in general. Until this is done, the recommended relative permeability end points and Corey parameters provided by ResLab, which seems very reasonable based on this review, should be used further for modeling the Frøy wettability.

4 Reservoir simulation

4.1 Introduction

The main objective of this thesis is to find out if the wettability variation in the Frøy field is modeled adequately in Det norske's reservoir simulation model. To be able to define the expression "adequately", we need to find out how big the effect of the uncertainty in the wettability is on the production profiles and on the reservoir performance in general. Six years of production data are available which means that the reservoir parameters can be history matched to find the correct values. The idea is that if one is able to make a simulation model that manages to reproduce the historical production data, this model can accurately predict future production. If simulation shows that changing wettability in the model does not significantly affect the reservoir performance, there is no need to do an in depth study of the wettability variations to model it more accurately. However, if simulation shows the opposite result, that wettability heavily affects the reservoir performance, then more effort is needed to define this parameter and its variation properly in the simulation model.

The reservoir simulator which is used by Det norske to model the Frøy field and which also is used in this thesis is the Schlumberger program Eclipse 100, version 2011.1, which is a fully-implicit, three phase, three dimensional, general purpose black oil simulator (Eclipse Technical Description 2010). In Eclipse, wettability is not a separate input parameter, but is given implicitly through the relative permeability and capillary pressure data. These data, which define the endpoints and shapes of the capillary pressure and relative permeability curves, are given as table values in saturation function tables. Different tables can be assigned to different saturation function regions of the reservoir to account for wettability variations. Each grid cell in the model is assigned to a saturation function region by using the keyword SATNUM.

In the Frøy model every grid cell is assigned the same SATNUM number. In other words, only one set of relative permeability curves is used throughout the whole model. The curves can be seen in Appendix B. The whole purpose of this master's thesis is to find out if these curves are adequate to describe the Frøy wettability. The original plan when starting on this thesis was to try to find wettability trends based on the measurements and reports reviewed in the previous chapter. The idea was to implement the trends into the reservoir simulation model, perform a new history match and then run predictions on future production. The new production profile could then be compared with the current profile given in the PDO. But unfortunately, no clear trends could be identified. Therefore, different scenarios will be described and tested with the simulator in order to be able to say something about the importance of the wettability on the Frøy field. For each scenario, the relative permeability setup will be different. For this reason, a full history match should have been performed for every scenario if we wanted to try to match the historical production data. But this is considered to be too time consuming for this thesis and it will most likely not help us to find a more correct wettability variation. Except in cases where the relative permeability setup is very far off, it is likely that the history match procedure is able to tweak and tune the other reservoir parameters to give a good fit with the historical data, and we have no way

of knowing if one history match is more correct than the others. Hence, history matching will not be performed, and the different scenarios will only be compared relative to one another.

4.2 Description of the Frøy simulation model

A reservoir simulation model is available for the Frøy field. It consists of 285 048 grid cells in total with 74, 107 and 36 cells in the x, y and z direction, respectively. Several faults are implemented in the model. The minimum acceptable pore volume is set to 5.0 m³. If a cell's pore volume is less than this value, it will be deactivated (by using the keyword ACTNUM in Eclipse). For this reason, the number of active cells is 88 856. The reservoir section of the Frøy field is located in the Hugin and Sleipner formations, which were deposited during the mid/late Jurassic, and is divided into six reservoir units (RU 1 to RU 6) based on depositional environment.

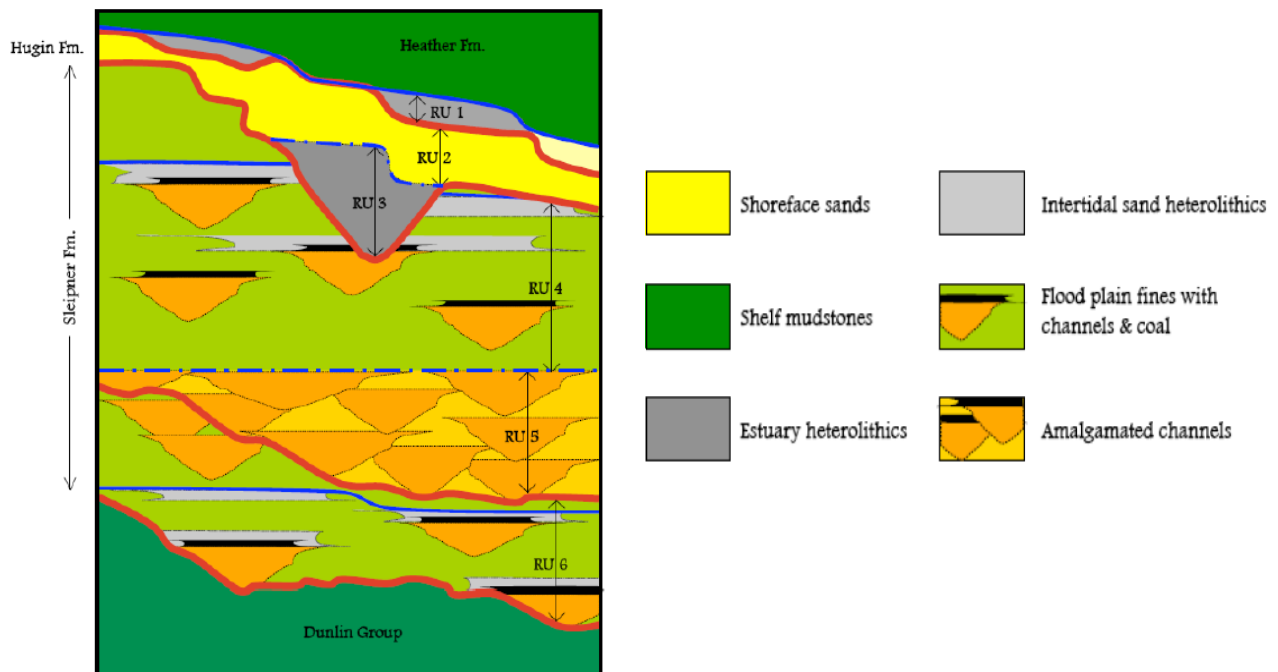


Figure 4.1 – Sequence stratigraphic model for the Sleipner and Hugin formations, showing the six reservoir units (PDO, Det norske 2008)

As we can see from the figure above, the reservoir is far from homogeneous. We have several depositional environments in the reservoir zone that will lead to varying properties of the reservoir rocks. Most of the hydrocarbons in place are found in RU 1 and RU 2 on top of a horst structure. The best reservoir properties are found in the channel sands in RU 5. RU 5 works as a “highway” through the reservoir, capable of quickly transporting big volumes of fluids. Because of high resolution of the facies analysis, the reservoir units have been subdivided into several parasequences. The following table shows the relationship between the formations, reservoir units and simulation layers (z –direction):

Formation	Reservoir Unit	Simulation Layers
Hugin Formation	RU_1	1
Hugin Formation	RU_2	2-4
Sleipner Formation	RU_3	5-7
Sleipner Formation	RU_4_1, RU_4_2, RU_4_3	8-10, 11-13, 14-16
Sleipner Formation	RU_5_1, RU_5_2, RU_5_3, RU_5_4	17-20, 21-24, 25-28, 29-30
Sleipner Formation	RU_6_1, RU_6_2	31-33, 34-36

Table 4.1 – Relationship between geological formation, reservoir unit and simulation layer gradients (Frøy DG2 report, Det norske 2011)

In table 4.2 some of the grid properties are given:

Grid property	Min	Max	Mean
Cell x dimension [m]	47	156	99
Cell y dimension [m]	58	135	100
Cell z dimension [m]	0.01	9.43	1.84
Porosity	0,1 %	26,7 %	11,8 %
Permeability in x- and y-direction [mD]	0.0001	12143	302
Permeability in z-direction [mD]	0.0001	7290	54

Table 4.2 – Grid properties in the simulation model

The top cell is located at $z = 2950$ meters and the lowest cell is located at $z = 3392$ meters. The depth of the WOC is 3175 meters. No gas cap is present initially. This is modeled by setting the GOC above the reservoir. The initial reservoir pressure and temperature are estimated at 308 bars and 103°C at 2970 MSL TVD. The Frøy oil is a light, slightly under-saturated, low viscosity reservoir oil. The saturation pressure and hence the initial oil formation volume factor and solution gas oil ratio have strong depth gradients (Frøy PDO, Det norske 2008).

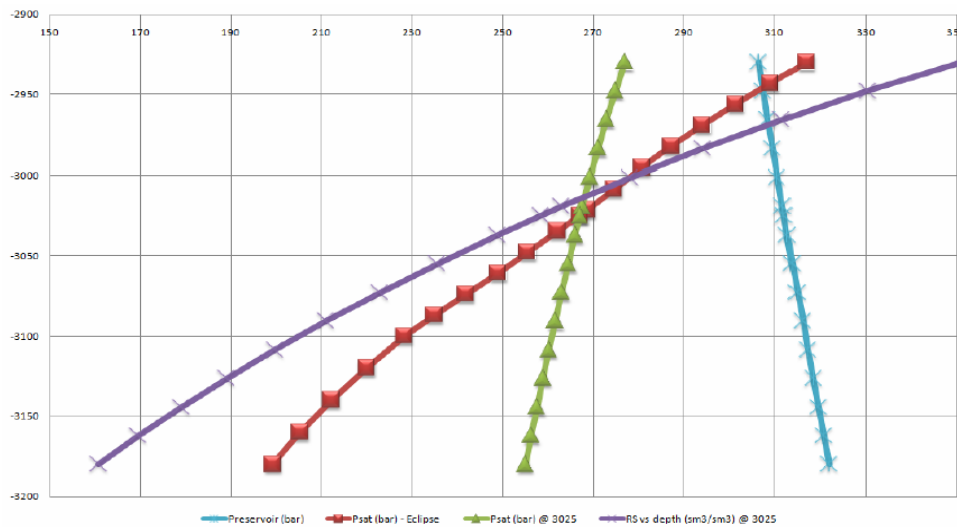


Figure 4.2 – R_s (purple) and saturation pressure (green) both show strong depth gradients (Frøy DG2 report, Det norske 2011)

The relative permeability curves used in the simulation model are derived from the Corey equations described in Chapter 2 and are based on the Corey exponents and the relative permeability end points recommended by ResLab (2007). The oil and water relative permeabilities and the capillary pressure are given as functions of water saturation in an input table using the Eclipse keyword SWOF. The SWOF table and a plot of the curves are given in Appendix B.

The dynamic simulation model is an upscaled version of a finer gridded static geological model. According to the PDO, the difference in STOIP between the geological model and the simulation model is less than 1 %. The initial water saturation in the static model is distributed using a saturation height function (SHF), based on SCAL-data and log measurements. Eclipse can calculate the initial water saturation in every grid block based on hydrostatic equilibrium. Eclipse first calculates the phase pressure in every grid block. The difference between the oil and water phase pressures is defined as the capillary pressure. Eclipse looks up this capillary pressure in column 4 in the SWOF table and distributes the corresponding water saturation in column 1 to the grid block. But in the Frøy case, the water saturation is already known from the geological model. The water saturation distribution in the upscaled simulation model is the pore-volume weighted arithmetic average of the geological model given by the SWATINIT keyword. The capillary pressure in the SWOF table will then be scaled in such a way that hydrostatic equilibrium is obtained and at the same time the SWATINIT values are honored. The ENDSCALE keyword in the RUNSPEC section must be specified if SWATINIT is used for distributing the initial water saturation, and the capillary pressure values in the SWOF table must be monotonically decreasing with increasing water saturation. The scaling process is described in detail in the Eclipse Technical Description and will not be reproduced here.

To make sure that the water is not moving initially in the model, the critical water saturation (keyword SWCR) is set equal to the initial water saturation (SWATINIT). The connate water saturation is specified by the keyword SWL and is equal to 0.12. The maximum water saturation (SWU) equals 1. The critical oil in water saturation (SOWCR) is uncertain and is used as a history matching parameter. The endpoints and critical saturations in the model used for the PDO are discussed in more detail in the Frøy PDO and will not be reproduced here.

Several simulation cases were prepared and run in this master's thesis. A black oil simulation case defined in BO_8_001.DATA, created by Det norske was used as template for defining the new simulation cases. A slightly modified copy of this data file is given in Appendix C. Important remarks on this data file are:

- End point scaling is activated by the keyword ENDSCALE in the RUNSPEC section. This allows the input capillary pressure in the saturation function (SWOF) to be scaled such that the input water saturation given by SWATINIT (included in the PROPS section by "SWAT1.INC") can be honored.
- Several faults are implemented in the model by the include files in the GRID section.
- The relative permeability data and saturation end points are given in the PROPS section.
- The historical production from 1995 to 2001 is given as an include file in the SUMMARY section.

- History matching has been performed, using the SPT Group (now Schlumberger) software program MEPO. Uncertainty parameters like transmissibility factors across faults, size of aquifer, relative permeability Corey parameters and critical saturations are used as input in MEPO, and the program calculates best fit values based on history matching. The results from MEPO are used in the Eclipse data file and can be recognized by the file extension .MINC on the include files.

The relative permeability curves, defined by their end points and Corey parameters, are used as matching parameters together with the other uncertainty parameters in the MEPO history match procedure. Hence, if the relative permeability curves are changed in an Eclipse data file while at the same time keeping the other uncertainty parameters constant (which in practice means using the same .MINC include files), the match between the simulation results and the historical performance will not be as good as with the original curves. To be able to compare new simulation cases with BO_001.DATA, history matching must be performed for every case, and the .MINC files must be replaced. We want to be able to see the effect of wettability on the reservoir performance. As discussed previously in Chapter 2, the wettability will affect the fluid flow through the reservoir, the water breakthrough time and the oil recovery. The faults and the size of the aquifer also influence the same parameters. This means that if history matching is performed for every simulation case, there is no way of knowing how much of the change in reservoir performance is due to the change in wettability (relative permeability) and how much is due to the change in aquifer size and fault transmissibility factors. For this reason it was decided not to perform history matching, which means that comparing the simulation results with the performance of BO_8_001.DATA has no purpose. Instead it was decided to remove all the .MINC files, except "SGOF5_BVI.MINC" which is the oil-gas relative permeability, such that none of the faults acts as flow barriers and the aquifer is removed. The gas-oil relative permeability curves will be kept similar to the curves in BO_8_001.DATA in all the new simulation cases. The reason is that no gas cap is present initially and no recommendations for gas-oil relative permeability curves for production below bubble point pressure are given. The "stripped down version" of BO_8_001.DATA was saved as VBASECASE.DATA and was used as template for the other simulation cases. The reservoir performance of the new simulation cases will be compared relative to one another and compared to the historical performance.

4.3 New simulation cases for studying the effect of wettability on the Frøy reservoir performance

Six different sets of relative permeability curves were made for the purpose of testing the effect of wettability on the reservoir performance. Three of the curves are based on the recommendations from ResLab (2008) given in table 3.2. The other three curves are based on recommended Corey parameters for different wetting characteristics given by table 2.2. "ResLab's low case" is the most oil-wet set of the curves and "Water zone" is the most water-wet set of the curves. The curves are calculated by using the Corey equations given in Chapter 2 of the thesis. It must be emphasized that the three last sets of curves

are made based on engineering judgments, not on relative permeability measurements on the Frøy field. The chosen Corey parameters and the saturation end points are summarized in table 4.3 below.

	n_o	n_w	S_{wi}	S_{or}	$k_{ro}(S_{wi})$	$k_{rw}(S_{or})$
ResLab's Low Case	6	1	0.12	0.12	1	1
ResLab's Base Case	5.5	1.3	0.12	0.08	1	0.8
ResLab's High Case	5	1.8	0.12	0.05	1	0.6
Mixed-wet	4	2	0.12	0.05	1	0.4
Slightly water-wet	3	4	0.12	0.05	1	0.35
Water zone	2	7	0.12	0	1	0.25

Table 4.3 – End points and Corey parameters for calculation of new relative permeability curves

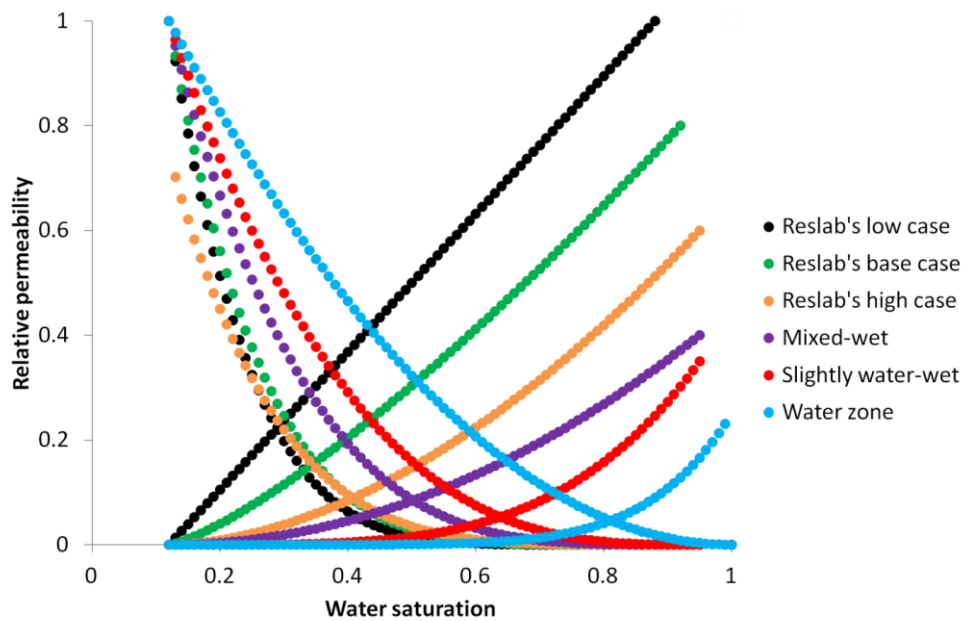


Figure 4.3 – New calculated relative permeability curves

Five simulation cases were run with only 1 SATNUM. That means that the same set of relative permeability curves were used in the whole reservoir. The cases simulated what the reservoir performance would have been if the whole reservoir was given the relative permeability “ResLab’s low case”, “ResLab’s base case”, “ResLab’s high case”, “Mixed-wet” or “Slightly water-wet”. From this point on, these curves and the water zone curve will be referred to as LC, BC, HC, MX, SWW and WZ, respectively. The only difference between the five simulation cases is the input SWOF table, which is the oil-water saturation function table. The following end points that are based on the values from VBASECASE.DATA were used in the new simulation cases:

SOWCR	0.15
SWL	0.12
SWCR	= SWATINIT
MINVALUE SWCR	0.12
MAXVALUE SWCR	0.7799
SWU	1
SGL	0
SGCR	0.06
SGU	0.88
SOGCR	0.10

Table 4.4 – Saturation end points used in the new simulation cases

The results from these simulation runs are presented in subchapter 4.5.

4.4 Introducing more SATNUMs for studying the effect of wettability variation on the reservoir performance

In the previous subchapter we defined simulation cases where the same wettability (relative permeability) is used in the entire reservoir. In this subchapter we will define simulation cases where we investigate how variations in wettability affect the reservoir performance. The reservoir will be divided into several saturation function regions (using the keyword SATNUM) and different sets of relative permeability curves will be given to the different SATNUM regions. The SATNUMs can be based on initial oil saturation, rock permeability, rock type or whatever we believe is the main factor controlling the wettability variation in the reservoir. In the Frøy case, we do not know what the dominant factor is, but we do know from the literature review that in a typical reservoir the wettability is dependent on the distance above the water-oil contact. For this reason, we will divide the reservoir into SATNUMs based on depth levels.

The division of Frøy into SATNUM regions was done by using the calculator in Petrel. Two different scenarios were created. In the first scenario, the grid cells below the WOC was given the value 1, and the reservoir zone above the WOC was split into three equal depth intervals (75 m per interval), and the grid cells in these intervals were given the values 2, 3 and 4. In the second scenario, the reservoir zone above the WOC was split into five equal depth intervals (45 m per interval), and the grid cells in these intervals were given the values 2, 3, 4, 5 and 6. Illustrations of the two different scenarios are given in figure 4.4 and figure 4.5 below.

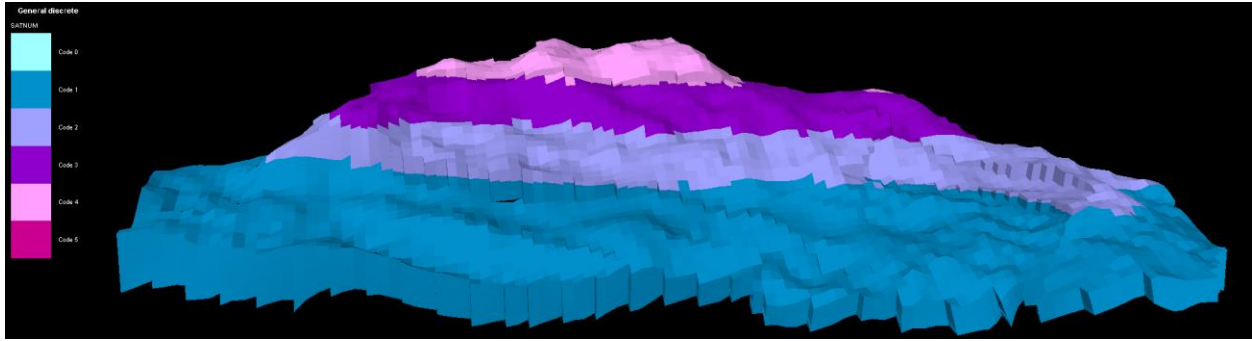


Figure 4.4 – Illustration of the division of the reservoir into 4 SATNUMs

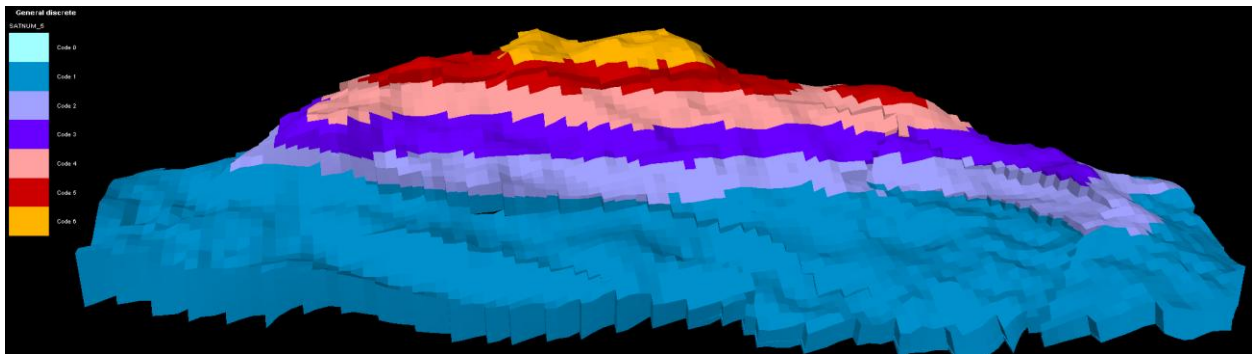


Figure 4.5 – Illustration of the division of the reservoir into 6 SATNUMs

In the new simulation cases with several SATNUMs, the WZ curves were assigned to SATNUM 1 and different combinations of SWW, MX, HC, BC and LC were tried out on the other SATNUMs above the WOC. Actually the water zone will behave the same, independent of its relative permeability curves because it will be fully saturated with water during the entire simulation period in all of the simulation cases, but the WZ curves were assigned to the water zone anyway to be consistent. The new simulation cases are given names based on their combination of relative permeability curves, e.g. the name WZ_SWW_HC_LC means that the WZ curves are assigned to SATNUM 1, the SWW curves are assigned to SATNUM 2, the HC curves are assigned to SATNUM 3, and the LC curves are assigned to the last SATNUM. Eleven cases were run with four SATNUM regions and seven cases were run with six SATNUM regions.

4.5 Simulation results

4.5.1 Results from simulation cases using only 1 SATNUM

The field performances for the five simulation cases, using only one SATNUM, are given in figure 4.6 and the cases are compared with the historical performance in figure 4.7. The performance of each of the six producing wells A1, A4, A5, A6, A7 and A8, including oil production rate, water production rate, bottom hole pressure and gas oil ratio are given in the figures D.1 through D.12 in Appendix D.

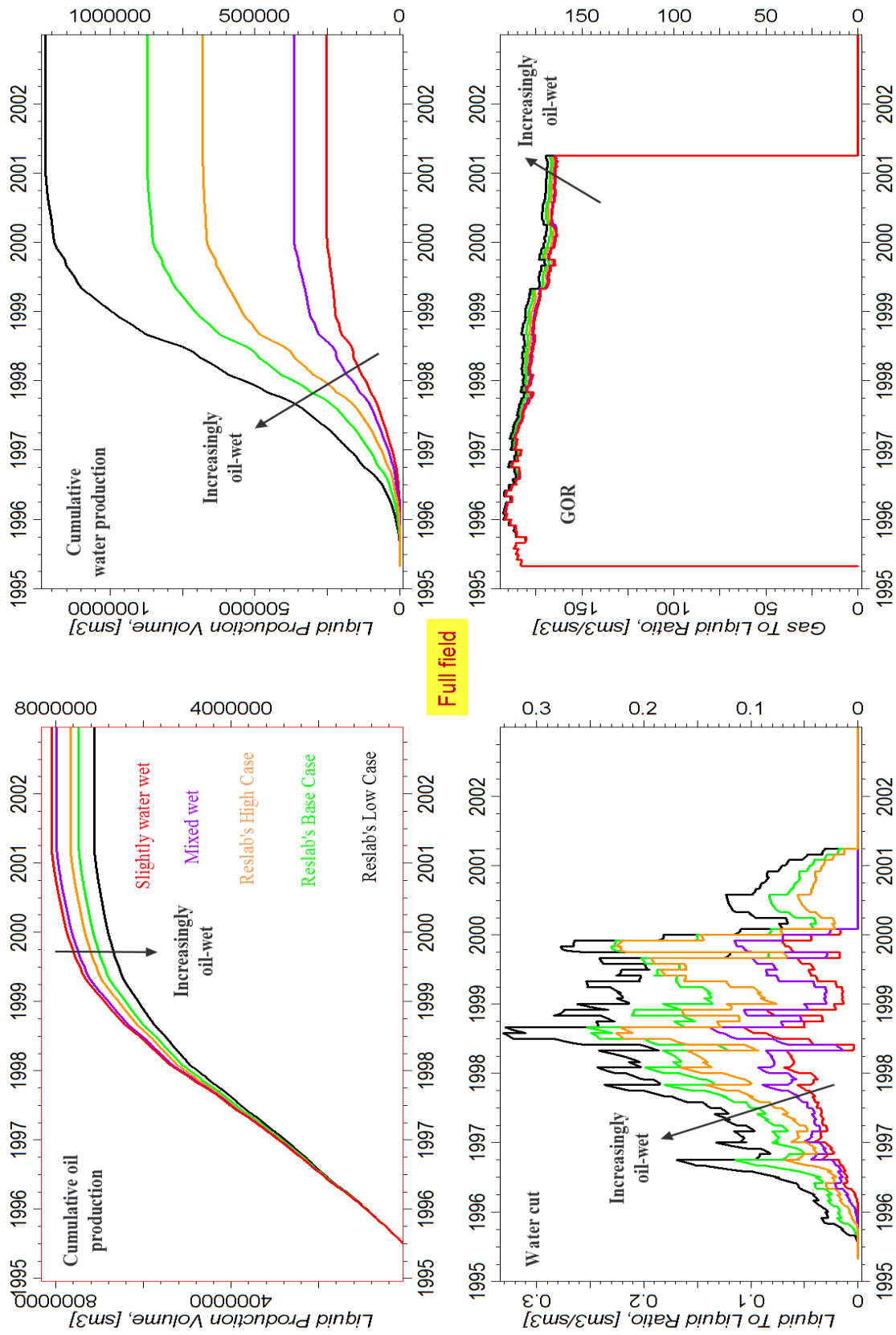


Figure 4.6 – Field performance as a function of wettability, 1 SATNUM

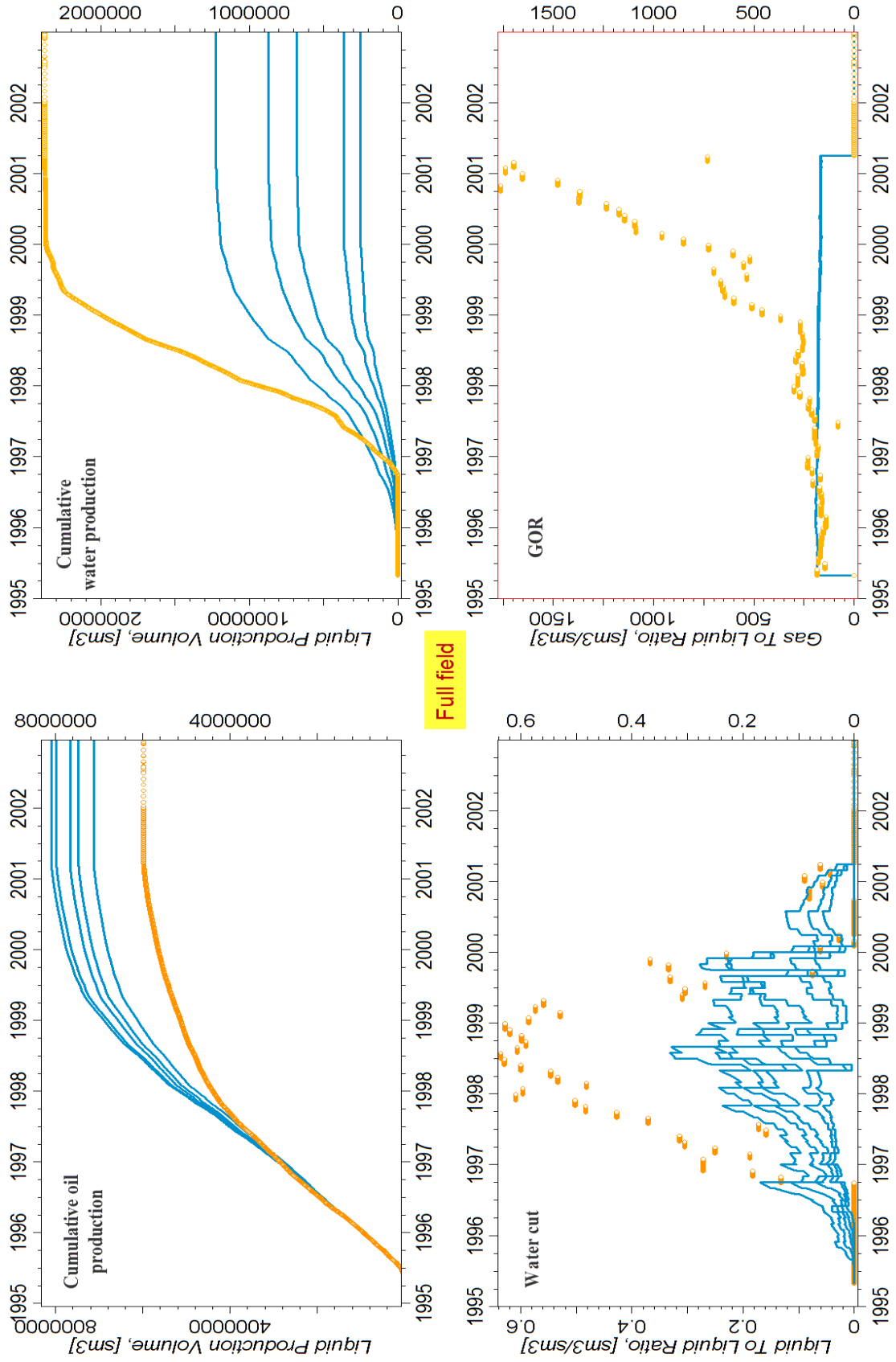


Figure 4.7 – Comparison of simulation cases and historic performance, 1 SATNUM

The field performance summarizes the well performances very well in these cases. We observe that when the reservoir goes towards more oil-wet, the oil production goes down, the water production goes up and the water breakthrough occurs earlier. As a consequence of the oil and water production, the water cut also increases when the rock becomes more oil-wet. We observe that the gas-oil ratio is approximately constant through the whole simulation period.

Figure 4.8 shows that the cumulative oil production for the different wells is not equally sensitive to changes in wettability. The difference in oil production for A4 between the SWW and LC cases is $371\,425\text{ Sm}^3$ which corresponds to a 24 % increase in production when the wettability goes from oil-wet to slightly water-wet. The difference in oil production for A6 is only 1750 Sm^3 which corresponds to 2 % increase in production.

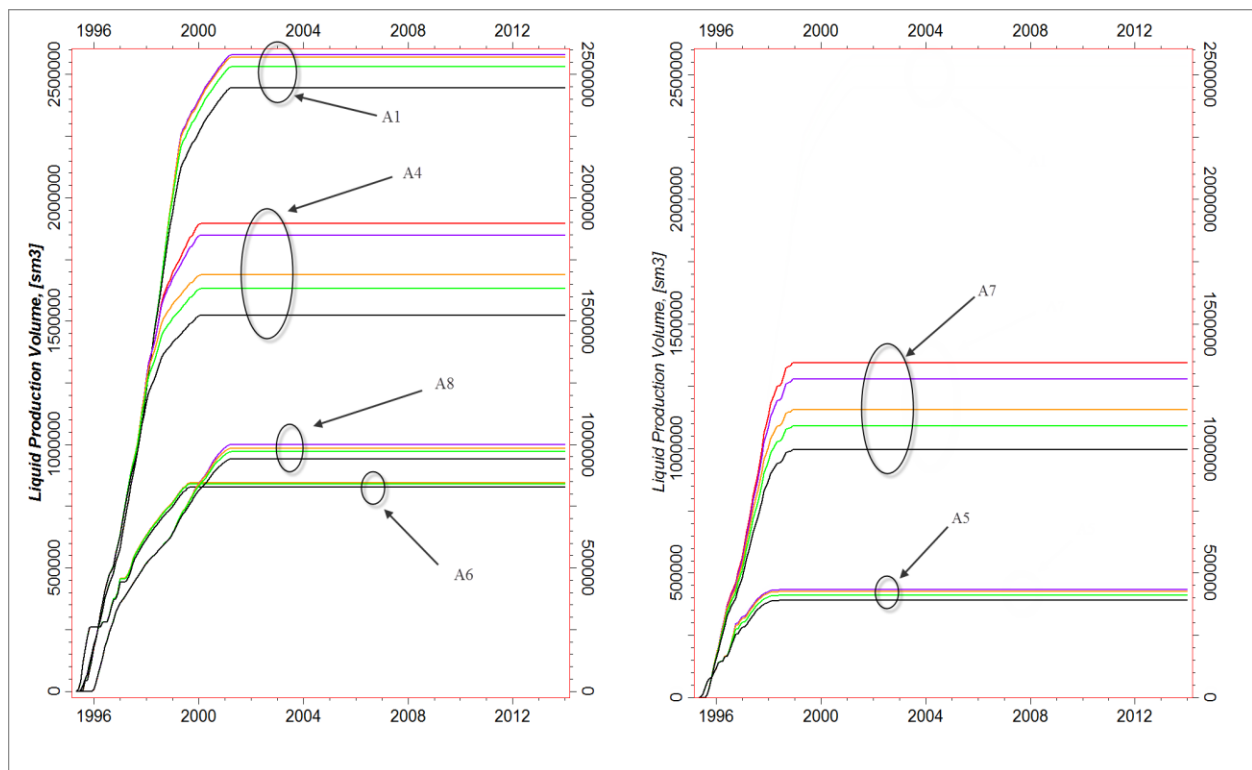


Figure 4.8 – Cumulative oil production as a function of wettability (figure split in two for readability)

4.5.2 Results from simulation cases using 4 and 6 SATNUMs

The SWW case and LC case from when we only used 1 SATNUM are the two extreme cases where the entire reservoir is slightly water-wet or very oil-wet, respectively. When we use several SATNUMs and use a combination of the SWW, MX, HC, BC and LC relative permeabilities, it is reasonable to assume that the production profiles of these cases will fall somewhere between these two extremes. In figure 4.9 we see the field results of the reservoir performance of the new cases using several SATNUMs compared to the LC and SWW case where we use only 1 SATNUM.

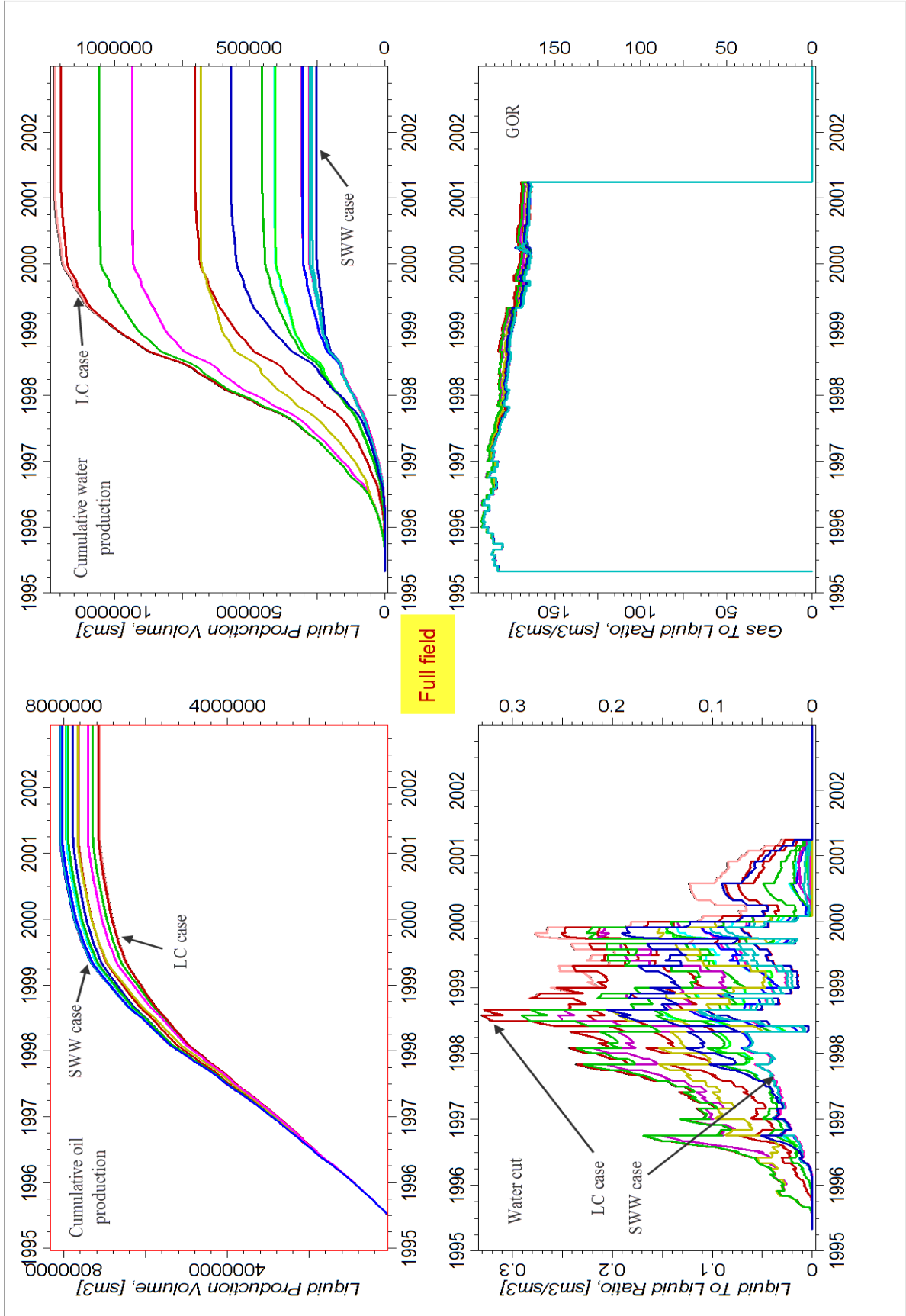


Figure 4.9 – Field performance as a function of wettability variations using 4 and 6 SATNUMs compared to LC and SWW using 1 SATNUM

Some of the results from A1 and A7 are given in the figures D.13, D.14 and D.15 in Appendix D. Figure D.13 presents the performance of A1 for different cases using 4 SATNUMs. If we look at the cumulative oil production, it appears like that the WZ_LC_LC_SWW case is identical to the LC case and that there is a negligible difference between

- WZ_SWW_LC_LC
- WZ_SWW_SWW_LC
- WZ_LC_SWW_SWW
- WZ_LC_SWW_LC
- WZ_SWW_LC_SWW
- SWW

Figure D.15 presents the performance of A7 for different cases using 6 SATNUMs. If we look at the cumulative oil production, we see the following:

- WZ_LC_LC_SWW = WZ_LC_SWW_SWW = WZ_LC_SWW_LC = LC
- WZ_SWW_SWW_LC = WZ_SWW_LC_LC = SWW_LC_SWW = SWW

In other words, the performance of A7 in these cases is only dependent on the relative permeability curves used in SATNUM 2, which is the first 75 meters above the WOC.

5 Discussion on the simulation results

5.1 Simulation cases using only 1 SATNUM

The performance of A1 has the same trends as the field performance, except that there is no difference between the oil production for the MX and SWW case. The reason is simple. The wells in the simulation cases are controlled by historical liquid rates because LRAT is specified in the Eclipse keyword WHISTCTL in the included file "G4_SCHED_BUILDUP_BO.INC" in the SUMMARY section. This means that the wells produce with the exact same liquid rates (water + oil) as the historical wells once did. For the MX and SWW case, A1 does not produce any water which implies (because of LRAT) that the oil rates for the two cases will be exactly the same. Well A4 and A7 show the same trends as the field performance when changing the wettability. The performance of A6 appears to be almost independent of the wettability. The water production is approximately zero for the HC, MX and SWW case which implies that the oil rate profiles will be approximately identical. The bottom hole pressure and gas oil ratio show very small differences between the five simulation cases. A8 also shows very small differences in BHP and GOR but the A8 production profiles are more sensitive to the wettability than the A6 production profiles. There is no water production in the SWW and MX cases, but water is produced in the HC, BC and LC cases, where the highest water production is observed in the LC (most oil-wet) case.

If we compare the simulated field performance with the historical field performance (figure 4.7), it appears like that if we assign a relative permeability to the field that corresponds to an extremely oil-wetting behavior, we will get a good match on the oil production, water production and water cut. The comparison with the historical performance show that there was produced less oil and correspondingly more water during 1995 – 2001 than we produce in our new simulation cases. This can most likely be handled by introducing aquifer support. As described in subchapter 4.2, the aquifer was removed from the simulation model. If a strong aquifer is acting on the reservoir it is plausible that the water breakthrough will come earlier and that more water will be produced. If we look at the GOR for the different wells, we see that our simulation cases underestimate the GOR at the end of the life of the wells. Gas is released from the oil when the pressure drops below the saturation pressure, which is depth dependent. For Well A8 we observe that we overestimate the BHP which may be the reason the GOR is underestimated. The overestimation of the BHP may be explained by the removal of all barriers in the model. A sealing fault located close to A8 can increase the pressure drop close to the well and gas may be released. But at A4 and A7 we underestimate the BHP and still the simulated GOR is too low, which emphasizes that this is a complex reservoir. The oil production rates at A8 are matched perfectly with the historical production for the SWW and MX cases. The historical water production is zero and this can only be simulated by not using oil-wet relative permeability curves because the oil-wet curves causes the injected water to move more rapidly through the reservoir and towards the producers, and no flow barriers that could have stopped the advancing water front are implemented in the model. When the water production is zero, the liquid rate equals the oil rate, and since the wells are controlled with LRAT, the simulated oil rate will match the historical oil rate.

5.2 Simulation cases using 4 and 6 SATNUMs

The full field results are as expected. The simulation cases where we use several SATNUMs give field results that falls between the SWW and LC cases (using 1 SATNUM), which indicates that the new simulation cases are modeled correctly. There is however, for an unknown reason, a small spike in the GOR in the beginning of year 2000 for some of the cases, but this will be ignored.

If we look at the cumulative water production for the cases using 4 SATNUMs, we can see that some of the cases have exactly the same production profiles. What we actually observe is that if two cases have the same relative permeability curves in SATNUM 2 and SATNUM 3, they will have the same production profiles, regardless of which relative permeability curve that is used in SATNUM 4. Figure D.13 only presents the results from A1, but we see the same results for the other wells.

When using 5 SATNUM regions above the water-oil contact instead of 3, we can define the depth intervals that influence the performance of the wells more precisely. Figure D.14 and figure D.15 show the well performances of A1 and A7 for the simulation cases using 6 SATNUMs. As mentioned previously, in the cases with 4 SATNUMs each depth interval above the WOC is 75 meters, and in the cases with 6 SATNUMs each depth interval is 45 meters. WZ_LC_LC_SWW (150 meters with LC curves above the WOC) equals LC (the whole reservoir uses the LC curves) and WZ_LC_LC_LC_SWW_SWW (135 meters) equals LC, but WZ_LC_LC_SWW_SWW_SWW (90 meters) produces less water and more oil than the LC case. This means that a “critical depth” is located between 90 and 135 meters above the WOC and if the reservoir rock between the WOC and this depth is oil-wet, the performance of the A1 well will be as if the entire reservoir was oil-wet. On the other hand, WZ_SWW_SWW_LC_LC_LC = SWW, but WZ_SWW_LC_LC has a higher water production (almost negligible) and lower oil production than the SWW case. This means that the “critical depth” for SWW is located between 75 and 90 meters above the WOC and if the reservoir rock between the WOC and this depth is slightly water-wet, the performance of the A1 well will be as if the entire reservoir was slightly water-wet. By following this logic, we can define two depth values for each well within which the “critical depth” will be located.

Let us assume that the LC curves are assigned to SATNUM 2 which is the depth interval directly above the water-oil contact. Table 5.1 then shows how thick SATNUM 2 must be in order for the different wells to perform as if the LC curves were assigned to the entire reservoir. The exact thickness values are not known because of the resolution of the simulation cases, but they will be somewhere within the given intervals. In these cases the SWW curves are assigned to the reservoir zone above SATNUM 2.

Well name	A1	A4	A5	A6	A7	A8
Thickness [m]	90 - 135	90 - 135	90 - 135	45 - 75	45 - 75	135 - 150

Table 5.1 – Thickness of SATNUM 2, LC

If we assume that the SWW curves are assigned to SATNUM 2, then Table 5.2 shows how thick SATNUM 2 must be in order for the different wells to perform as if the SWW curves were assigned to the entire reservoir. In these cases, the LC curves are assigned to the reservoir zone above SATNUM 2.

Well name	A1	A4	A5	A6	A7	A8
Thickness [m]	45 - 75	90 - 135	45 - 75	< 45	45 - 75	75 - 90

Table 5.2 – Thickness of SATNUM 2, SWW

Another observation was made when plotting WZ_LC_SWW_SWW_SWW_SWW for the A1 case. This case showed no water production and gave the same results as the SWW case. This means that even though the depth interval closest to the WOC has the most significant effect on the production profiles, it will in some cases not influence the production at all if it is thin enough.

If we assume that the LC curves are assigned to the reservoir zone above SATNUM 2, this table shows how thick this zone must be in order for the different wells to perform as if the LC curves were assigned to the entire reservoir. In these cases the SWW curves are assigned to SATNUM 2.

Well name	A1	A4	A5	A6	A7	A8
Thickness [m]	> 180	> 180	> 180	> 180	> 180	> 180

Table 5.3 – Thickness of the reservoir zone above SATNUM 2, LC

If we assume that the SWW curves are assigned to the reservoir zone above SATNUM 2, this table shows how thick this zone must be in order for the different wells to perform as if the SWW curves were assigned to the entire reservoir. In these cases the LC curves are assigned to SATNUM 2.

Well name	A1	A4	A5	A6	A7	A8
Thickness [m]	135 - 150	> 180	150 - 180	150 - 180	> 180	135 - 150

Table 5.4 – Thickness of the reservoir zone above SATNUM 2, SWW

We can summarize the observations from the simulation cases where we are using saturation function regions with the following: It is the wettability characteristic (relative permeability) of the depth interval closest to the WOC that affects the production profiles the most. If it is thick enough, the wells will perform as if the entire reservoir had the same wettability as this depth interval. But the thickness of the interval is well dependent. For example if less than 45 meters above the WOC is slightly water-wet, the performance of Well A6 will be as if the entire reservoir was water-wet, even though the rest of the reservoir is oil-wet, but for Well A4 more than 90 meters of the reservoir zone directly above the WOC must be slightly water-wet. If not, it will be affected by the oil-wet zone above. On the other hand, if we have a depth interval directly above the WOC that has a different wettability than the rest of the

reservoir it will not affect the performance of the wells at all if it is too thin. For example, the simulation results in this thesis show that if the top reservoir zone is slightly water-wet and that this zone is more than 150 meters thick, meaning that the oil-wet zone directly above the WOC is less than 75 meters thick (the reservoir zone is 225 meters in total), A1 will perform as if the entire reservoir was slightly water-wet.

More generally speaking, wettability variations with depth affect the oil and water production profiles of the wells at the Frøy field, but the different wells are not equally affected. Exactly how much the performance of the wells is affected depends on at which depth levels the wettability variations occur.

5.3 Discussion on the validity of the presented data

Results from a number of simulation cases have been presented, but in order to say something about their validity, we need to discuss the uncertainties in the parameters involved, and discuss some of the consequences of the assumptions and choices that were made when defining the simulation cases.

Defining the importance of wettability variations within the Frøy field is a challenging task. First of all, we only have a few reliable wettability measurements available that does not show any clear trends throughout the reservoir. This means that we don't know how much the wettability indices are varying in the reservoir or where in the reservoir they are varying. Because of this fact, relative permeability curves that was meant to correspond to wettabilities ranging from slightly water-wet to very oil-wet was defined and the plan was to make simulation cases where these relative permeability curves could be used. But how can we make simulation cases that are directly comparable and how can we know with certainty that one simulation case is more correct than the other? We have several years of production data available which means that we can compare our simulation results to the historical production to see if we are getting closer or further away from the correct values. The wettability will affect the oil and water production profiles and the time of water breakthrough. The problem is that these simulation results also are affected by other uncertain reservoir parameters like aquifer support and fault transmissibility factors. If we use a history matching software program that provides best fit values of the unknowns, we can actually get several complete different combinations of wettability, size of aquifer and fault transmissibility factors that will give a good fit with the historical production, and we will still not know if we have the correct wettabilities. Hence, in order to be able to compare the simulation cases properly, it is necessary to keep the other parameters constant. This is the only way we can be sure that the changes we see in the results comes from the changes in wettability and not from the changes in some of the other parameters. It was decided to remove the aquifer completely and also to open the flow across the implemented faults.

Five simulation cases were run where the new relative permeability curves were tried out. In these cases only one saturation function region was defined such that one set of relative permeability curves was used for the whole reservoir. We saw what the literature review predicted which was lower oil production and higher water production and earlier water breakthrough when the reservoir went from

slightly water-wet to very oil-wet. When these cases were compared to the historical production we saw that the historical oil production was a lot lower than our most oil-wet case. But that does not mean that the reservoir has to be extremely oil-wet. The same five sets of relative permeability curves were tried out on the simulation case BO_8_001 created by Det norske. In this case faults and an aquifer are present in the simulation model. The results, which can be studied in figure D.19 show that we get a fairly good match with the BC case but we have no way of knowing how correct the results are because we don't know if the aquifer and faults are modeled properly. The point is that we cannot find out what the correct wettabilities in the Frøy reservoir are based on these simulations. Either more wettability measurements must be performed or the uncertainty of the other reservoir parameters that affect the production must be reduced such that the wettability can be determined accurately from history matching.

To be able to say something about the effect of wettability on Frøy, the reservoir performance for the different simulation cases using only one saturation function region were compared, looking at the performance of the entire field and also the performance of each well. Here we saw that the wells were not equally affected by the change in wettability. The A4 well was affected the most. There was a 24 % increase in oil production when the wettability was changed from oil-wet to slightly water-wet and A6 was affected the least. But by looking at figure D.16 we can see that the difference between the results from the SWW case and the LC case are bigger when the aquifer and faults are included. When the aquifer and fault transmissibility factors are not included, the difference in field oil production between the SWW and LC case is approximately $1.0 \cdot 10^6 \text{ Sm}^3$ (14 % increase when the reservoir goes from oil-wet to slightly water-wet), but when they are included, the difference is approximately $1.7 \cdot 10^6 \text{ Sm}^3$ (31 % increase). In other words, how big the effect of changing the wettability will be is also dependent on the aquifer size and the fault transmissibility factors, which means that there is no way of telling how big the effect of changing the wettability will be if we don't give the aquifer size and fault transmissibility factors their proper values.

The results from the simulations are also dependent on the way we choose to initialize the model and in particular how we choose to model the critical saturations.

If capillary forces are strong within a reservoir, they will affect the production. We know from the literature that the capillary pressure is a function of the rock properties, including porosity, permeability and wettability. But the same capillary pressure curve has been used in all the simulation cases presented in this thesis. As mentioned, the model is initialized with an initial water saturation distribution map by using the keyword SWATINIT. Eclipse will scale the given capillary pressure curve such that the SWATINIT values can be honored. The scaling process may in some grid cells give high, unphysical capillary pressure values, especially in grid cells above the WOC that has high water saturation. How this affects the reservoir performance has not been studied in detail, but an alternative way of initializing the model was tested. Instead of assigning the initial water saturation distribution map to the SWATINIT keyword, it was assigned to the SWL keyword. By doing this, we are saying that the water saturation from the distribution map (which as explained earlier is the upscaled water saturation from the geological model) is the lowest water saturation the given grid cells can have. When

initializing with SWL we can actually remove the capillary pressure curve by inserting only zeros in column four in the SWOF table. When Eclipse calculates the capillary pressure in a given grid cell based on hydrostatic equilibrium as explained earlier, Eclipse normally looks up the capillary pressure in the SWOF table and assigns the corresponding water saturation in column one to the grid cell. If the calculated capillary pressure is higher than the highest value in column four (which corresponds to the lowest water saturation in the table), the grid cell will be given the lowest water saturation, which in our case is 0.12. But the keyword SWL overwrites the lowest table saturation (Eclipse technical description, 2010). When every value in column four is zero, the calculated capillary pressure will always be higher than the table value. Hence, the SWL value will be given to the grid cell. In this way the initial water distribution map may be implemented into the model without scaling the capillary pressure. Since we only have one capillary pressure curve available, this alternative way of initializing the model may be more correct than initializing with SWATINIT. The 1 SATNUM cases initialized with SWL are compared to the LC and SWW cases initialized with SWATINIT in figure D.17. The figure indicates that the difference in results between the two initialization methods is negligible.

In Det norske's simulation model, the critical oil in water saturation (SOWCR) is a constant and is used as a history matching parameter. In the simulation cases presented in this thesis, the SOWCR is a constant and equals 0.15. The critical oil in water saturation is another expression for the residual oil saturation. It has been known for a long time that the residual oil saturation is a function of the initial oil saturation (Land 1968), and Spiteri et al. (2008) showed that the relation between initial and residual oil is dependent on the wettability of the rock. The initial oil saturation is varying in the reservoir. It is therefore a reason to believe that the residual oil saturation will be different from grid cell to grid cell. Spiteri et al.'s trapping model

$$S_{or} = \alpha S_{oi} - \beta S_{oi}^2 \quad (5.1)$$

where α and β are wettability dependent parameters, was implemented into the simulation model.

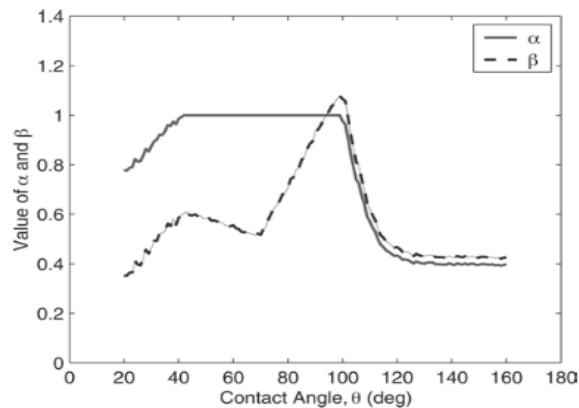


Figure 5.1 – The relation between the parameters alpha and beta and the intrinsic contact angle (Spiteri et al. 2008)

Based on figure 5.1 and figure 2.2 which gives the relation between the intrinsic contact angle and the receding and advancing contact angel, the following values of alpha and beta were chosen for the different sets of relative permeability curves:

Relative permeability	α	β
SWW	1	0.55
MX	1	0.9
HC	0.9	0.9
BC	0.5	0.5
LC	0.4	0.4

Table 5.5 – Values of alpha and beta for the different sets of relative permeability curves

The 1 SATNUM cases with Spiteri et al.'s trapping model implemented are compared to the SWW and LC cases in figure D.18. We can see that the MX case gives the highest oil production for the Spiteri cases and that the SWW case is almost as bad as the LC case. Spiteri et al.'s trapping model is fairly new and it is unknown if the model has been tested in the industry. Even though SOWCR is dependent on the initial oil saturation, it is difficult to say if the "Spiteri cases" are more correct than the other simulation cases where the SOWCR is constant and equal to 0.15.

There are most likely more issues and problems that affect the reservoir performance in the simulation model that will disturb the analysis of effect from wettability variations and that should have been discussed, but the last thing that will be mentioned is the gas phase. There is no gas cap present in the reservoir initially, but at the end of the simulation period the reservoir pressure has dropped below the bubble point pressure on the top of the horst structure. This is illustrated in the last figure in the appendix. No recommendations for the gas-oil relative permeability are given and it is specified in the Frøy PDO that the given gas-oil relative permeability that is used in the simulation models are only valid for gas injection and not for production below bubble point. The effect of the gas-oil relative permeability on the Frøy production is unknown.

6 Conclusions

Based on the literature review in Chapter 2, we can draw the following conclusions:

- Wettability is one of the most important parameters regarding the rate of oil recovery from a porous medium. Wettability controls the displacement and trapping mechanisms in a reservoir.
- The wettability in reservoir rocks depends on
 - Rock mineralogy
 - Rock quality (permeability)
 - Properties and composition of the oil, including the asphaltene content
 - Properties and composition of the formation water, including pH and salinity
 - Reservoir conditions (temperature and pressure)
 - Saturation and saturation history

Based on the reports on SCAL measurements presented in Chapter 3, we can draw the following conclusions:

- A review of the studies related to relative permeability and wettability on the Frøy field shows that the oil zone is on the oil-wetting side of the wettability scale, with Amott-Harvey wettability indices ranging from -0.00189 to -0.73.
- There are not enough reliable wettability measurements available to establish wettability trends within the Frøy field. Because of the lack of a good statistical dataset, the wettabilities observed cannot be related specifically to permeability, staining level, rock type, the distance above the WOC or any other parameters that are likely to affect the reservoir wettability.
- Several wettability tests on native state cores should be performed in order to provide a good statistical dataset that can be used for establishing wettability trends. The samples should represent different permeabilities, staining levels, distances from the WOC, rock types and parts of the reservoir in general.
- The relative permeability curves used in the 2008 PDO should be used further for modeling the Frøy wettability until new wettability studies are initiated.

Based on the simulation results presented in Chapter 4, we can draw the following conclusions:

- Simulation results show that when the Frøy reservoir rock goes from water-wet to oil-wet, the oil production goes down, the water production goes up, the water breakthrough occurs earlier and the oil recovery factor goes down.

- The results also show that there is no way of telling how big the effect of wettability variations is on the production profiles, unless the aquifer support and the fault transmissibility factors are modeled correctly, since these parameters also affect the production. In these simulations, the six historical producers are not equally affected by changes in the wettability.
- We cannot conclude on whether the relative permeability curves that are currently used in the simulation model are adequate or not to model the Frøy wettability.
- If we assume that there is no aquifer support at Frøy and that the flow across the faults are completely open, simulations show that Well A4 is the producer that is the most affected by changes in wettability with an increase in oil production up to 24 % when going from slightly water-wet to oil-wet, while A6 is hardly affected by wettability changes at all.
- It is the wettability of the bottom half of the 225 meter thick reservoir zone that affects the production profiles of the wells. The wettability of the top half of the reservoir zone hardly affects the production profiles at all.

7 Nomenclature

Symbols and parameters

A_1 – Area under secondary drainage curve
 A_2 – Area under imbibition curve
 α – Wettability dependent curve parameter in Spiteri's trapping model
 β – Wettability dependent curve parameter in Spiteri's trapping model
 ΔS_w – Total water production from core
 Θ – Contact angle
 Θ_A – Advancing contact angle
 Θ_R – Receding contact angle
 Φ – Porosity
 Φ_e – Effective porosity
 σ_{SO} – Interfacial tension between solid and oil
 σ_{SW} – Interfacial tension between solid and water
 σ_{WO} – Interfacial tension between water and oil
 I_o - Wettability index for oil
 I_w - Wettability index for water
 I_{WO} – Amott-Harvey wettability index
 k – Permeability
 k_o – Effective oil permeability
 k_{ro} – Oil relative permeability
 k_{rw} – Water relative permeability
 L_o, E_o, T_o – LET parameters for oil relative permeability
 L_w, E_w, T_w – LET parameters for water relative permeability
 n_o – Corey parameter for the oil relative permeability
 n_w – Corey parameter for the water relative permeability
 R_s – Solution gas-oil ratio
 S_g – Gas saturation
 S_{gr} – Residual gas saturation
 S_o – Oil saturation
 S_{or} – Residual oil saturation
 S_w – Water saturation
 $S_{w,f}$ – Forced water production from core

S_{wi} – Initial water saturation
 S_{wirr} – Irreducible water saturation
 $S_{w,sp}$ – Spontaneous water production from core
 V_g – Volume of gas
 V_o – Volume of oil
 V_w – Volume of water
 V_p – Pore volume
 WI – Wettability index
 $WI_{W,Amott}$ – Amott wettability index for water
 WI_{USBM} – USBM wettability index

Relative permeability curves

WZ – Water zone
SWW – Slightly water-wet
MX – Mixed-wet
HC – ResLab's high case
BC – ResLab's base case
LC – ResLab's low case

Eclipse keywords

ACTNUM – Activation/deactivation of grid cells
ENDSCALE – Activate end point scaling
INCLUDE – Including external files
MAXVALUE – Maximum value
MINVALUE – Minimum value
SATNUM – Saturation function number
SGOF – Saturation function table for gas-water
SGL – Lower value of gas saturation
SGCR – Critical gas saturation
SGU – Upper gas saturation
SOGCR – Critical oil in gas saturation
SOWCR – Critical oil in water saturation
SWATINIT – Initial water saturation distribution map
SWCR – Critical water saturation
SWL – Lower value of water saturation
SWOF – Saturation function table for oil-water
SWU – Upper value of water saturation

8 References

- Agbalaka, C., Dandekar, A.Y., Patil, S.L. et al. 2008. The Effect of Wettability on Oil Recovery: A Review. Paper 114496 presented at the SPE Asia Pacific Oil and Gas Conference and Exhibition, Perth, Australia, 20-22 October. <http://dx.doi.org/10.2118/114496-MS>.
- Al-Maamari, R.S.H. and Buckley, J.S. 2003. Asphaltene Precipitation and Alteration of Wetting: The Potential for Wettability Changes During Oil Production. *SPE Journal* **6** (4): 210-214. SPE-84938-PA. <http://dx.doi.org/10.2118/84938-PA>.
- Amott, E. 1959. Observations Relating to the Wettability of Porous Rock. *Trans, AIME* **216**: 156-162.
- Brown, R.J.S. and Fatt, I. 1956. Measurements Of Fractional Wettability Of Oil Fields' Rocks By The Nuclear Magnetic Relaxation Method. SPE 743 presented at the Fall Meeting of the Petroleum Branch of AIME, Los Angeles, California, 14-17 October. <http://dx.doi.org/10.2118/743-G>.
- Buckley, J.S., Liu, Y., and Monsterleet, S. 1998. Mechanisms of Wetting Alteration by Crude Oils. *SPE Journal* **3** (1): 54-61. SPE-37230-PA. <http://dx.doi.org/10.2118/37230-PA>.
- Carlson, F.M. 1981. Simulation of Relative Permeability Hysteresis to the Nonwetting Phase. Paper SPE 10157 presented at the SPE Annual Technical Conference and Exhibition, San Antonio, Texas, USA, 4-7 October. <http://dx.doi.org/10.2118/10157-MS>.
- Craig, F.F. 1971. *The Reservoir Engineering Aspects of Waterflooding*, Vol. 2. Millet the Printer, Texas: Monograph Series, SPE.
- Det norske oljeselskap: *Frøy PDO Subsurface Support Document*. March 2008.
- Det norske oljeselskap: *Frøy Project DG2 Subsurface Report*. May 2008.
- Det norske oljeselskap: *PL 364 Frøy Redevelopment Project, Plan for Development and Operation*. August 2008.
- Dixit, A.B., McDougall, S.R., Sorbie, K.S. et al. 1999. Pore-Scale Modeling of Wettability Effects and Their Influence on Oil Recovery. *SPE Journal* **2** (1): 25-36. SPE-54454-PA. <http://dx.doi.org/10.2118/54454-PA>.
- Donaldson, E.C. and Alam, W. 2008. *Wettability*. Houston: Gulf Publishing Company.
- Donaldson, E.C., Thomas, R.D., and Lorenz, P.B. 1969. Wettability Determination and Its Effect on Recovery Efficiency. *SPE Journal* **9** (1): 13-20. SPE-2338-PA. <http://dx.doi.org/10.2118/2338-PA>.

Elf Petroleum Norge: *End of Well Report 25/5-A1 Anadrill Schlumberger*. (NODOC01-#858865-v1-FRØY_END_OF_WELL_REPORT). 1993.

Elf Petroleum Norge: *Maersk Gallant – Frøy, End of Well Report, Well: 25/5-A-7*. (NODOC01-#857456-v1-FRØY_END_OF_WELL_REPORT). 1995.

Fugro Geolab Nor: *Aspects of the Reservoir Geochemistry of the Frøy Field*. March 2009.

Geco Petroleum Laboratory: *Well 25/5-1, special core analysis*. September 1988.

Geffen, T.M., Owens, W.W., Parrish, D.R. et al. 1951. Experimental Investigation of Factors Affecting Laboratory Relative Permeability Measurements. *Trans, AIME*, **192**: 99-110.

Ghedan, S., Canbaz, C.H., Boyd, D. et al. 2010. Wettability Profile of a Thick Carbonate Reservoir by the New Rise in Core Wettability Characterization Method. Paper SPE 138697 presented at the Abu Dhabi International Petroleum Exhibition and Conference, Abu Dhabi, UAE, 1-4 November.
<http://dx.doi.org/10.2118/138697-MS>.

Ghorayeb, K., Tan, L.H., Limsukhon, M. et al. 2009. Ensuring Water Saturation Consistency Between Static (Fine-Grid) and Dynamic (Upscaled) Models – A Case Study of the North Kuwait Jurassic Complex. Paper SPE 125568 presented at the SPE/EAGE Reservoir Characterization and Simulation Conference, Abu Dhabi, UAE, 19-21 October. <http://dx.doi.org/10.2118/125568-MS>.

Goda, H.M. and Behrenbruch, P. 2004. Using a Modified Brooks-Corey Model to Study Oil-Water Relative Permeability for Diverse Pore Structures. Paper SPE 88538 presented at the SPE Asia Pacific Oil and Gas Conference and Exhibition, Perth, Australia, 18-20 October.
<http://dx.doi.org/10.2118/88538-MS>.

Hamon, G. 2000. Field-Wide Variations of Wettability. SPE 63144 presented at the SPE Annual Technical Conference and Exhibition, Dallas, Texas, 1-4 October. <http://dx.doi.org/10.2118/63144-MS>.

Holmes, M. 2002. Capillary Pressure & Relative Permeability Petrophysical Reservoir Models. Digital Formation, Inc. Denver, Colorado, USA, May 2002.
<http://www.digitalformation.com/Documents/CPRP.pdf>.

Jackson, M.D., Valvatne, P.H., and Blunt, M.J. 2005. Prediction of Wettability Variation Within an Oil/Water Transition Zone and Its Impact on Recovery. *SPE Journal* **10** (2): 185-195. SPE-77543-PA.
<http://dx.doi.org/10.2118/77543-PA>.

Jadhunandan, P.P. and Morrow, N.R. 1995. Effect of Wettability on Waterflood Recovery on Crude-Oil/Brine/Rock Systems. *SPE Journal* **10** (1): 40-46. SPE-22597-PA. <http://dx.doi.org/10.2118/22597-PA>.

Jerauld, G.R. and Rathmell, J.J. 1997. Wettability and Relative Permeability of Prudhoe Bay: A Case Study in Mixed-Wet Reservoirs. *SPE Journal* **12** (1): 58-65. SPE-28576-PA. <http://dx.doi.org/10.2118/28576-PA>.

Killough, J.E. 1976. Reservoir Simulation With History-Dependent Saturation Functions. *SPE Journal* **16** (1): 37-48. SPE-5106-PA. <http://dx.doi.org/10.2118/5106-PA>.

Land, C.S. 1968. Calculation of Imbibition Relative Permeability for Two- and Three-Phase Flow From Rock Properties. *SPE Journal* **8** (2): 149-156. SPE-1942-PA. <http://dx.doi.org/10.2118/1942-PA>.

Lenormand, R., Zarcone, C., and Sarr, A. 1983. Mechanisms of the displacement of one fluid by another in a network of capillary ducts. *J. Fluid Mech.* **135**: 337-353.
<http://dx.doi.org/10.1017/S0022112083003110>.

Lomeland F., Ebeltoft E., and Thomas W.H. 2005. A New Versatile Relative Permeability Correlation. Reviewed Proceedings of the 2005 International Symposium of the SCA, Abu Dhabi, United Arab Emirates, October 31 - November 2. SCA 2005-32.

Morrow, N.R. 1990. Wettability and its Effect on Oil Recovery. *SPE Journal* **42** (12): 1476-1484. SPE-21621-PA. <http://dx.doi.org/10.2118/21621-PA>.

Morrow, N.R., Ma, S., Zhou, X. et al. 1994. Characterization of Wettability From Spontaneous Imbibition Measurements. Paper PETSOC 94-47 presented at the Annual Technical Meeting, Calgary, Alberta, Jun 12 - 15. <http://dx.doi.org/10.2118/94-47>.

Numerical Rocks: *eCore Modelling on Frøy*. April 2009.

Owens, W.W. and Archer, D.L. 1971. The Effect of Rock Wettability on Oil-Water Relative Permeability Relationships. *SPE Journal* **23** (7): 873-878. SPE-3034-PA. <http://dx.doi.org/10.2118/3034-PA>.

Reslab Integration: *Verification of available water-oil and gas-oil relative permeability data*. RI 100009101107, October 2007.

Reslab Integration: *Validation of available relative permeability data from Frøy*. RI 100063010808, August 2008.

Reslab Integration: *Verification and recommendation of available water-oil relative permeability data for the Frøy field*. RI 100063020808. September 2008.

Reslab, Reservoir Laboratories: *Review of Frøy Requirements and Analytical Recommendations*. April 2008.

Roosta, A., Escrochi, M., Varzandeh, F. et al. 2009. Investigating the Mechanism of Thermally Induced Wettability Alteration. Paper SPE 120354 presented at the SPE Middle East Oil and Gas Show and Conference, Bahrain, Bahrain, 15-18 March. <http://dx.doi.org/10.2118/120354-MS>.

Salathiel, R.A. 1973. Oil Recovery by Surface Film Drainage In Mixed-Wettability Rocks. *SPE Journal* **25** (10): 1216-1224. SPE-4104-PA. <http://dx.doi.org/10.2118/4104-PA>.

Schlumberger: *ECLIPSE reservoir simulation software, ECLIPSE Technical Description*. Version 2010.2. 2010.

Seethepalli, A., Adibhatla, B., and Mohanty, K.K. 2004. Wettability Alteration During Surfactant Flooding of Carbonate Reservoirs. Paper SPE 89423 presented at the SPE/DOE Symposium on Improved Oil Recovery, Tulsa, Oklahoma, 17-21 April. <http://dx.doi.org/10.2118/89423-MS>.

Selboe, K. 2010. Low Salinity Waterflooding in North Sea Reservoir Rocks: An Experimental Investigation with emphasis on Wettability Effects. MS thesis, NTNU, Trondheim, Norway (June 2010).

Sintef Petroleum Research: *Polar compounds in the Frøy field reservoir (PL 364)*. July 2008.

Spiteri, E.J., Juanes, R., Blunt, M.J. et al. 2008. A New Model of Trapping and Relative Permeability Hysteresis for All Wettability Characteristics. *SPE Journal* **13** (3): 277-288. SPE-96448-PA. <http://dx.doi.org/10.2118/96448-PA>.

Stensen, J.Å. and Førlund, T. *Aspects of Reservoir Geochemistry on Productivity of the Frøy Field – A Summary Report*. October 2009.

Tangen, M. Modeling Relative Permeability for Different Wettability Characteristics. Specialization Project in reservoir engineering, NTNU, Trondheim, Norway (December 2012).

Torsæter, O. and Abtahi, M. 2003. Experimental Reservoir Engineering Laboratory Workbook. Department of Petroleum Engineering and Applied Geophysics, Norwegian University of Science and Petroleum (NTNU), Norway.

Valvatne, P.H. and Blunt, M.J. 2004. Predictive pore-scale modeling of two-phase flow in mixed wet media. *Water Resources Research* **40**. <http://dx.doi.org/10.1029/2003WR002627>.

Vledder, P., Fonseca, J.C., Wells, T. et al. 2010. Low Salinity Water Flooding: Proof Of Wettability Alteration On A Field Wide Scale. Paper SPE 129564 presented at the SPE Improved Oil Recovery Symposium, Tulsa, Oklahoma, USA, 24-28 April. <http://dx.doi.org/10.2118/129564-MS>.

Weatherford Laboratories: *Frøy – Wettability Study of Native State Core*. August 2009.

Weatherford Petroleum Consultants, product description, SENDRA: <http://www.wftpc.com/sendra.aspx>.

Wendel, D.J., Anderson, W.G., and Meyers, J.D. 1987. Restored-State Core Analysis for the Hutton Reservoir. *SPE Journal* **2** (4): 509-517. SPE-14298-PA. <http://dx.doi.org/10.2118/14298-PA>.

Yildiz, H.O., Ozturun, F.B., and Sirkecki, A.A. 2010. Determination of Reservoir Rock Wettability By Thin Layer Wicking Approach. Paper SPE 136936 presented at the SPE/DGS Saudi Arabia Section Technical Symposium and Exhibition, Al-Khobar, Saudi Arabia, 4-7 April. <http://dx.doi.org/10.2118/136936-MS>.

Yu, L., Evje, S., Kleppe, H. et al. 2008. Analysis of the Wettability Alteration Process During Seawater Imbibition Into Preferentially Oil-Wet Chalk Cores. Paper SPE 113304 presented at the SPE/DOE Symposium on Improved Oil Recovery, Tulsa, Oklahoma, USA, 20-23 April. <http://dx.doi.org/10.2118/113304-MS>.

Zolotukhin, A.B. and Ursin, J-R. 2000. *Introduction to Petroleum Reservoir Engineering*. Norway: Høyskoleforlaget.

APPENDICES

A APPENDIX A – Key figures and tables regarding SCAL measurements on Frøy

Case	N_o	N_w	S_{or}	$k_{rw}(S_{or})$
High	4.5	2	0.05	0.45
Base	5.5	1.8	0.08	0.55
Low	6.5	1.6	0.12	0.65

Table A.1 – Recommendations for Well 25/5-A1, $S_{wi} = 0.2$ (ResLab Integration 2008)

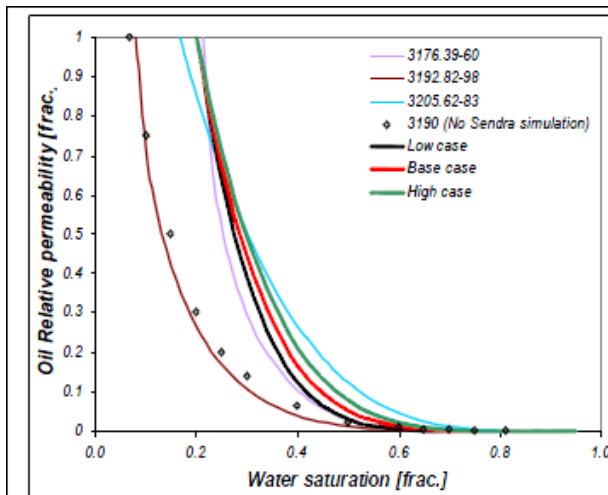


Figure 3.1 Recommended oil relative permeability, lin-lin plot.

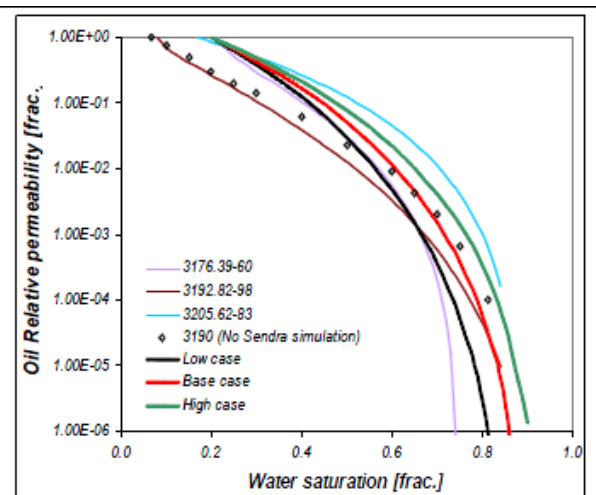


Figure 3.2 Recommended oil relative permeability, semilog plot.

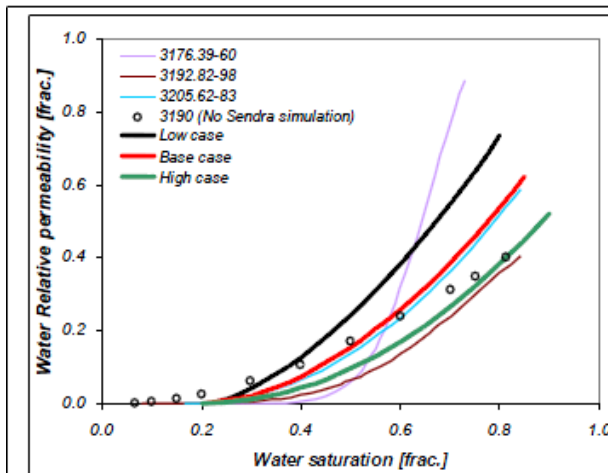


Figure 3.3 Recommended water relative permeability, lin-lin plot.

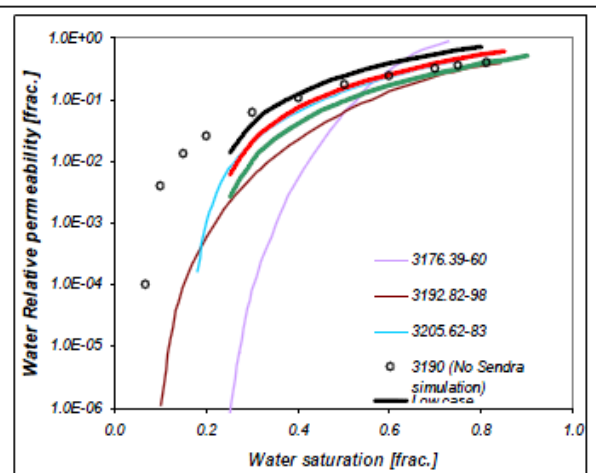


Figure 3.4 Recommended water relative permeability, semilog plot.

Figure A.1 – Recommendations for Well 25/5-A1, $S_{wi} = 0.2$ (ResLab Integration 2008)

Case	N_o	N_w	S_{or}	$K_{rw}(S_{or})$
High	5	2	0.05	0.6
Base	5.5	1.8	0.08	0.75
Low	6	1.6	0.12	0.9

Table A.2 – Recommendations for Well 25/5-A7, $S_{wi} = 0.2$ (ResLab Integration 2008)

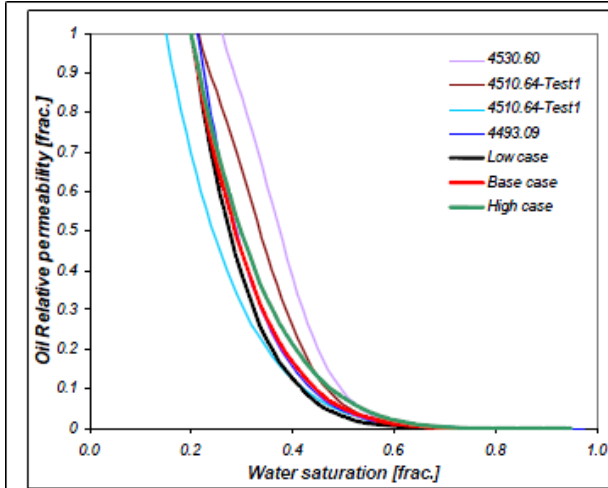


Figure 3.5 Recommended oil relative permeability, lin-lin plot.

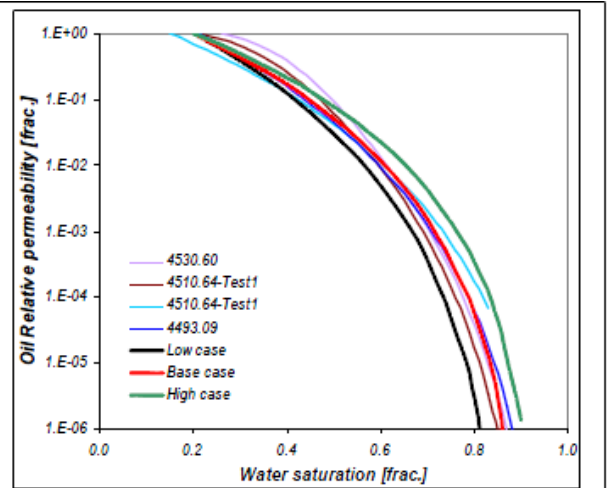


Figure 3.6 Recommended oil relative permeability, semilog plot.

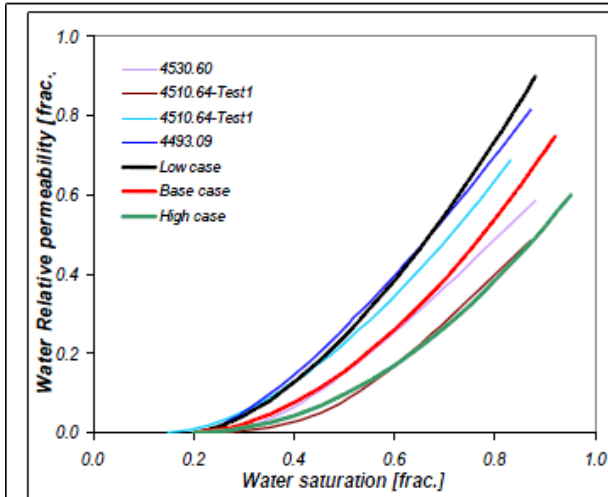


Figure 3.7 Recommended water relative permeability, lin-lin plot.

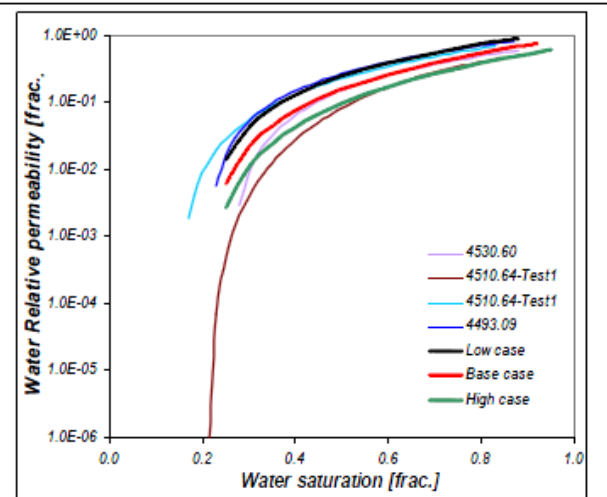


Figure 3.8 Recommended water relative permeability, semilog plot.

Figure A.2 – Recommendations for Well 25/5-A7, $S_{wi} = 0.2$ (ResLab Integration 2008)

Case	N_o	N_w	S_{or}	$k_{rw}(S_{or})$
High	5	2	0.1	0.3
Base	5.7	1.8	0.12	0.37
Low	6.3	1.3	0.15	0.4

Table A.3 – Recommendations for Well 25/5-1, $S_{wi} = 0.2$ (ResLab Integration 2008)

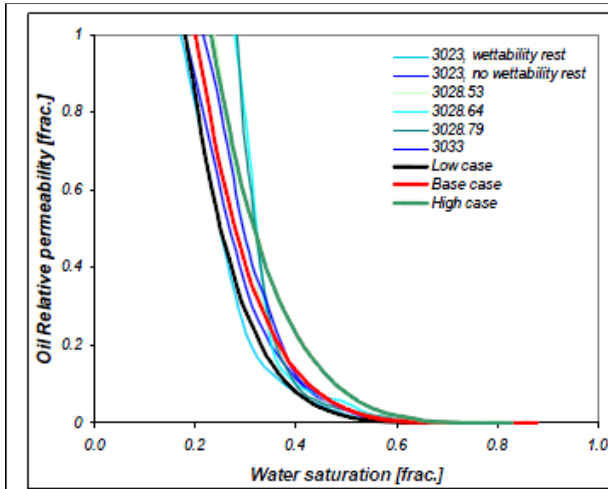


Figure 3.9 Recommended oil relative permeability, lin-lin plot.

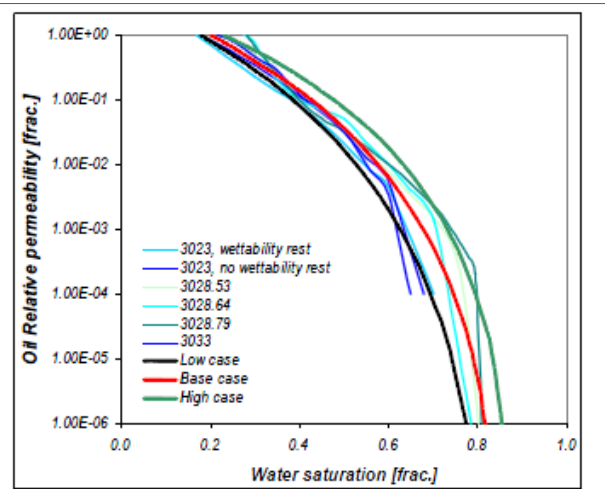


Figure 3.10 Recommended oil relative permeability, semilog plot.

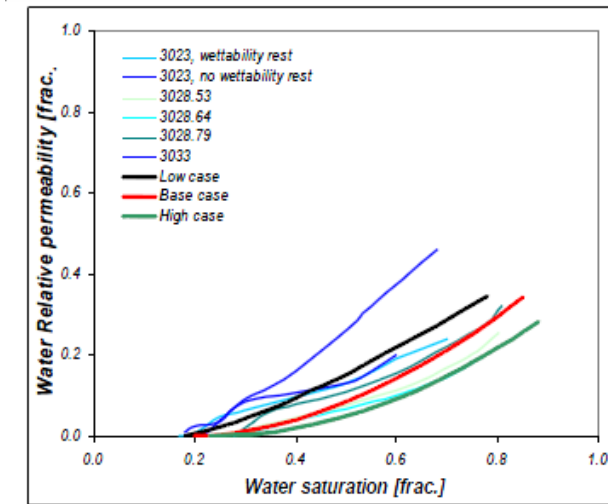


Figure 3.11 Recommended water relative permeability, lin-lin plot.

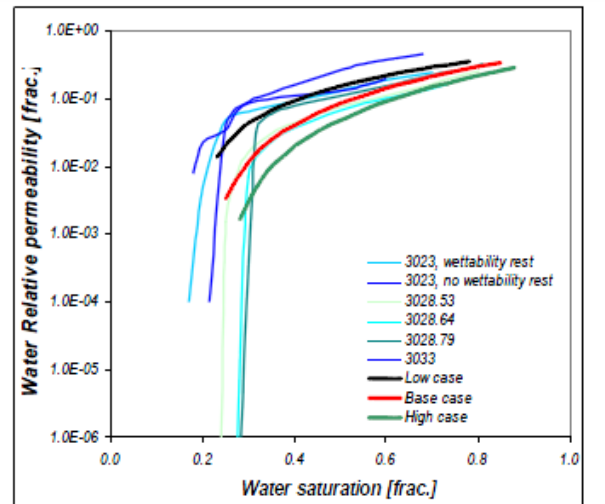


Figure 3.12 Recommended water relative permeability, semilog plot.

Figure A.3 – Recommendations for Well 25/5-1, $S_{wi} = 0.2$ (ResLab Integration 2008)

Sample	S_{wi} [frac]	k_{ro} (S_{wi})	L_w	E_w	T_w	L_o	E_o	T_o
3031.93	0.22	1	2.55	2.4	0.82	3.1	4.9	0.9
3205.55	0.17	1	2.8	7	1.24	4.05	1.1	1.02
3215.52	0.24	1	2.85	2.8	0.7	2.8	2.3	0.9
3221.83	0.25	1	2.6	7.4	0.9	2.35	1.2	0.9

Table A.4 – Simulated drainage data (Numerical Rocks 2009)

Sample	S_{orw}	$k_{rw}(S_{orw})$	L_w	E_w	T_w	L_o	E_o	T_o	AI
3031.93	0.10	0.70	2.45	2.5	0.54	3.1	2.4	0.76	-0.2
3205.55	0.08	0.72	1.85	3.3	1.29	4.6	1	0.69	0
3215.52	0.07	0.78	2	4.9	1.1	2.9	3.8	1.18	-0.23
3221.83	0.05	0.77	2.45	5.7	1.74	3.4	4.2	1.33	-0.25

Table A.5 – Simulated waterflood data (Numerical Rocks 2009)

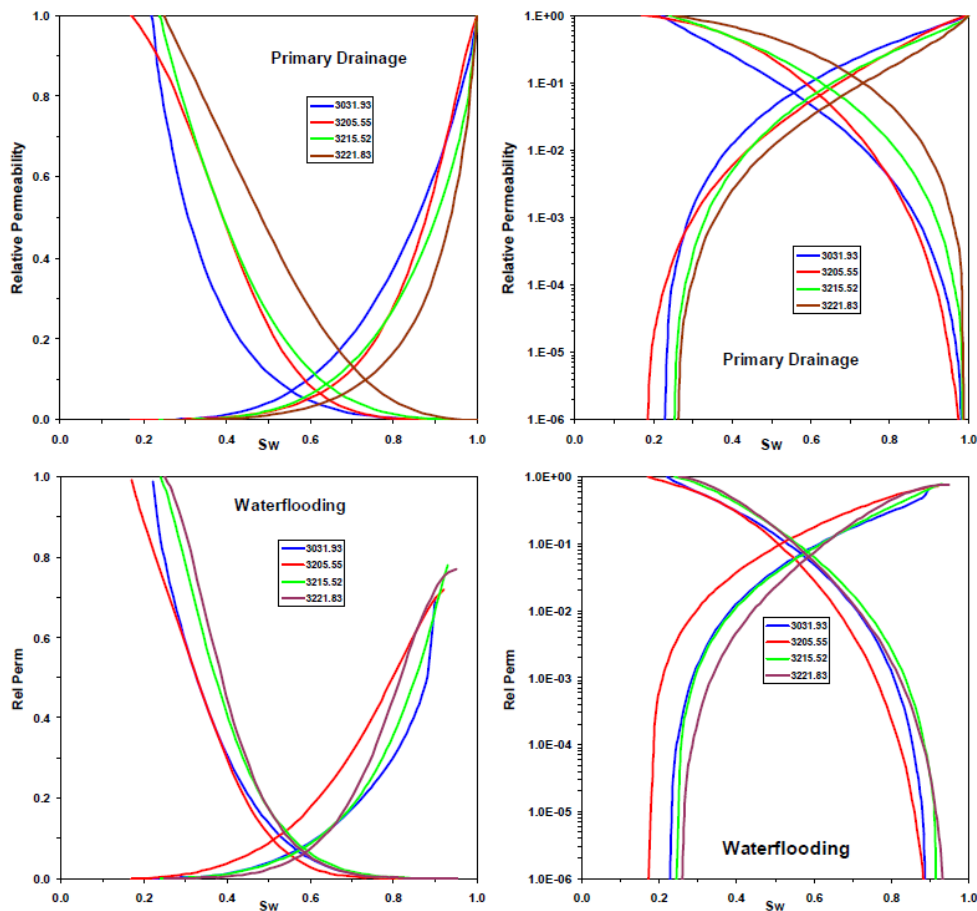


Figure A.4 – Relative permeability curves generated by pore scale models (Numerical Rocks 2009)

Fraction oil wet pores	Water-wet Adv. Angles	Oil-wet Adv. Angles	Simulated Amott Index
0.4	30-80	110-140	0.4
0.6	30-80	120-160	0
0.8	30-80	130-170	-0.4

Table A.6 – Input data for wettability sensitivity study (Numerical Rocks 2009)

Sample	Amott Index	S_{orw}	$kr_w(S_{orw})$	L_w	E_w	T_w	L_o	E_o	T_o
3205.55	0.4	0.19	0.43	2.95	1.7	0.61	3.1	1.7	1.23
3205.55	-0.4	0.03	0.92	1.7	6.7	1.71	3.7	7.2	1.55

Table A.7 – Endpoints and optimized LET-parameters for simulated relative permeability curves (Numerical Rocks 2009)

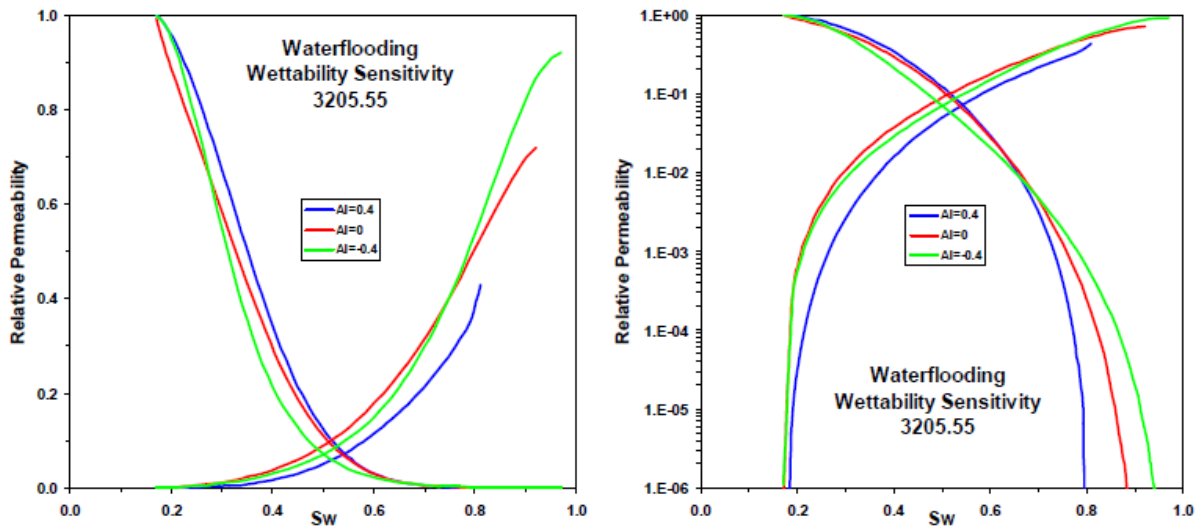


Figure A.5 – Relative permeability curves for wettability sensitivity study (Numerical Rocks 2009)

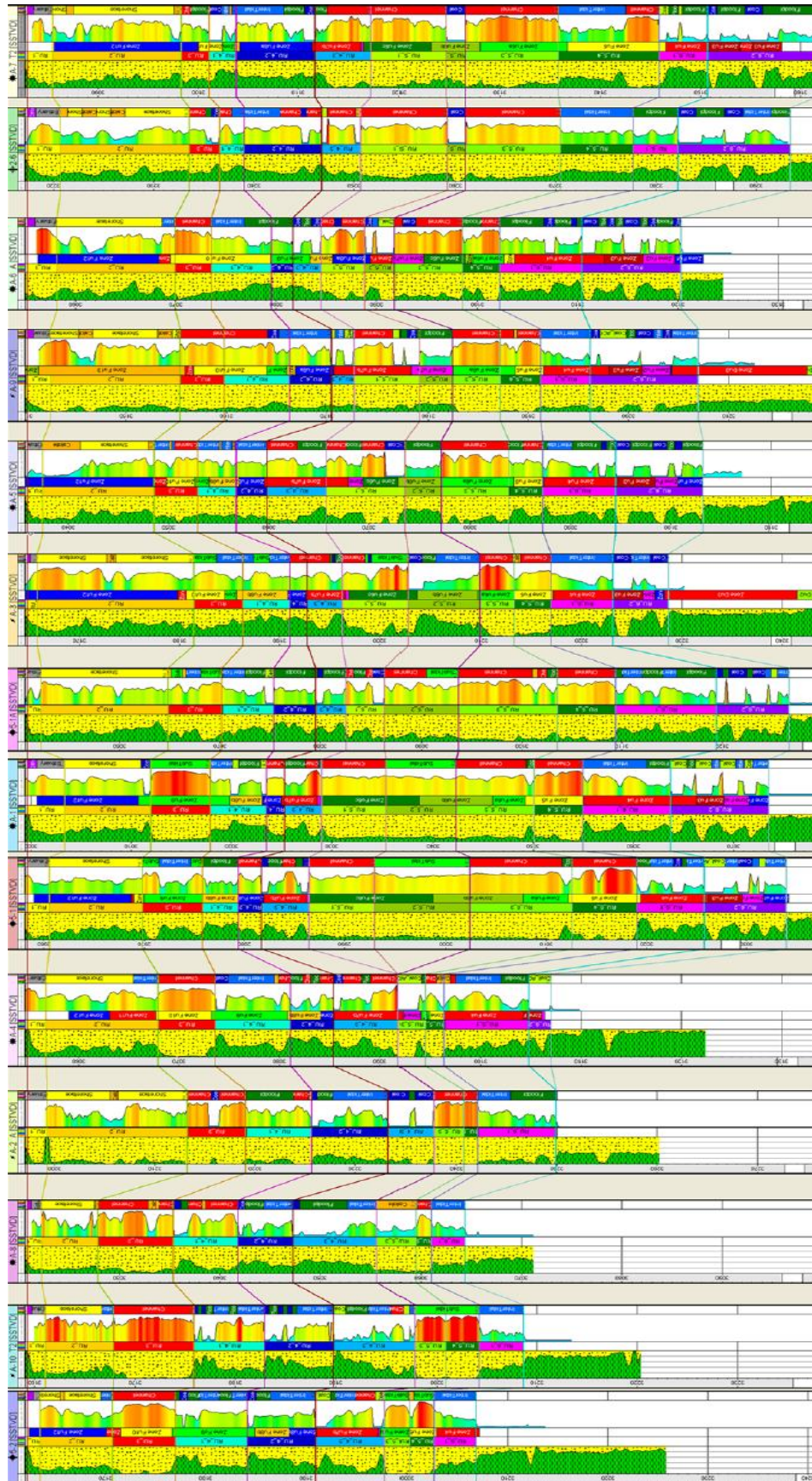


Figure A.6 – Well correlations (Frøy PDO, Det norske)

B APPENDIX B – Data describing the PDO simulation model

SWOF							
-- Sw	Krw	Krow	Pcowc				
0.12	0.000000	1.0	0.54430772				
0.13	0.000581764239574	0.936683655937	0.445641469	0.56	0.361923324167	0.0157291433924	8.20452E-05
0.14	0.00189015759083	0.876645487498	0.364860376	0.57	0.376017705977	0.0135858213134	6.71729E-05
0.15	0.00376576448375	0.819754555029	0.298722241	0.58	0.390333059764	0.0116848310208	5.49965E-05
0.16	0.00614114013058	0.765883560325	0.244573224	0.59	0.404867933152	0.0100047111625	4.50273E-05
0.17	0.00897420589841	0.714908790675	0.20023962	0.60	0.419620914249	0.0085253448438	3.68653E-05
0.18	0.0122350049042	0.666710063056	0.163942335	0.61	0.434590629691	0.00722791231962	3.01827E-05
0.19	0.0159006065044	0.621170668483	0.134224631	0.62	0.449775742823	0.00609484397236	2.47115E-05
0.20	0.0199526231497	0.578177316491	0.109893833	0.63	0.465174951991	0.00510977358292	2.02321E-05
0.21	0.0243758230266	0.53762007978	0.089973461	0.64	0.480786988961	0.00425749190239	1.65646E-05
0.22	0.0291572809855	0.499392339008	0.073664039	0.65	0.496610617422	0.00352390053237	1.3562E-05
0.23	0.0342858236404	0.46339072773	0.060311014	0.66	0.512644631598	0.0028959661224	1.11036E-05
0.24	0.0397516482113	0.429515077505	0.049378482	0.67	0.528887854935	0.00236167489359	9.09086E-06
0.25	0.0455460502581	0.397668363149	0.040427682	0.68	0.545339138869	0.001909987498	7.44297E-06
0.26	0.0516612229469	0.367756648147	0.033099387	0.69	0.561997361676	0.00153079422421	6.09379E-06
0.27	0.0580901051375	0.339689030234	0.027099486	0.70	0.578861427372	0.00121487056	4.98917E-06
0.28	0.0648262638677	0.313377587131	0.022187182	0.71	0.595930264696	0.000953833124101	4.08479E-06
0.29	0.0718638017279	0.288737322443	0.018165328	0.72	0.613202826133	0.000740095979741	3.34434E-06
0.30	0.0791972826661	0.265686111732	0.014872513	0.73	0.630678087	0.000566827343947	2.73812E-06
0.31	0.0868216717133	0.244144648748	0.012176584	0.74	0.648355044584	0.000427906707512	2.24178E-06
0.32	0.0947322854069	0.22403639184	0.009969344	0.75	0.666232717314	0.0003178823821	1.83541E-06
0.33	0.102924750563	0.205287510536	0.008162208	0.76	0.684310143994	0.000231929492377	1.50271E-06
0.34	0.111394969652	0.187826832291	0.006682651	0.77	0.702586383061	0.000165808432917	1.23031E-06
0.35	0.120139091468	0.171585789425	0.005471292	0.78	0.721060511885	0.000115823811683	1.0073E-06
0.36	0.129153486075	0.15649836623	0.004479515	0.79	0.739731626111	7.87839043483e-05	8.24705E-07
0.37	0.138434723259	0.142501046264	0.003667517	0.80	0.758598839025	5.19606466335e-05	6.75211E-07
0.38	0.147979553867	0.129532759831	0.003002709	0.81	0.777661280954	3.30501953232e-05	5.52816E-07
0.39	0.157784893556	0.117534831641	0.00245841	0.82	0.796918098694	2.01340928768e-05	4.52608E-07
0.40	0.167847808549	0.10645092867	0.002012776	0.83	0.816368454971	1.16410757895e-05	3.70564E-07
0.41	0.178165503103	0.0962270082054	0.001647921	0.84	0.836011527917	6.3095734448e-06	3.03392E-07
0.42	0.18873530841	0.0868112660897	0.001349204	0.85	0.855846510576	3.15095264074e-06	2.48396E-07
0.43	0.199554672751	0.0781540851625	0.001104635	0.86	0.875872610435	1.41357406863e-06	2.0337E-07
0.44	0.210621152693	0.0702079839046	0.000904398	0.87	0.89608904897	5.47742059229e-07	1.66505E-07
0.45	0.221932405223	0.0629275652874	0.000740459	0.88	0.916495061218	1.71650084892e-07	1.36323E-07
0.46	0.233486180659	0.0562694658301	0.000606236	0.89	0.93708989536	3.84558656782e-08	1.11612E-07
0.47	0.245280316275	0.0501923048689	0.000496344	0.90	0.957872812329	4.66968994038e-09	9.13799E-08
0.48	0.257312730522	0.044656634042	0.000406372	0.91	0.978843085436	1.27037537751e-10	7.48155E-08
0.49	0.269581417785	0.0396248869931	0.00033271	0.92	1.000000	0.0000000	6.12538E-08
0.50	0.282084443619	0.0350613292991	0.0002724	1	1.000000	0.0000000	1.00E-32
0.51	0.294819940399	0.0309320086236	0.000223022				
0.52	0.307786103336	0.027204705103	0.000182595				
0.53	0.320981186839	0.0238488819672	0.000149496				
0.54	0.334403501155	0.0208356364019	0.000122397				
0.55	0.348051409292	0.0181376506546	0.00010021				

Table B.1 – Oil-water saturation function table used by Det norske (table split in two)

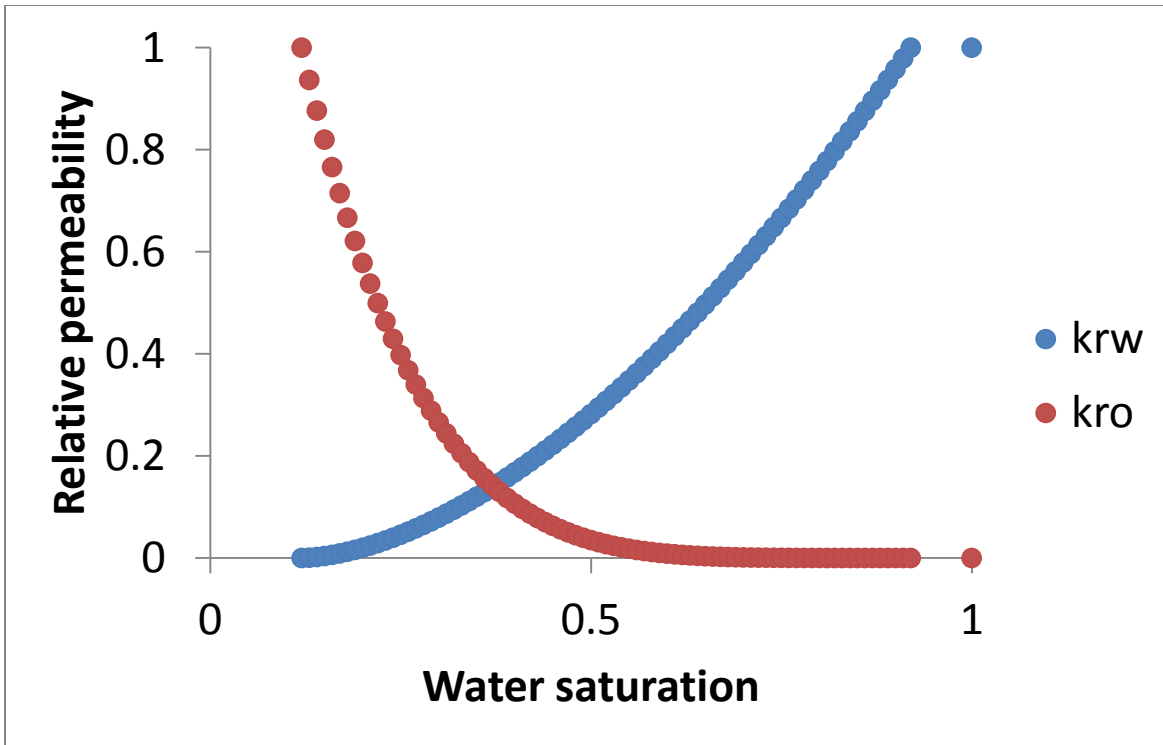


Figure B.1 – Relative permeability curves used by Det norske for the Frøy field

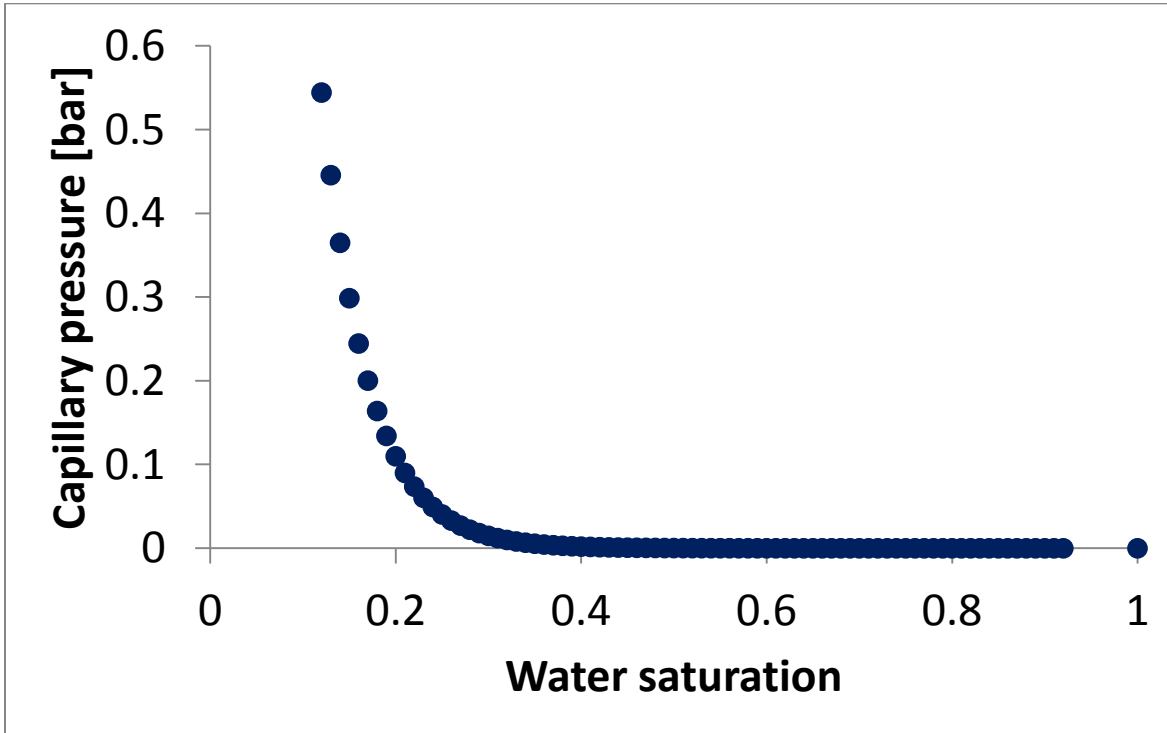


Figure B.2 – Capillary pressure curve used by Det norske for the Frøy field

C APPENDIX C – A modified copy of BO_8_001.DATA

RUNSPEC

MULTREAL
'd90f8a00-7e8a-446a-95b2-b2758e43d261' 'YES' /

TITLE
Frøy Field History Match Production from May 1995 to June 2001

DIMENS
74 107 36 /

METRIC
DISGAS
WATER
OIL
GAS

-- Use end point scaling for saturation regions
ENDSCALE
/

START
1 MAY 1995 /

GRIDOPTS
YES 30 /

REGDIMS
10 30 /

FAULTDIM
1750 /

EQLOPTS
/

EQLDIMS
1 100 40 /

WELLDIMS
30 200 7 10 5* 33 /

VFPPDIMS
10 8 10 8 8 1 /

UNIFIN
UNIFOUT

TABDIMS
2 1 100 197 1* 197 197 /

AQUDIMS
4* 1 5000 /

SAVE
/

NSTACK
50 /

MESSAGES

1* 1* 1* 1* 1* 1*
100000 50000 10000 3333333 100 1* /

GRID

INIT
GRIDFILE
2 1 /

MINPV
5 /

INCLUDE
'../INCLUDE/G5_NOACT.GRDECL' /

INCLUDE
'../INCLUDE/G5_ACTNUM.INC' /
NOECHO

INCLUDE
'../INCLUDE/PORO1.INC' /

INCLUDE
'../INCLUDE/PERMX1.INC' /

INCLUDE
'../INCLUDE/PERMY1.INC' /

INCLUDE
'../INCLUDE/PERMZ1.INC' /

INCLUDE
'../INCLUDE/FACIES1.INC' /

--Faults
INCLUDE
'../INCLUDE/G4_FAULTS_PURPLECX_ADJUSTED.INC' /

INCLUDE
'../INCLUDE/G3TOG4_NEWG4_FAULTS_HM99_BVI2.INC' /

INCLUDE
'../INCLUDE/G3-F11-A_BOTTOM.INC' /

INCLUDE
'../INCLUDE/G5FA7NN2_FAULTS.INC' /

INCLUDE
'../INCLUDE/TS_FAULTS.INC' /

INCLUDE
'../INCLUDE/A5A6BARRIERS.INC' /

INCLUDE
'MULTFLT_NEW2.MINC' /

INCLUDE
'G3TOG4_NEWG4_MULTFLT.MINC' /

INCLUDE
'G3-F11-A_BOTTOM_MULTFLT.MINC' /

```

INCLUDE
'G5FA7NN2_MULTFLT.MINC' /

INCLUDE
'TS_MULTFLT.MINC' /

INCLUDE
'././INCLUDE/A4A10AREA_FAULTS.INC' /

INCLUDE
'././INCLUDE/A9A6AREA_FAULTS.INC' /

INCLUDE
'A5A6_MULTFLT.MINC' /

MULTFLT
'BEIGE_B' 0.0 /
'WHITEB' 0.0 /
/

EQUALS
MULTX 1.0 1 74 1 107 1 36 /
MULTY 1.0 1 74 1 107 1 36 /
MULTZ 1.0 1 74 1 107 1 36 /
MULTZ- 1.0 1 74 1 107 1 36 /
/

INCLUDE
'MULTZ.MINC' /

INCLUDE
'MULTY_A8N.MINC' /

INCLUDE
'A-2BARRIER.MINC' /

EDIT

INCLUDE
'MULTPV.MINC' /

PROPS

INCLUDE
'././INCLUDE/SCALECRS.INC' /

-- Initial water saturations using SWATINIT from Petrel
INCLUDE
'././INCLUDE/SWAT1.INC' /

FILLEPS

-- Rock compressibility
INCLUDE
'././INCLUDE/ROCK.INC' /

INCLUDE
'././INCLUDE/PVT_DEWPOINT_2011/DEWPOINT_BO_18-01-
2011_OLDPROCESS_PVDG_3025.PVT' /

INCLUDE
'SGOF5_BVI.MINC' /

INCLUDE
'SWOF5_SW1_BVI.MINC' /

INCLUDE
'SOWCR_MULTNUM.MINC' /

EQUALS
SOWCR 0.08 1 74 1 107 1 4 /
/

-- Connate water 12 %; i.e. smallest water saturation in an
SATFUNC
SWL
285048*0.12 /

-- Critical water saturation; equal initial SWATINIT
INCLUDE
'././INCLUDE/SWCR_FROM_SWATINIT.INC' /

INCLUDE
'MULTSWCR_BVI.MINC' /

MINVALUE
SWCR 0.12 /
/

MAXVALUE
SWCR 0.7799 /
/

--Adjust the gas saturation table for connate water
SGU
285048*0.88 /

INCLUDE
'SGCR_MULTNUM.MINC' /

EQUALS
SGCR 0.07 1 74 1 107 1 4 /
/

INCLUDE
'SOGCR_MULTNUM.MINC' /

EQUALS
SOGCR 0.08 1 74 1 107 1 4 /
/

INCLUDE
'KRWR_MULTNUM.MINC' /

EQUALS
KRWR 0.8 1 74 1 107 1 4 /
/

KRW
285048*1.0000 /

REGIONS

INCLUDE
'././INCLUDE/SATNUM_BVI.INC' /

INCLUDE
'././INCLUDE/FIPNUM_BVI.INC' /

```


SOLUTION

```
EQUIL
-- datum pressure owc Pcowc GOC Pcgoc RSVD RVVD equil
 2930 306 3176 0 2870 0 1 1 0/
```

```
RPTSOL
'FIP=3' 'FIPRESV' 'RESTART=2' /
```

```
RPTSOL
RESTART=2 SWAT SOIL SGAS 'FIP=3' 'FIPRESV' PBUB RSSAT
PRESSURE /
```

```
INCLUDE
'AQUIFER.MINC' /
```

```
INCLUDE
'../INCLUDE/PVT_DEWPOINT_2011/DEWPOINT_BO_18-01-
2011_OLDPROCESS_RSVD.INC' /
```

SUMMARY

```
INCLUDE
'../INCLUDE/HIST_SUM_BVI.INC' /
```

```
PERFORMA
```

```
SCHEDULE
```

```
TSTEP
0.01 /
```

```
INCLUDE
'G4_SCHED_BUILDUP_BO.INC' /
```

```
END
```


D APPENDIX D – Simulation results

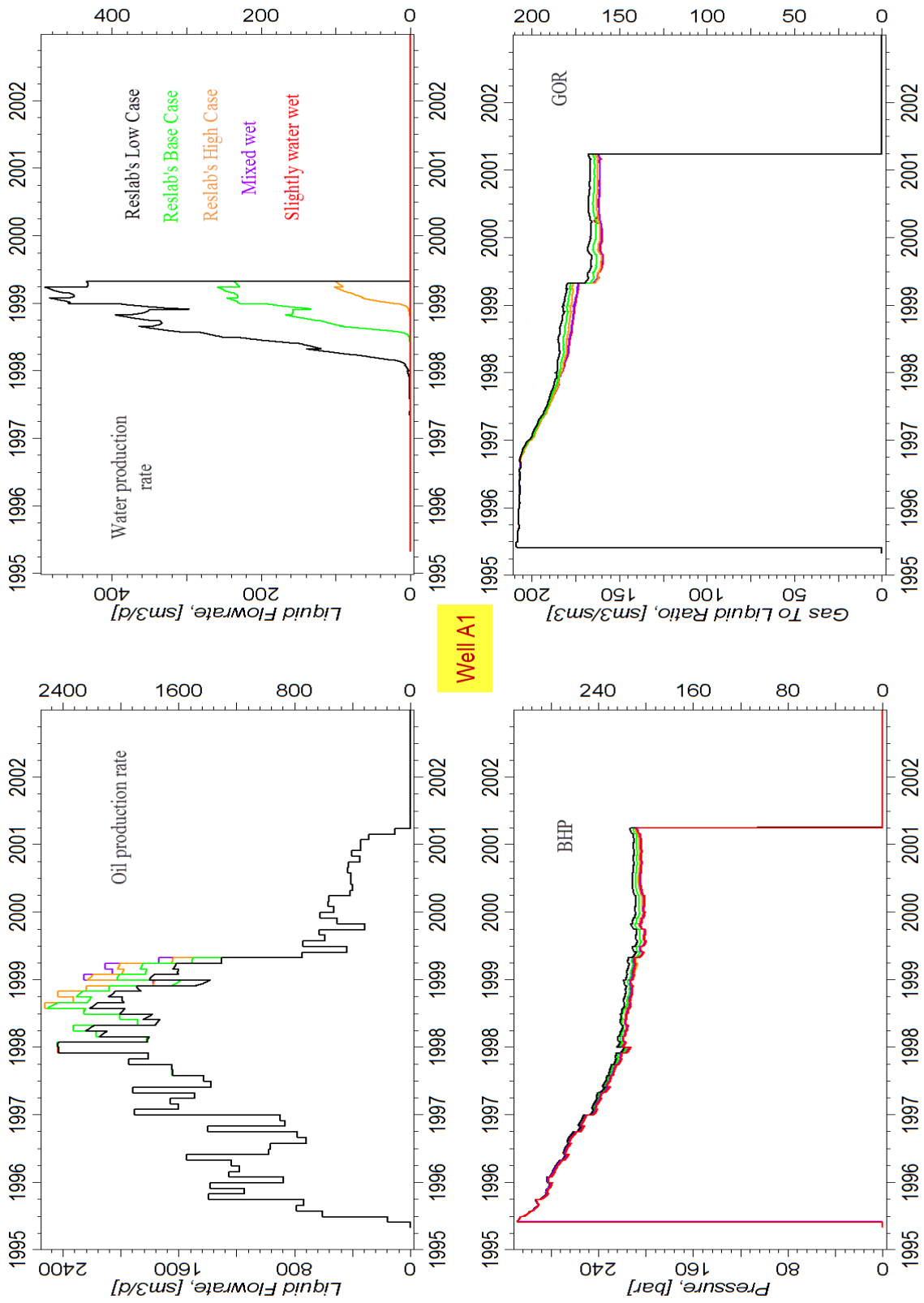


Figure D.1 – Performance of A1 as a function of wettability, 1 SATNUM region

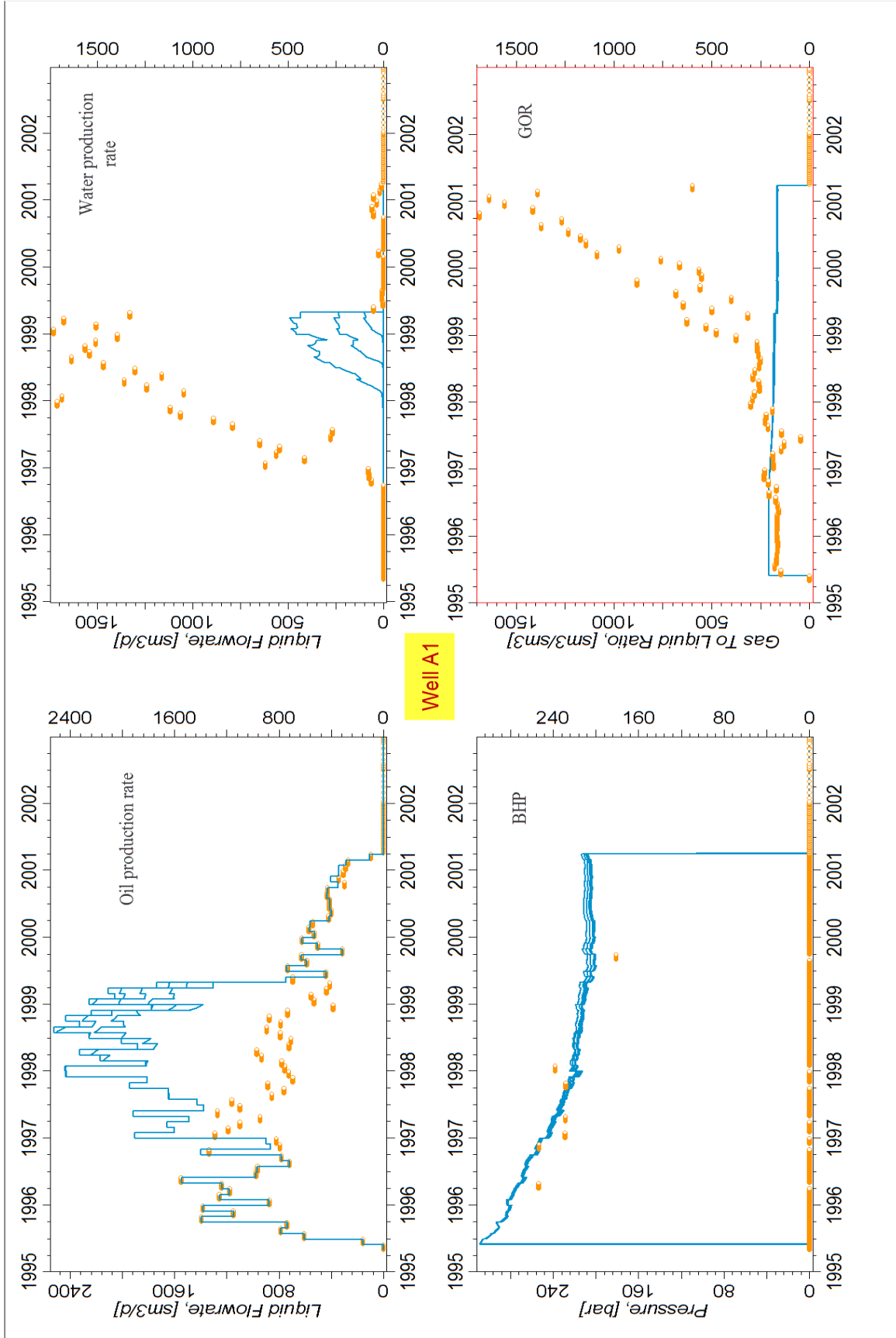


Figure D.2 – Comparison of simulation cases and historic performance of A1, 1 SATNUM region

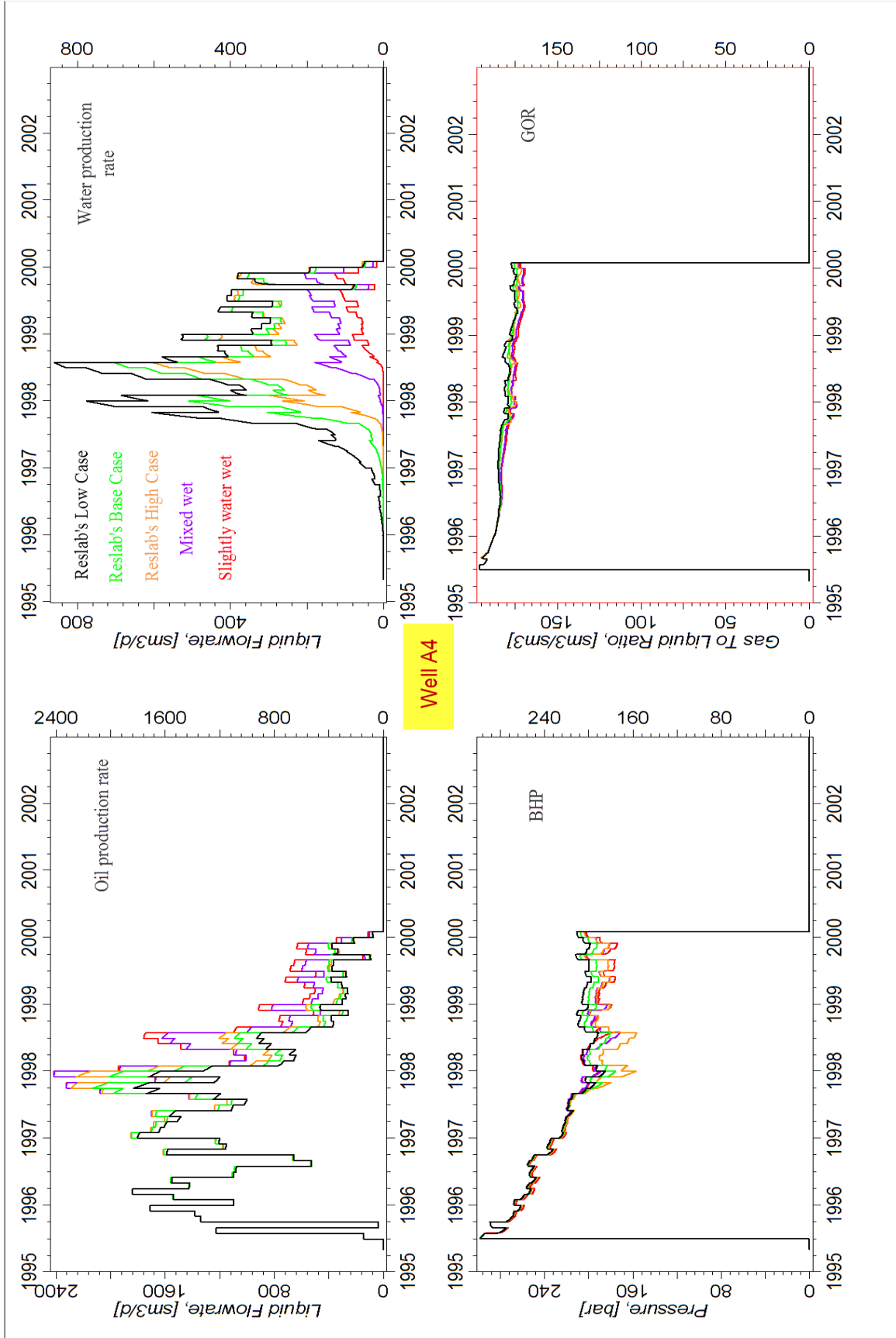


Figure D.3 – Performance of A4 as a function of wettability, 1 SATNUM region

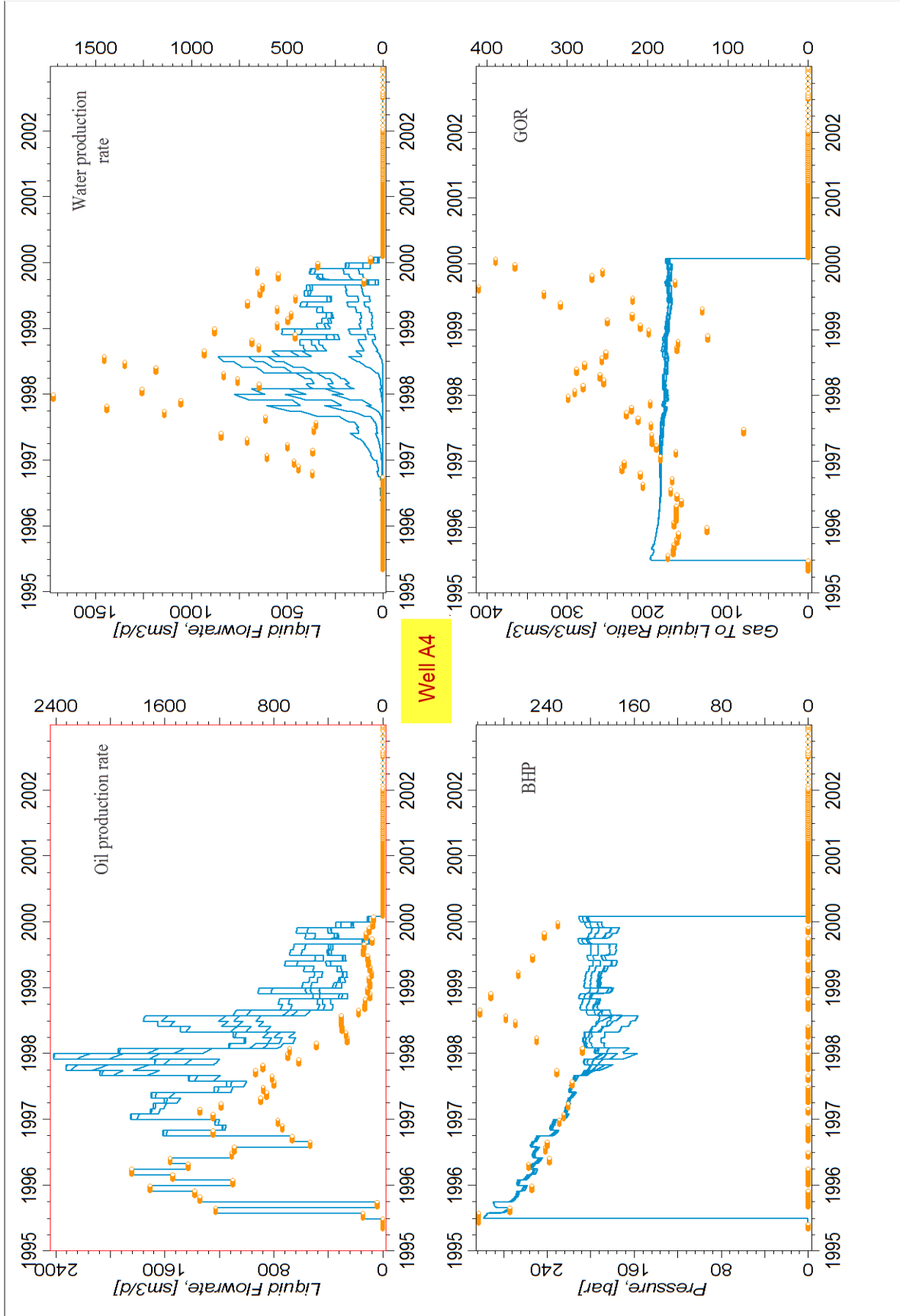


Figure D.4— Comparison of simulation cases and historic performance of A4, 1 SATNUM region

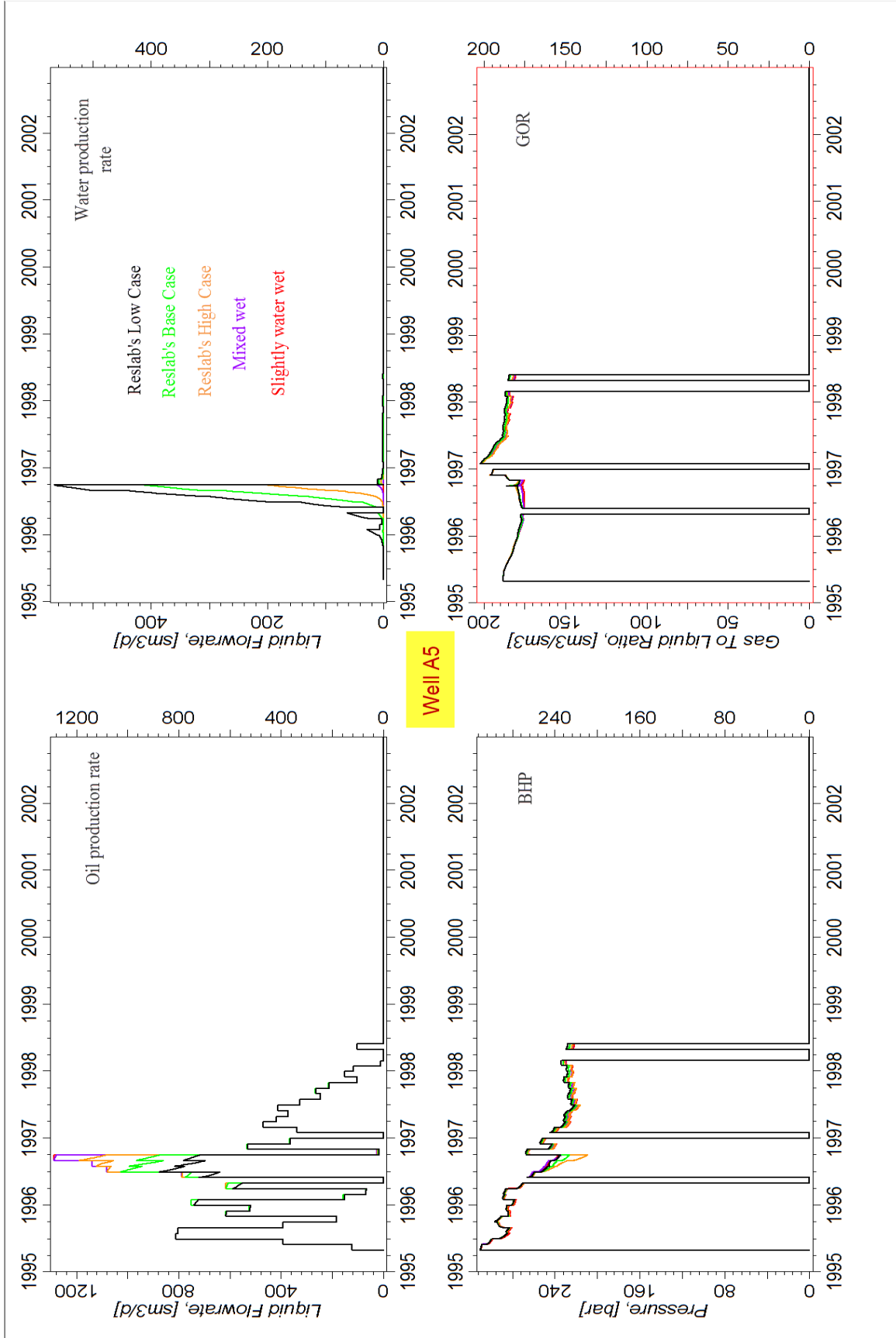


Figure D.5 – Performance of A5 as a function of wettability, 1 SATNUM region

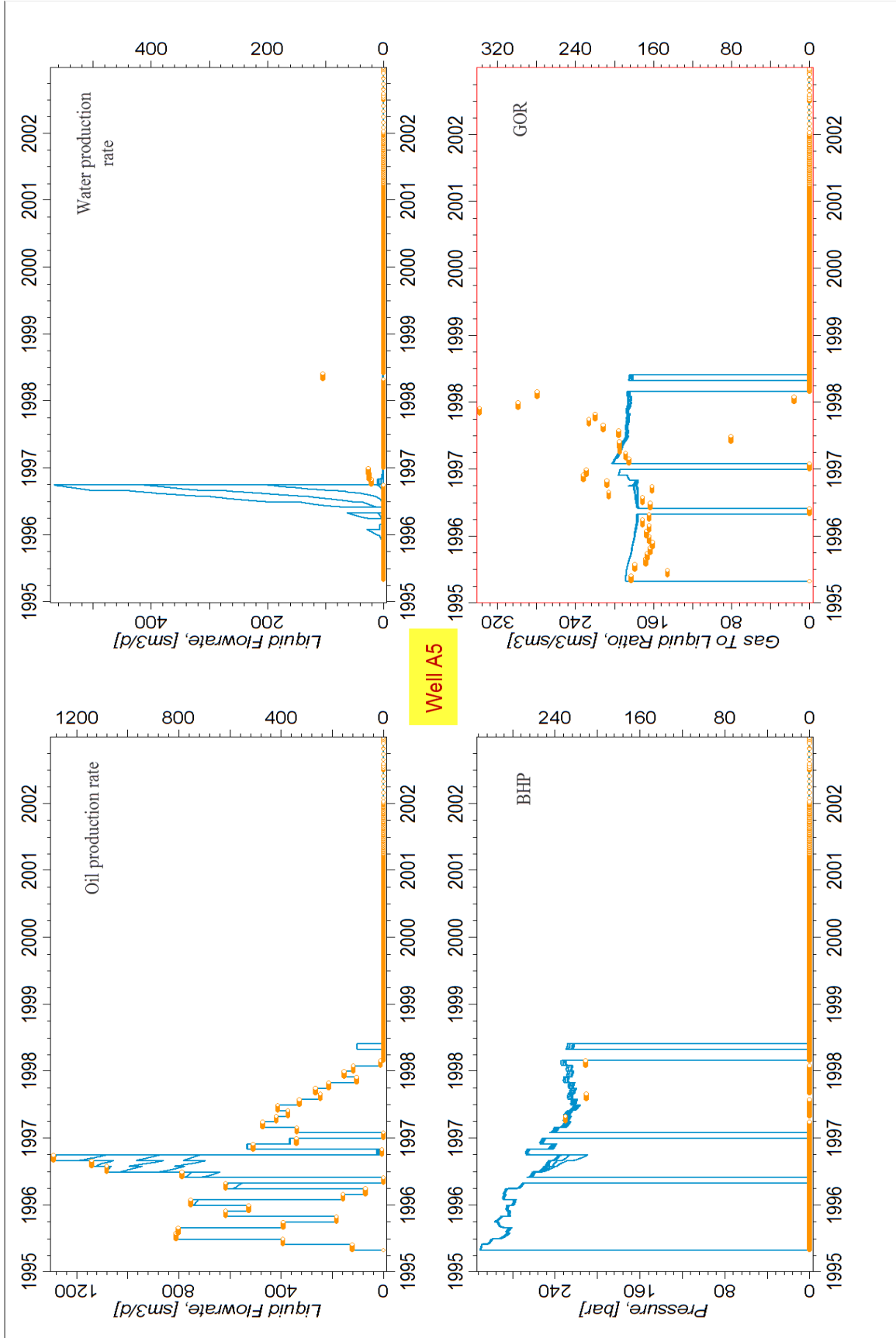


Figure D.6 – Comparison of simulation cases and historic performance of A5, 1 SATNUM region

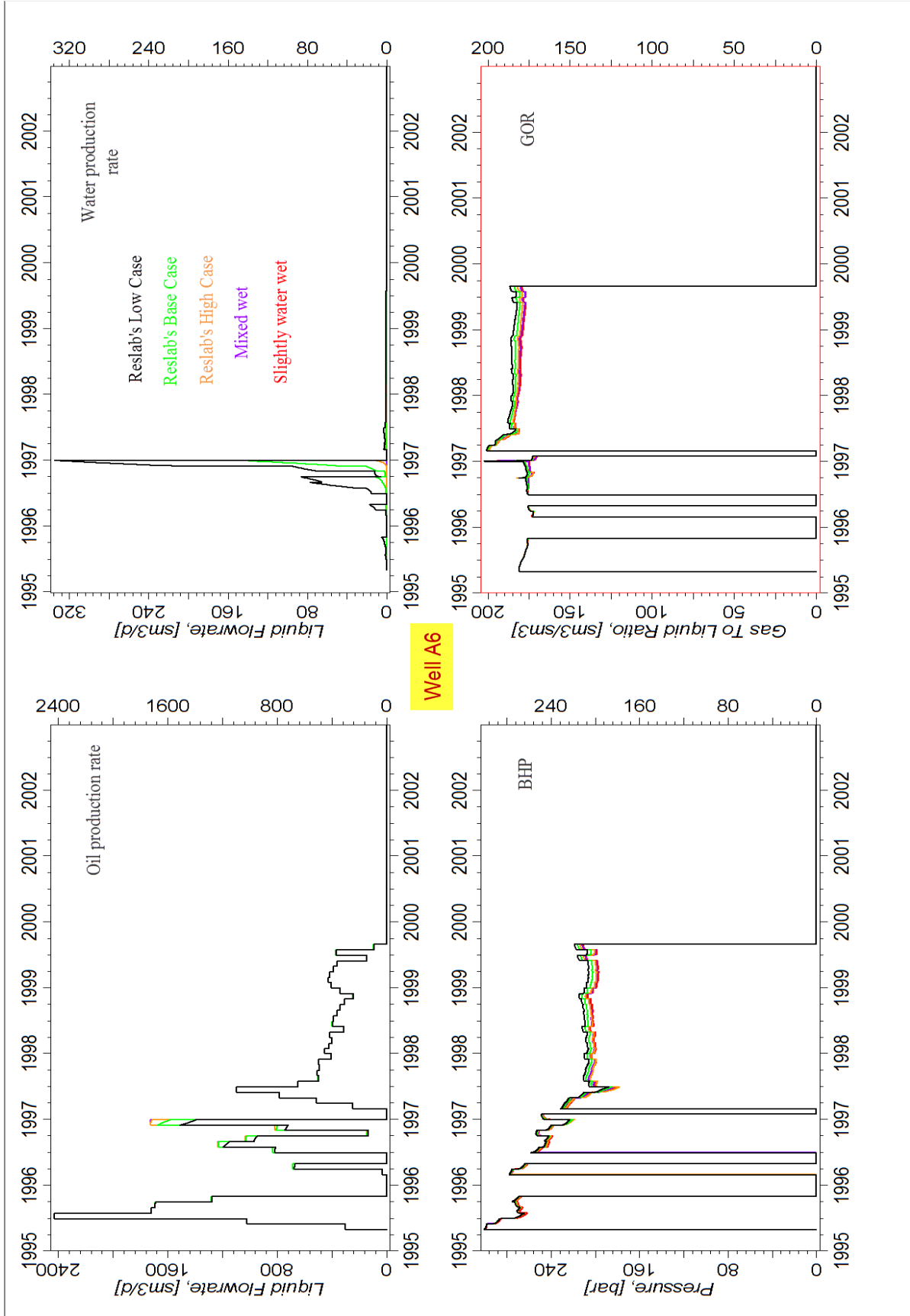


Figure D.7 – Performance of A6 as a function of wettability, 1 SATNUM region

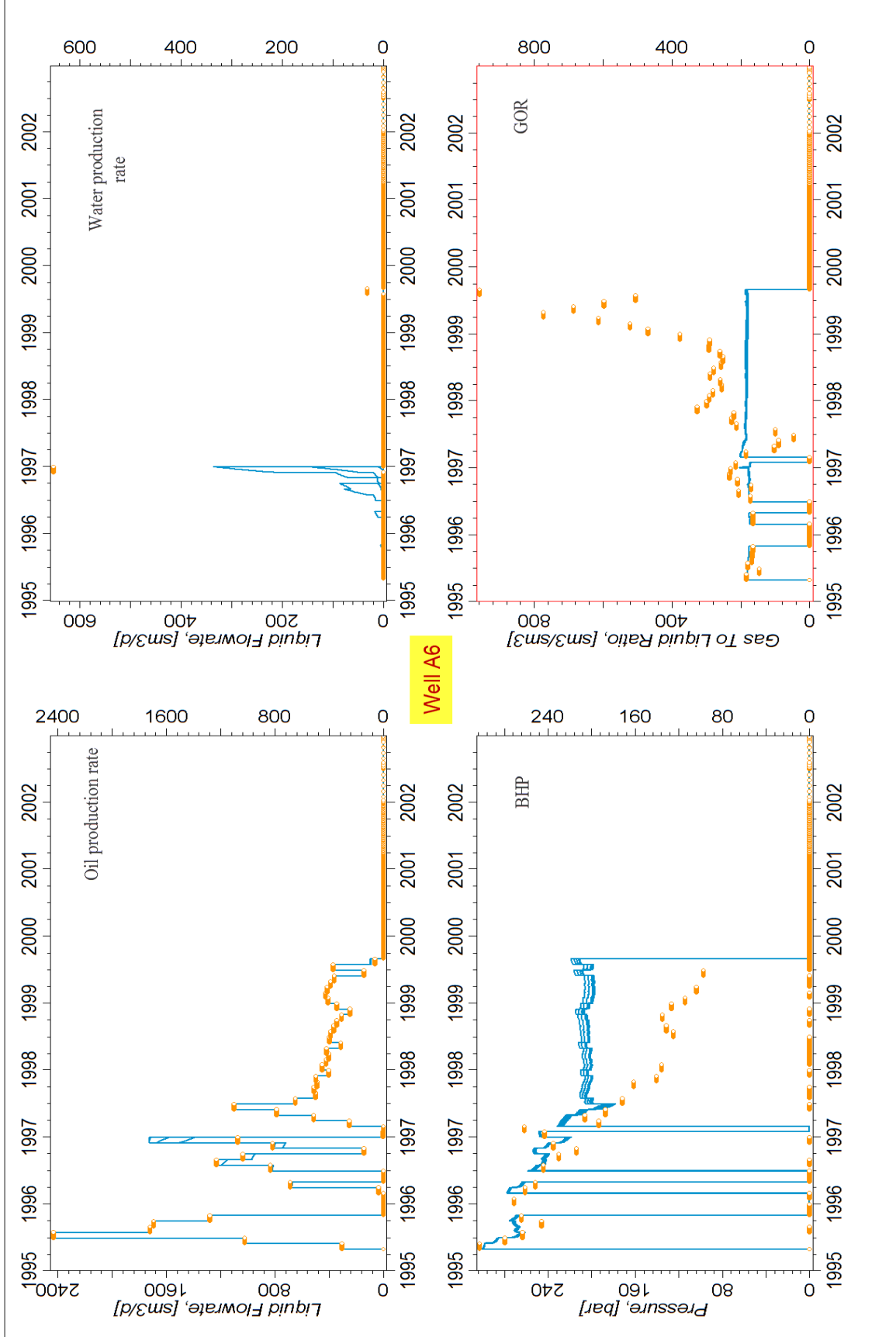


Figure D.8 – Comparison of simulation cases and historic performance A6, 1 SATNUM region

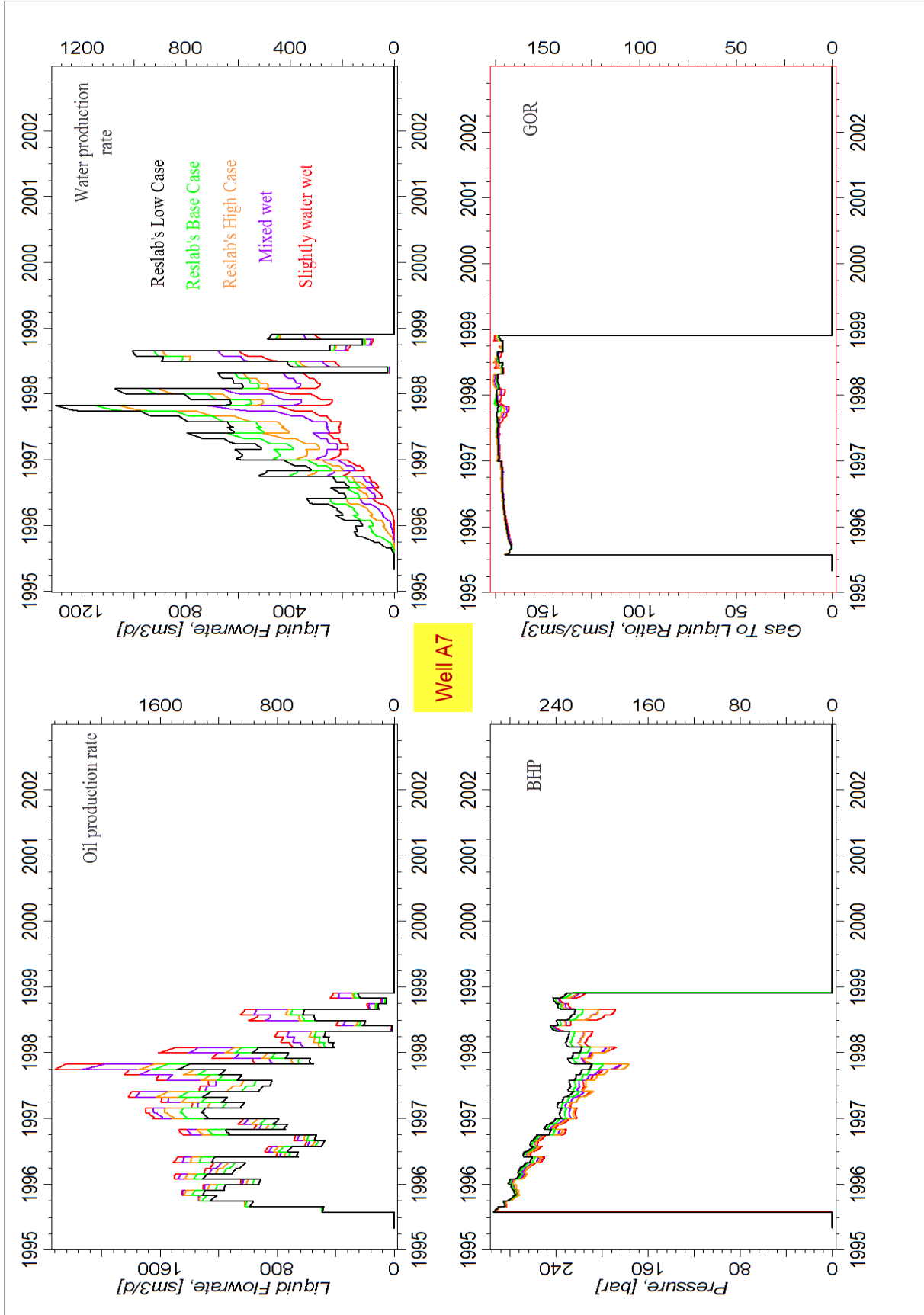


Figure D.9 – Performance of A7 as a function of wettability, 1 SATNUM region

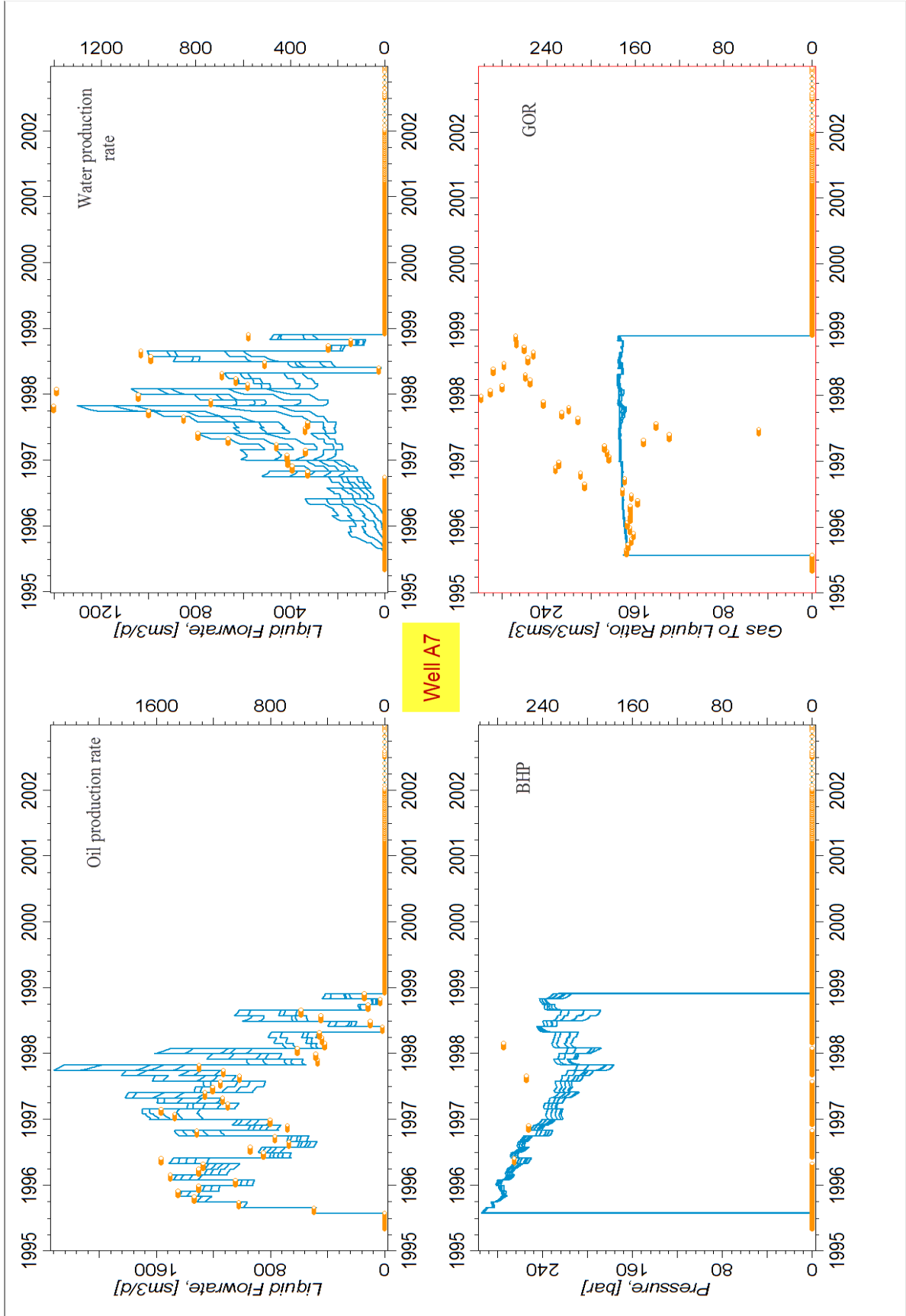


Figure D.10 – Comparison of simulation cases and historic performance of A7, 1 SATNUM region

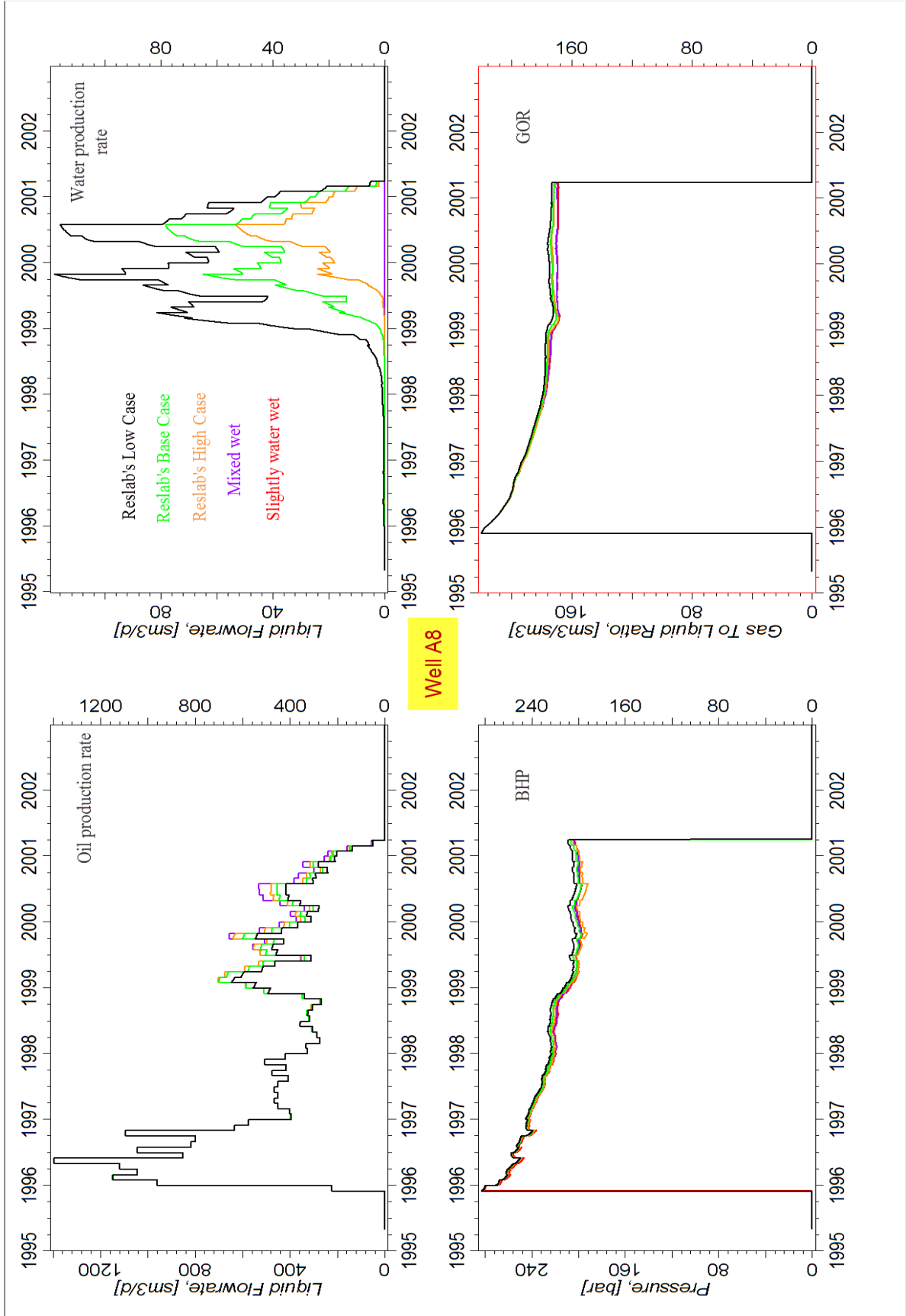


Figure D.11 – Performance of A8 as a function of wettability, 1 SATNUM region

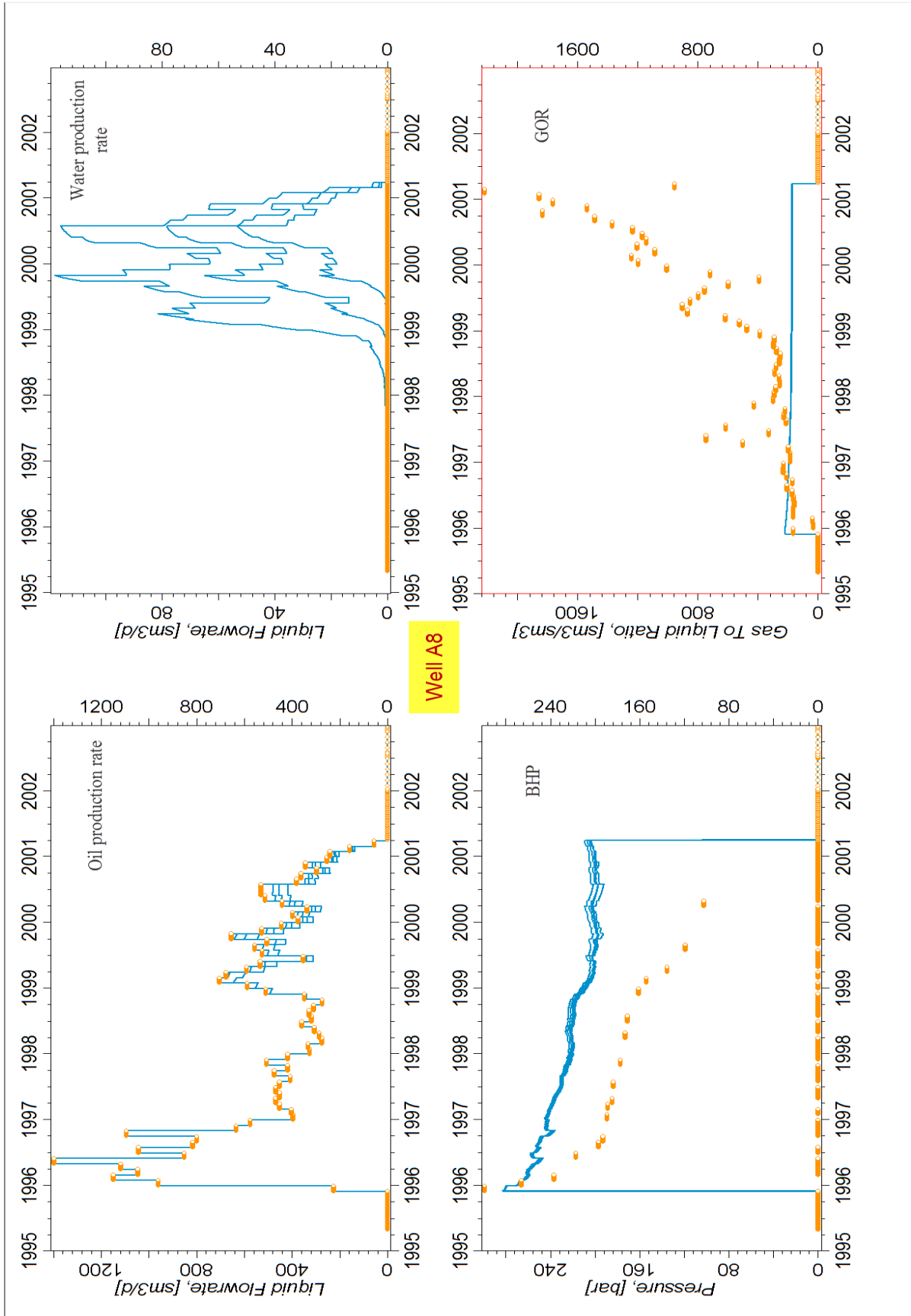


Figure D.12 – Comparison of simulation cases and historic performance of A8, 1 SATNUM region

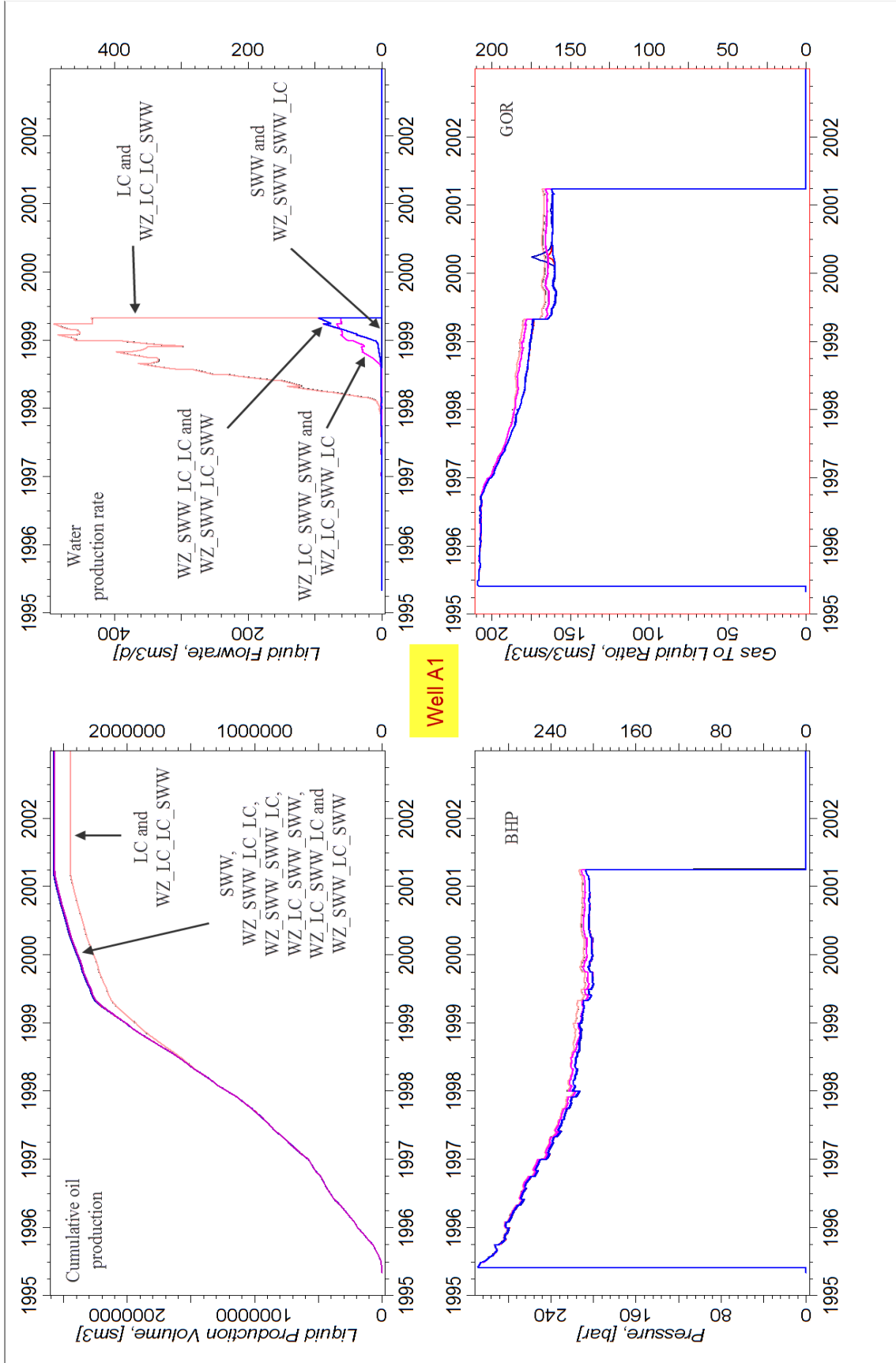


Figure D.13 – Performance of A1 as a function of wettability variations, 4 SATNUMs

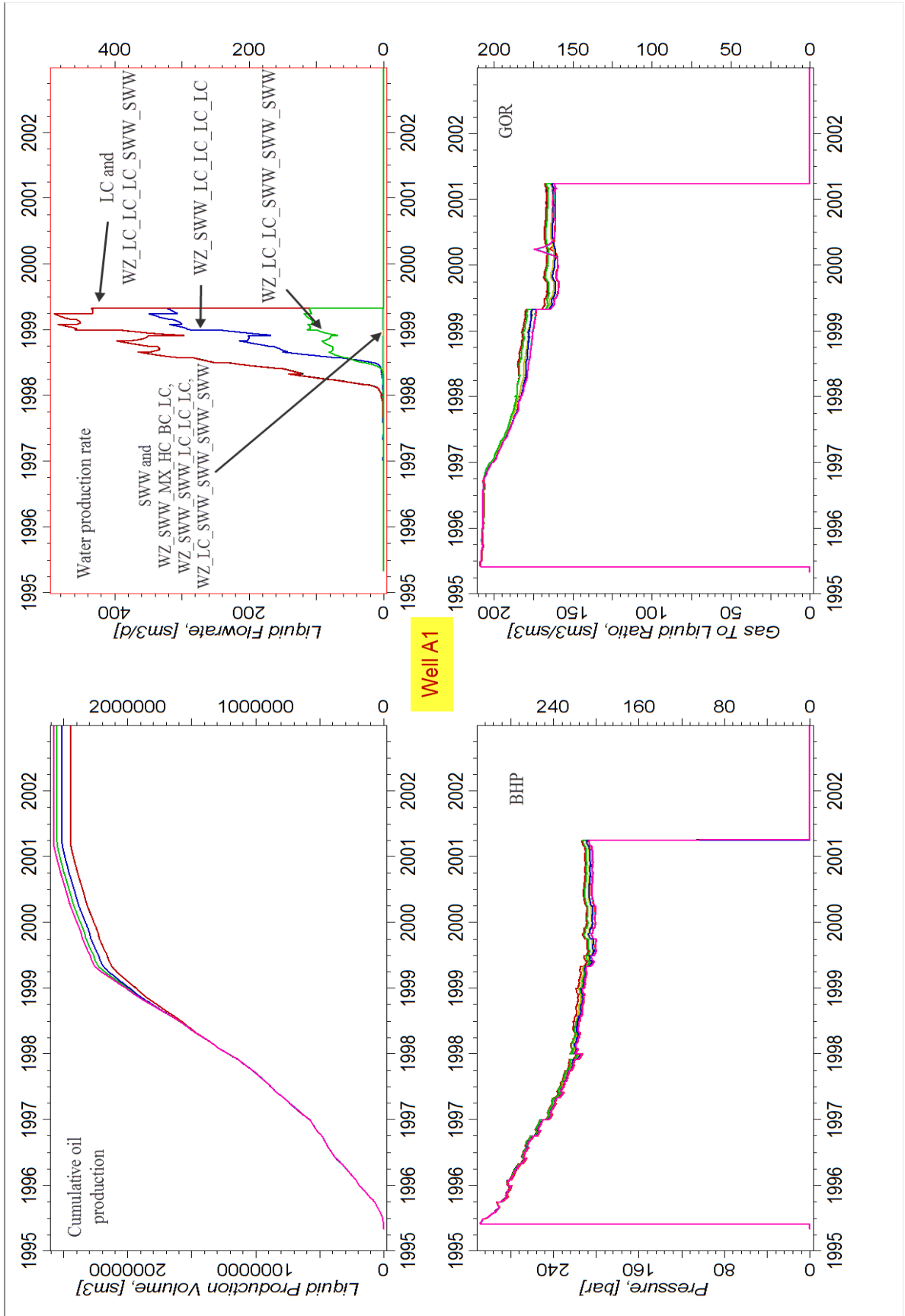


Figure D.14 – Performance of A1 as a function of wettability variations, 6 SATNUMs

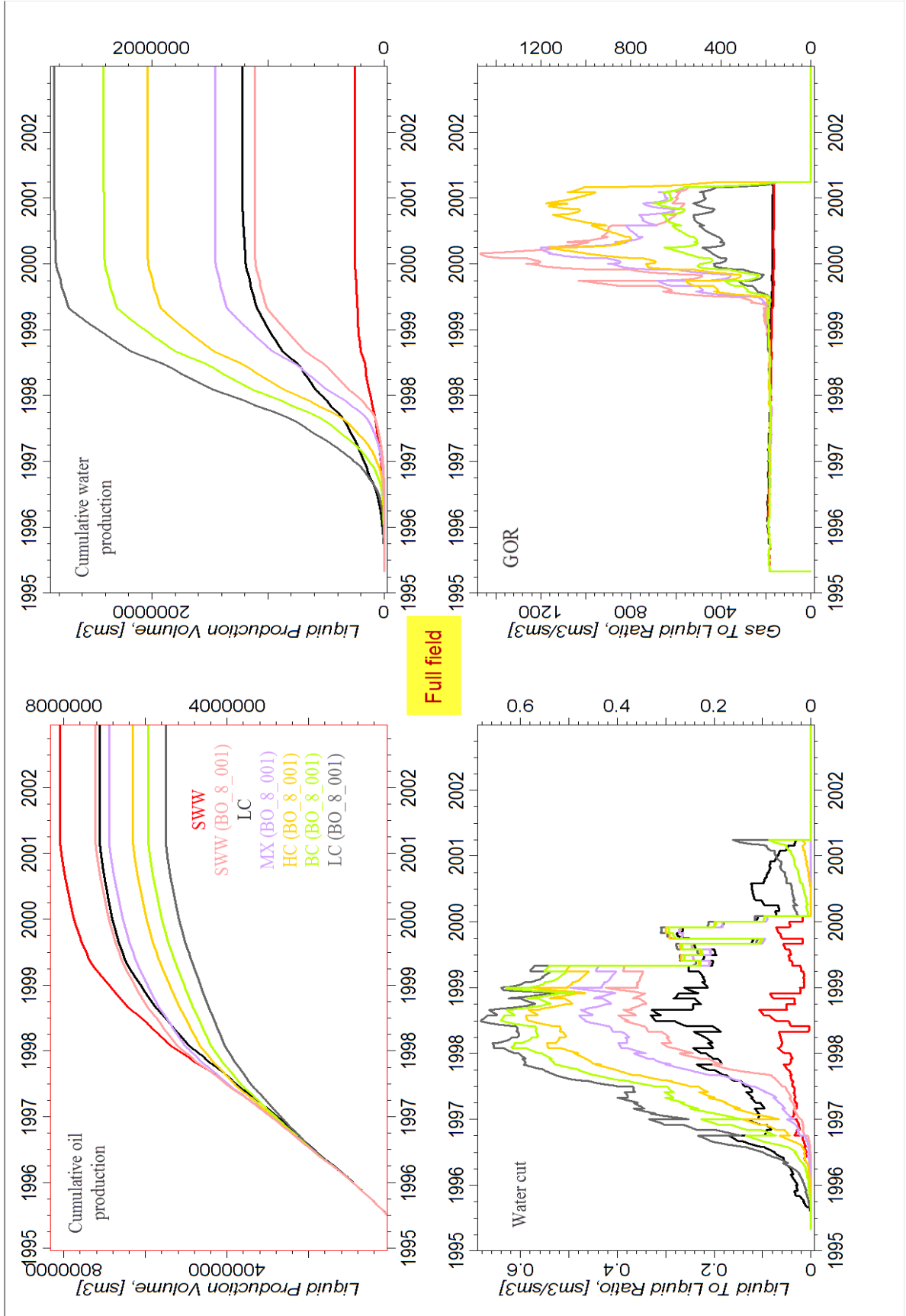


Figure D.16 – Field performance, comparing the SWW and LC cases with simulation cases including aquifer and fault transmissibility factors

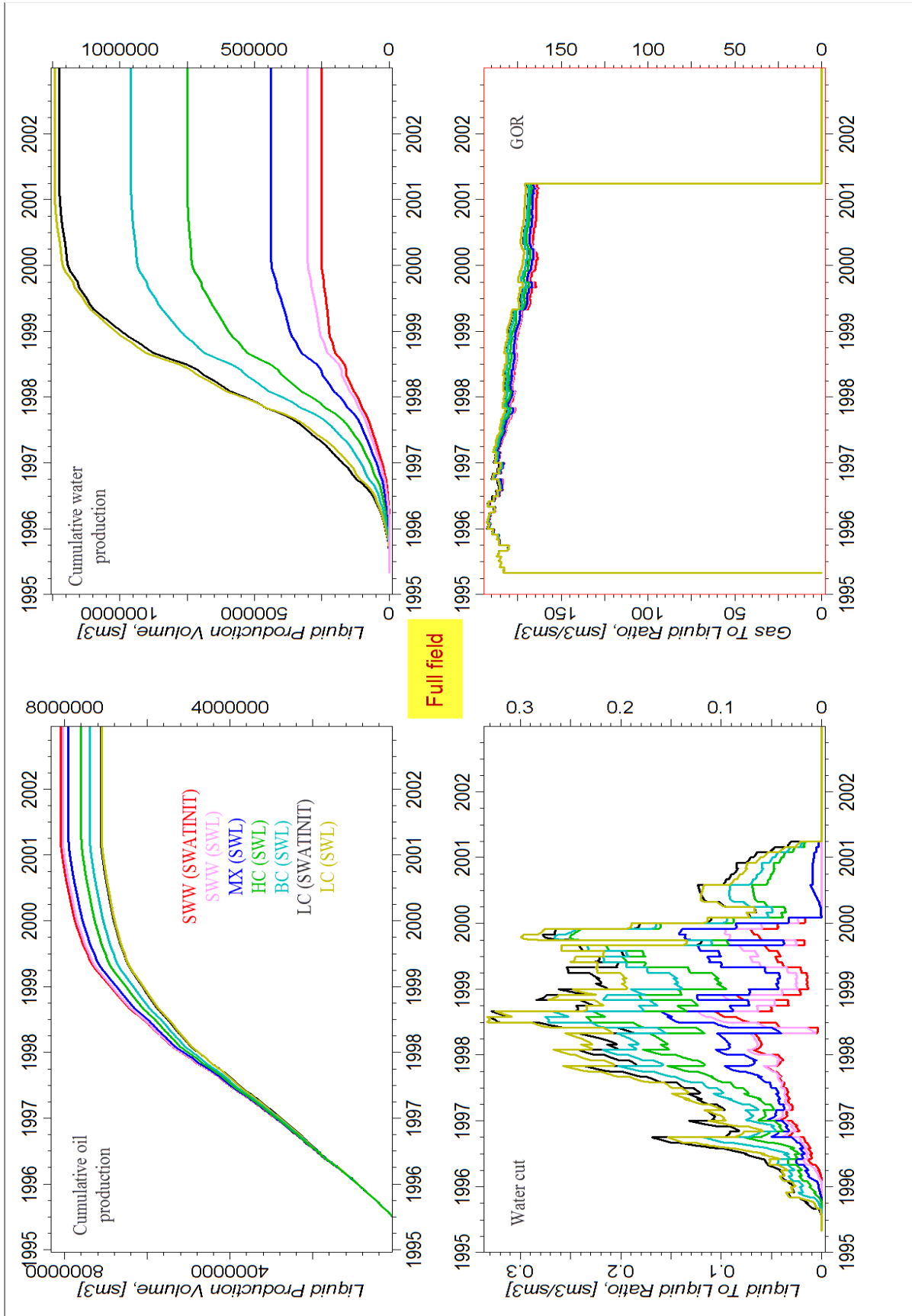


Figure D.17 – Field performance, comparing the SWW and LC cases with simulation cases using the SWL initialization method (PC = 0)

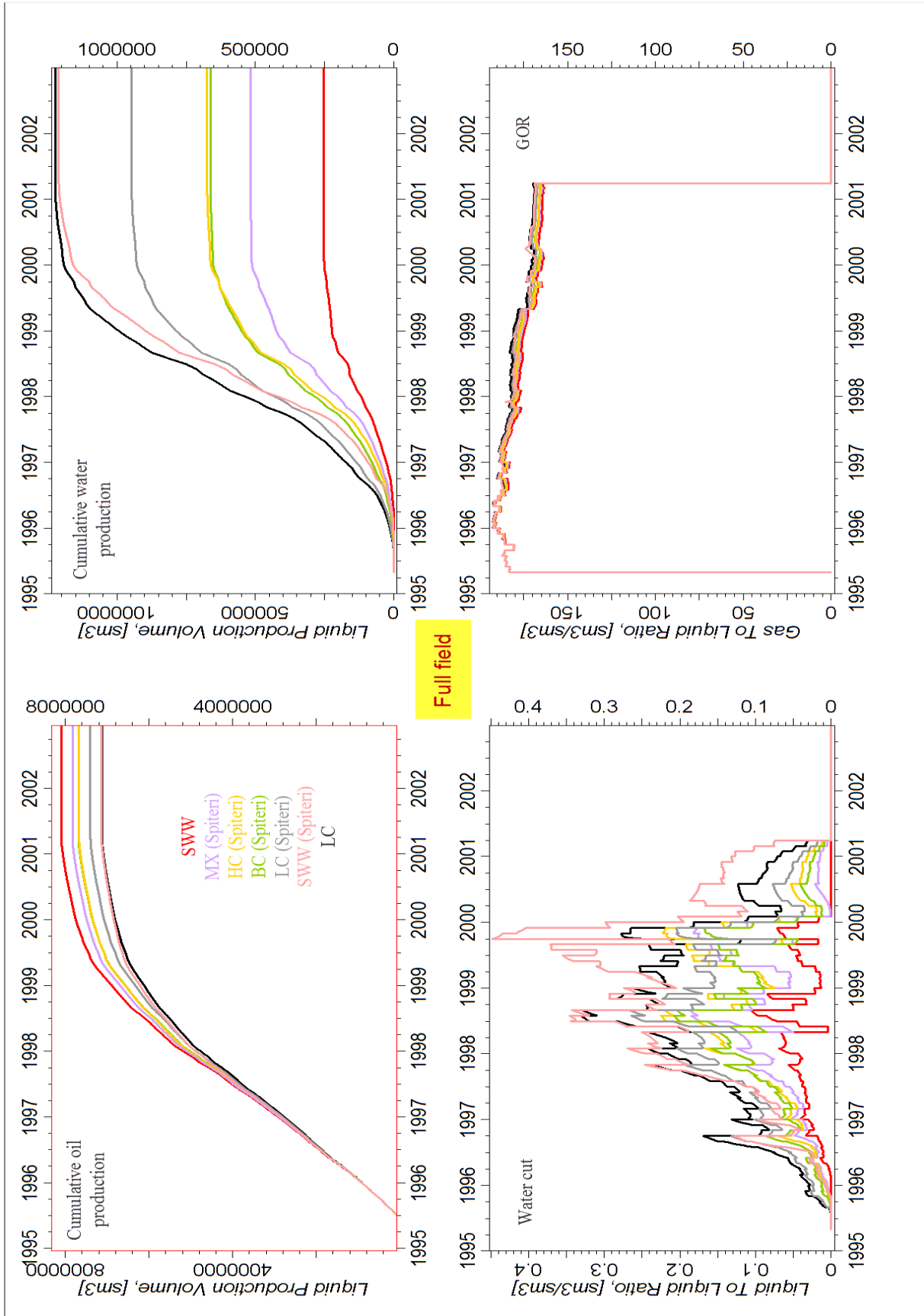


Figure D.18 – Field performance, comparing the SWW and LC cases with simulation cases including Spiteri et al.'s trapping model

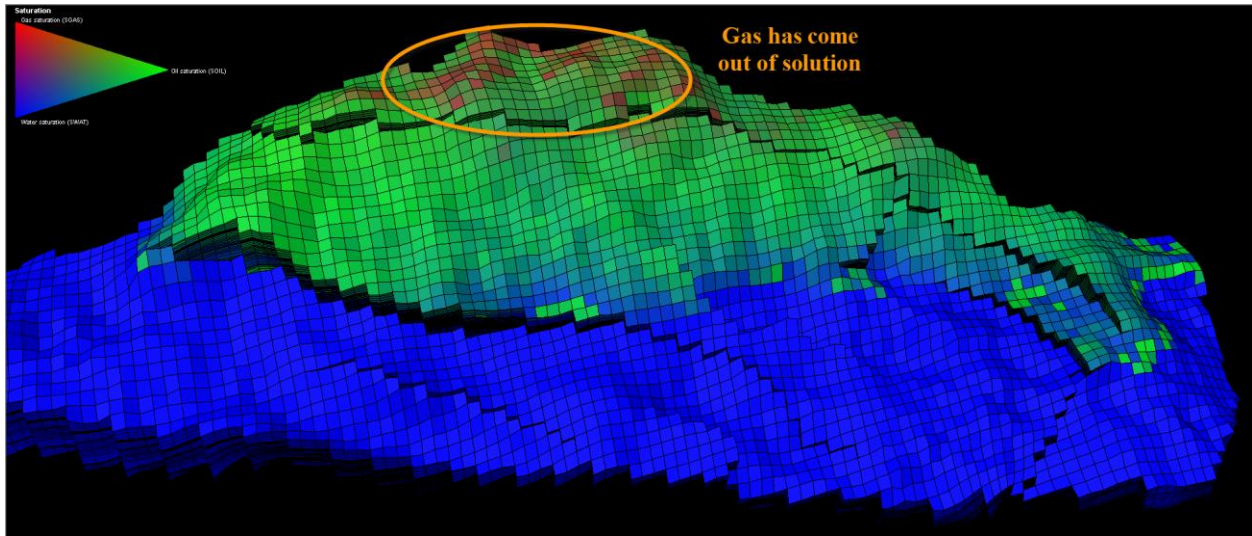


Figure D.19 – The reservoir pressure has dropped below the bubble point pressure at the top of the horst structure at the end of the simulation period